U.S. DEPARTMENT OF COMMERCE
National Technical Information Service

PB-256 910

Development Strategy for Pollutant Dosimetry

Research Triangle Inst.

Prepared For
Environmental Sciences Research Lab.

February 1976

TECHNICAL REPORT DATA

(Please read Instructions on the reverse before completing)

1. REPORT NO. EPA-600/2-76-034	2.	3. RECIPIENT'S ACCESSION NO.
4. TITLE AND SUBTITLE DEVELOPMENT STRATEGY FOR POLLUTANT DOSIMETRY		5. REPORT DATE February 1976
		6. PERFORMING ORGANIZATION CODE
7. AUTHOR(S) J. W. Harrison, P. A. Lawless D. E. Gilbert, J. H. White		8. PERFORMING ORGANIZATION REPORT NO.
9. PERFORMING ORGANIZATION NAME AND ADDRESS Research Triangle Institute P. O. Box 12194 Research Triangle Park, NC 27709		10. PROGRAM ELEMENT NO. 1AA010
		11. CONTRACT/GRANT NO. 68-02-1731
12. SPONSORING AGENCY NAME AND ADDRESS Environmental Sciences Research Laboratory Office of Research and Development U. S. Environmental Protection Agency Research Triangle Park, NC 27711		13. TYPE OF REPORT AND PERIOD COVERED Final
		14. SPONSORING AGENCY CODE EPA-ORD

15. SUPPLEMENTARY NOTES

16. ABSTRACT

This report comprises the results of a study to: (1) Define and place realistic limits upon the needs of epidemiologists for personal pollutant dosimeters; (2) Identify pollutant-sensing principles that offer reasonable opportunity for early development of functioning dosimeters capable of operating with the limits of (1) above; (3) Project the impact of mechanical and electronic miniaturization techniques upon each of the principal options disclosed in (2) above; (4) Assess the cost/benefit aspects of active vs. passive sampling of the atmosphere, as applied to candidate sensors identified in (1), (2) and (3) above; (5) Assess the advantages, if any, of a systems approach to dosimeter development, in which the design of a sensor for a given pollutant would be constrained to make maximum use of components & subassemblies common to sensors for other pollutants.

The study reported on has been arbitrarily limited to consideration of devices applicable to the measurement of ozone, sulfur dioxide and nitrogen dioxide. The principles developed will apply in some degree to the eventual design of dosimeters for other pollutants.

17. KEY WORDS AND DOCUMENT ANALYSIS

a. DESCRIPTORS	b. IDENTIFIERS/OPEN ENDED TERMS	c. COSATI Field/Group
*Dosimeters Air pollution Ozone Sulfur dioxide Nitrogen dioxide		06R 13B 07B

PRICES SUBJECT TO CHANGE

18. DISTRIBUTION STATEMENT RELEASE TO PUBLIC	19. SECURITY CLASS *(This Report)* UNCLASSIFIED	21. NO. OF PAGES 195
	20. SECURITY CLASS *(This page)* UNCLASSIFIED	22. PRICE $7.50

EPA Form 2220-1 (9-73)

247078

PB 256 910

EPA-600/2-76-004
February 1976

Environmental Protection Technology Series

UNITED STATES ENVIRONMENTAL PROTECTION AGENCY

REPRODUCED BY
NATIONAL TECHNICAL
INFORMATION SERVICE
U. S. DEPARTMENT OF COMMERCE
SPRINGFIELD, VA. 22161

RESEARCH REPORTING SERIES

Research reports of the Office of Research and Development, U.S. Environmental Protection Agency, have been grouped into five series. These five broad categories were established to facilitate further development and application of environmental technology. Elimination of traditional grouping was consciously planned to foster technology transfer and a maximum interface in related fields. The five series are:

1. Environmental Health Effects Research
2. Environmental Protection Technology
3. Ecological Research
4. Environmental Monitoring
5. Socioeconomic Environmental Studies

This report has been assigned to the ECOLOGICAL RESEARCH series. This series describes research on the effects of pollution on humans, plant and animal species, and materials. Problems are assessed for their long- and short-term influences. Investigations include formation, transport, and pathway studies to determine the fate of pollutants and their effects. This work provides the technical basis for setting standards to minimize undesirable changes in living organisms in the aquatic, terrestrial, and atmospheric environments.

This document is available to the public through the National Technical Information Service, Springfield, Virginia 22161.

EPA-600/2-76-034
February 1976

DEVELOPMENT STRATEGY FOR POLLUTANT DOSIMETRY

J. W. Harrison
D. E. Gilbert
P. A. Lawless
J. H. White

Research Triangle Institute
P. O. Box 12194
Research Triangle Park, NC 27709

68-02-1731

Andrew E. O'Keeffe
Air Quality Measurement Methods Branch
Chemistry and Physics Laboratory
Research Triangle Park, N. C. 27711

U.S. ENVIRONMENTAL PROTECTION AGENCY
OFFICE OF RESEARCH AND DEVELOPMENT
CHEMISTRY AND PHYSICS LABORATORY
RESEARCH TRIANGLE PARK, N. C. 27711

i (b)

DISCLAIMER

This report has been reviewed by the Environmental Sciences Research Laboratory, U.S. Environmental Protection Agency, and approved for publication. Approval does not signify that the contents necessarily reflect the views and policies of the U.S. Environmental Protection Agency, endorsement or recommendation for use.

ABSTRACT

This report comprises the results of a study to:

(1) Define and place realistic limits upon the needs of epidemiologists for personal pollutant dosimeters;

(2) Identify pollutant-sensing principles that offer reasonable opportunity for early development of functioning dosimeters capable of operating within the limits of (1) above;

(3) Project the impact of mechanical and electronic miniaturization techniques upon each of the principal options disclosed in (2) above;

(4) Assess the cost/benefit aspects of active vs. passive sampling of the atmosphere, as applied to candidate sensors identified in (1), (2) and (3) above;

(5) Assess the advantages, if any, of a systems approach to dosimeter development, in which the design of a sensor for a given pollutant would be constrained to make maximum use of components & subassemblies common to sensors for other pollutants.

The study reported on has been arbitrarily limited to consideration of devices applicable to the measurement of ozone, sulfur dioxide and nitrogen dioxide. The principles developed will apply in some degree to the eventual design of dosimeters for other pollutants.

TABLE OF CONTENTS

PAGE

ABSTRACT iii

LIST OF FIGURES viii

LIST OF TABLES. xi

SECTION

1.0 INTRODUCTION. 1

1.1 Criteria for Method Selection. . . . , ... 2
1.2 Study Organization 5

2.0 SAMPLE ACQUISITION METHODS. 6

2.1 Passive Sampling 6
    2.1.1 Flat Plate Absorbers. 6
    2.1.2 Diffusion Tube Dosimeter. 7
    2.1.3 Summary 18

2.2 Active Sampling. 18

3.0 SORPTION METHODS. 21

3.1 Sorption Mechanisms. 21
    3.1.1 Reversible Sorption 21
    3.1.2 Irreversible Sorption 23

3.2 Sorbents for Sulfur Dioxide. 25
3.3 Sorbents for Nitrogen Dioxide. 30
3.4 Sorbents for Ozone 35

4.0 METHODS FOR CONTINUAL MONITORING. 39

4.1 Conductometric Analyzer. 40
    4.1.1 Prior Use 40
    4.1.2 Model 41
    4.1.3 Projected Performance 50
    4.1.4 Logistical Factors. 52
    4.1.5 Dose Rate Information 52

4.2 Halogen/Halide Redox Amperometry 52
    4.2.1 Prior Use 54
    4.2.2 Model 55
    4.2.3 Projected Performance 61
    4.2.4 Logistical Factors. 62
    4.2.5 Dose Rate Information 62

Preceding page blank

TABLE OF CONTENTS (continued)

SECTION PAGE

4.0 METHODS FOR CONTINUAL MONITORING (continued). . . . .

4.3 Halogen Generation Amperometry 62
4.3.1 Prior Use 62
4.3.2 Model 63
4.3.3 Projected Performance 66
4.3.4 Logistical Factors. 67
4.3.5 Dose Rate Information 67

4.4 Membrane Amperometers. 67
4.4.1 Prior Use 68
4.4.2 Model 69
4.4.3 Projected Performance 73
4.4.4 Logistical Factors. 74
4.4.5 Dose Rate Information 74

4.5 Colorimetric Methods 74
4.5.1 Prior Use 75
4.5.2 Model Detectors 78
4.5.3 Projected Performance 91
4.5.4 Logistical Factors. 92
4.5.5 Dose Rate Information 92

4.6 Gas Phase Luminescence 92
4.6.1 Prior Use 93
4.6.2 Model 94
4.6.3 Projected Performance 97
4.6.4 Logistical Factors. 98
4.6.5 Dose Rate Information 98

4.7 Gas/Liquid Phase Luminescence. 99
4.7.1 Prior Use 99
4.7.2 Model 100
4.7.3 Projected Performance 103
4.7.4 Logistical Factors. 103
4.7.5 Dose Rate Information 103

4.8 Gas/Solid Luminescence 104
4.8.1 Prior Use 104
4.8.2 Model 105
4.8.3 Projected Performance 105
4.8.4 Logistical Factors. 106
4.8.5 Dose Rate Information 106

TABLE OF CONTENTS (continued)

SECTION PAGE

4.0 METHODS FOR CONTINUAL MONITORING (continued)..............

4.9 Ionization and Electrophoresis........................ 106
4.9.1 Prior Use................................... 106
4.9.2 Model....................................... 109
4.9.3 Projected Performance....................... 115
4.9.4 Logistical Factors.......................... 115
4.9.5 Dose Rate Information....................... 115

4.10 Piezoelectric Mass Monitor.......................... 115
4.10.1 Prior Use.................................. 115
4.10.2 Model...................................... 117
4.10.3 Projected Performance...................... 126
4.10.4 Logistical Factors......................... 127
4.10.5 Dose Rate Information...................... 127

5.0 DATA ACQUISITION.. 128

5.1 General.. 128
5.2 Magnetic Tape System................................... 137
5.3 Solid State Memory System.............................. 143
5.3.1 MOS-LSI Memory Systems...................... 145
5.3.2 MNOS Memory System......................... 148
5.3.3 Summary..................................... 149

6.0 INTEGRATED DOSE METHODS.................................. 152

6.1 Solid Adsorbents/Passive Sampling...................... 152
6.2 Solid Adsorbents/Active Sampling....................... 154
6.3 Liquid Adsorbents/Passive Sampling..................... 156
6.4 Liquid Adsorbents/Active Sampling...................... 156
6.5 Packaged Vacuum.. 157

7.0 DOSIMETRY SYSTEMS.. 159

7.1 Integrated Dose Methods................................ 159
7.2 Continual Dose Methods................................. 163

8.0 CONCLUSIONS AND RECOMMENDATIONS........................... 167

8.1 Recommendations.. 169

REFERENCES... 171

LIST OF FIGURES

FIGURE PAGE

1.1 Schematic Diagram of a Single Channel Pollutant Dosimeter for Continual Exposure Measurements 4

2.1 Air Incident upon Absorber and Substrate Only 8

2.2 Air Incident upon Absorber and Substrate Mounted on Larger Area Carrier. 8

2.3 Normalized Concentration in the Diffusion Tube as a Function of Position along the Tube for Various Times after a Step Change in Concentration. 12

2.4 Normalized Current in the Diffusion Tube as a Function of Position and Time 14

2.5 Normalized Amount of Material Passing the Inlet of the Diffusion Tube (x = 0) and Being Collected (x = L) as a Function of Time 15

2.6 Normalized Response of the Diffusion Tube Sampler to a Pulse Input, with the Amount of Material Passing the Inlet (x = 0), as a Function of Time. 17

3.1 Adsorption Hysteresis for Water Vapor in Titania Gel 24

3.2 Relation between Pore Size and Diffusion Coefficient 24

3.3 Sulfur Dioxide Reaction Mechanisms. 25

3.4 Cellulose Nitrate Matrix. 28

4.1 Basic Conductance Cell Arrangement. 42

4.2 Bridge Arrangement for Conductance Cells. 42

4.3 Conductivity Cell Design of Hall[38]. 46

4.4 Change in Conductivity Cell Current for Various Concentrations of Sulfur Dioxide. 49

4.5 Change in Conductivity Cell Current for Various Concentrations of Nitrogen Dioxide. 51

LIST OF FIGURES (continued)

FIGURE		PAGE
4.6	Schematic Diagram of Conductance Amplifier Circuit[39]	53
4.7	Kromhyr Cell	56
4.8	Lindqvist Cell	56
4.9	Signal Processor for Differential Current Measurements	59
4.10	Model Cell for Halogen Generation/Amperometric Measurement Method	64
4.11	Model Membrane Amperometer	70
4.12	Model Colorimeter Detectors	79
4.13	Transparent Film Substrate Colorimetric Detector	83
4.14	Tape System Using Fibrous Tape	86
4.15	Measurement Using Surface Reflectance Change due to Pollutant Exposure	88
4.16	Remission Spectra of Pure $CuSO_4.5H_2O$ at Five Different Crystal Sizes	89
4.17	Fraction R of Linearly Polarized Light after the Reflection on Paper Dye with Rhodamin, for Various Angles of Incidence α as Parameter and Dependent on the Observation Angle θ	90
4.18	Ionization/Electrophoresis Apparatus of Vree and Fontijn	108
4.19	Ionization/Electrophoresis Detector	110
4.20	Equilibrium Distributions of Clusters $H^+(H_2O)_n$ Predicted by Experimental Data[115]	111
4.21	Orientation of AT and DT Cuts with Respect to Major Axes of Quartz[121]	118

LIST OF FIGURES (Continued)

FIGURE PAGE

4.22 Effect of Minor Orientation Changes on Temperature Effects in AT Cut Quartz [122] 119

4.23 Family of Frequency vs. Temperature Curves for AT Cut Quartz[122] 120

4.24 Zero Temperature Coefficient Operating Temperatures for AT Cut Quartz as a Function of Orientation[122] 120

4.25 Detailed Portion of Figure 4.24 Near Room Temperature[122] 122

4.26 Typical Frequency Response to a Change in Ambient Temperature 122

5.1 Generalized Data Acquisition System 131

5.2 Incremental Digital Tape Recorder Data Collection System 141

5.3 Data Selection Control 144

5.4 MOS LSI Memory System 147

5.5 MNOS Memory System 150

6.1 Pressure Components in Packed Tube Samplers 154

7.1 Integrated Dosimeter Operation Scheme 160

7.2 Dose Measurements from Integral Methods 162

7.3 Continual Dose Rate Measurement Operational Scheme 164

7.4 Data Processing for Dose Rate Records from Continual Monitors 166

LIST OF TABLES

TABLE PAGE

1.1 Performance Goals for Champ Instruments 2

2.1 Characteristics of Commercially Available Sampling Pumps 19

3.1 Species with Lewis-Acid-Base Character 26

3.2 Typical Chemical and Physical Sulfur Dioxide Adsorbents 26

3.3 Relative Response of Amines and Non-Amines 29

3.4 Liquid Sorbents for Nitrogen Dioxide 32

3.5 Apparent Sorption Efficiencies 36

3.6 Molar Absorptivities 37

4.1 Projected Performance of Conductivity Cell Analyzers 50

4.2 Performance Summary for Differential Amperometric Method for Ozone Measurement 57

4.3 Projected Performance of Differential Amperometric Cell Analyzers 61

4.4 Projected Performance of Iodine Generator Amperometer 66

4.5 Features of ECT Analyzers 68

4.6 Model SS-310 Interference Data 68

4.7 Advantages and Disadvantages of ECT Analyzers[53] 69

4.8 Parameter Values for Permeation of NO_2 in Teflon[54] at 25°C 72

4.9 Relative Permeation of NO, NO_2 and SO_2 in Various Materials[53] 72

LIST OF TABLES (continued)

TABLE		PAGE
4.10	Projected Performance of Membrane Amperometers.	74
4.11	SO_2 Emission Quenching Data[88]	95
4.12	Performance Values for Chemiluminescent Monitors.	98
4.13	Effect of Hydration on Mobility of SO_2, NO_2, and O_3 Molecules.	112
5.1	Power Requirements and Other Logistic Factors for Tape Recorder Unit.	142
5.2	Comparison of Memory Systems of 64K Bits.	151

SECTION 1

1.0 INTRODUCTION

The assessments of the effects of various pollutants on human subjects requires measurements of the amounts of pollutant to which these subjects are exposed over some period of time and correlation of these dosages with the general state of health of these subjects. Dosimetry has been a long standing required practice for personnel exposed to x-ray, γ-ray and high energy particle radiations. Two forms are used. The integrated dosage is routinely measured by film badges which are periodically collected and developed to obtain a "read-out" of the cumulative exposure of the individual wearer to ionizing radiation. In non-routine measurement situations, the dose rate is measured continuously in order to determine the variations in intensity that may be encountered in a work situation. This is important when dose rates are apt to be highly variable and/or unpredictable.

Either form of measurement could be contemplated for personal pollutant dosimeter development. The integrated dose method is relatively simple and inexpensive; however, it does not give enough definition to the measurement to allow correlation of dose rate with activity. For example, a human subject will require greater ventilation under stress. If the periods of higher ventilation also occur simultaneously with exposure to high pollutant concentration, the ingestion of pollutants and, therefore, the dose may be significantly larger than if the subject were able to "idle" when exposed to high pollutant concentration.

This has been recognized in a discussion concerning a proposed change in the "significant harm" level and "emergency" action level for photochemical oxidants.[1] Here it was pointed out that although a one-hour average was being used as a practical basis in assessing monitoring results, exposure to high enough levels over periods of 15 minutes or shorter could also lead to significant adverse effects.

In view of this need, a major part of this study has been directed to determining how present detection methods could be miniaturized to provide reasonably accurate, portable instruments that could enable continuous or, more properly, continual measurement of ambient SO_2, NO_2 and ozone with the data recorded in a format suitable for synchronizing exposure history with the subject's activity during a realistic time period.

Because economic or other factors might dictate that integrated dose devices be used instead of, or as a complement to, continual monitors principles underlying the design of these devices have also been examined, particularly from the point of view of sample acquisition onto totally absorbing materials via diffusion transport.

1.1 Criteria for Method Selection

Selection of one or more measurement principles for miniaturization as a pollutant dosimeter is based upon several criteria:

1. Repeatibility - i.e. calibration stability,
2. Precision and accuracy of measurement,
3. Ease of maintenance and calibration,
4. Convenience of data readout,
5. Portability and ruggedness, and
6. Economic deployment.

These guidelines are interpreted as follows.

Any useful measurement device to be carried around by non-trained, non-technical people must be repeatable. The zero drift and span change with time and with ambient conditions must be minimal. This might be achieved by various compensation techniques in the design or by automatic, periodic internal re-zeroing and span setting cycles.

Precision and accuracy of these measurements are necessary if the data are to be useful. Design goals for these have been set for CHAMP program instruments as ±2% precision and ±5% accuracy. Table 1.1 lists these and other performance goals for CHAMP instruments, which could be also used as design goals for pollutant dosimeters.

Table 1.1. PERFORMANCE GOALS FOR CHAMP INSTRUMENTS

Pollutant	Drift/day Zero	Drift/day Span	Noise	Detection Limit	Precision	Response Time
O_3	<1%FS	<0.5%	<2%FS	4 ppb	2%FS	10 sec
NO_2	<2%FS	<5%	<0.5%FS	5 ppb	2%FS	3 sec
SO_2	<1%FS	<2%	<2 ppb	5 ppb	2%FS	3 min

The design should be amenable to rapid, periodic calibration checks with an "external" calibration source of pollutants. These checks should be administered by trained, technical personnel to assure that data quality is maintained. At the same time routine maintenance should be performed such as reagent replenishment (if required) and a step-by-step verification that each functional component is performing within specifications. A modular design concept should be employed that would simplify functional component checks and replacement, if necessary.

The data format should be convenient for readout and manipulation as necessary for interpretation. As will be seen later, there are many design options for data recording and readout. Whichever option is selected will be influenced by many factors, but the selection should be weighted by considerations of obtaining the data in a form that enables correlation of the exposure history with the subject's activity pattern, meteorological factors, etc., without excessive manpower being required to cast it into readily usable form. Figure 1.1 indicates schematically a dosimeter system. The last step from readout to "data ready for use" should require a minimum amount of skilled manpower, particularly if the number of subjects and periods of testing are large enough to provide an adequate statistical basis for projection onto exposure of the general population.

Portability and ruggedness are necessary design features if the dosimeter package is to be transported around by normal human subjects. Ideally, a lapel type device is desired. However, the current state of the art in miniaturization, particularly when the foregoing constraints are applied, does not allow this. A briefcase sized instrument package capable of 10 hours of operation on batteries is a realistic design goal. The weight of such a package should be less than 20 pounds. It should be capable of operating unhindered by the impulse forces encountered in normal activity. The magnitude of these forces is at present unknown, but they could be estimated from a few acceleration measurements carried out on a briefcase. It would be desirable if the dosimeter package could function in any orientation. Certainly it must not be rendered inoperable by being temporarily placed on its side. This places severe design

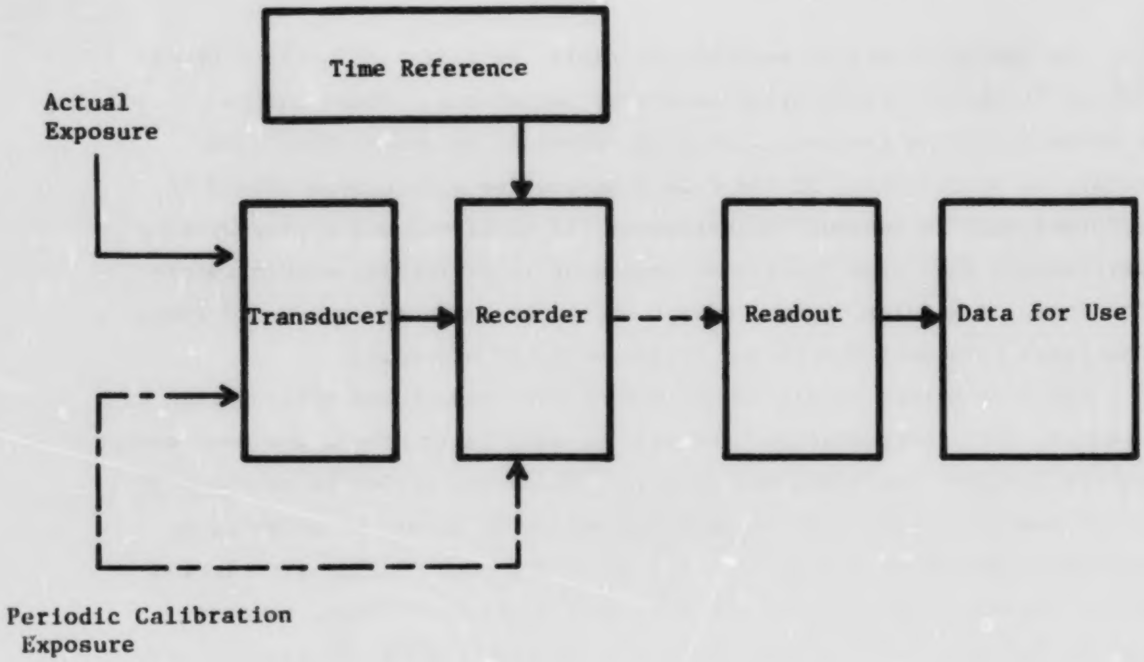

Figure 1.1. Schematic Diagram of a Single Channel Pollutant Dosimeter for Continual Exposure Measurements.

constraints on those measurement principles which use liquid reagents. It is possible that this requirement could be relaxed somewhat by cautioning the human subject to be careful about orientation. However, it seems unrealistic to expect complete compliance with such a request.

The deployment of a personal dosimeter network and operation of a system to maintain it, assure data quality and then process the data to obtain desired research information from it represents a sizable investment. The anticipated results must justify the commitment. The measurement methods chosen for development must depend upon existing technology for miniaturization. It is not feasible to launch a multiplicity of separate research efforts to obtain miniaturized components. Wherever possible, as many common components as possible should be used in the design of the separate dosimeter instruments for SO_2, NO_2 and ozone. These components should, if possible, be obtainable commercially from more than one source. If manufacture by special order is necessary, the manufacturing operations required should be routine and use commonly available materials. Only then can reasonable cost and delivery of initial items and replacement items be expected. In addition, the cost of maintenance and calibration must be taken into account as well as the cost of data retrieved. At this stage of development of the dosimeter concept, only guideline statements can be made about the economics of deployment. Realistic cost estimates can only be made on the basis of a firm prototype design.

1.2 Study Organization

This report is organized to cover the topic as follows. First, sample acquisition methods are discussed from the point of view of passive versus active sampling. Then the various methods in which pollutants can be extracted from the ambient air are discussed under the heading of sorption methods. Following this, a review of the principles of the methods used for SO_2, NO_2 and ozone detection is made and a mathematical model developed for each where practicable in order to assess their performance when "scaled down" to a convenient size for portable monitoring devices. A discussion of state-of-the-art methods for electronic data recording is next. Subsequently, various options for deployment and dosage read-out are reviewed. Finally, recommendations are made as to the methods which appear most feasible.

SECTION 2

2.0 SAMPLE ACQUISITION METHODS

Before a pollutant can be detected or collected to provide information on concentration or dosage, ambient air must be contacted with the detection or collection device. The contacting can be brought about either through natural convection and diffusion, hereinafter termed "passive sampling," or through forced convection, hereinafter called "active sampling." Passive sampling has advantages of simplicity, no power drain and, hence, low cost. It is suitable for applications where integrated dose measurements are sought and where response time is not an important factor. The characteristics, merits, and drawbacks are discussed below in Section 2.1.

Active sampling provides a continual supply of air to the detecting or collecting device. This is required by many measurement methods, particularly those classified as "dynamic," when the time resolution of the measurement must be small in order to register transient concentration changes. Such variations can occur due to "wafting" --i.e., eddy currents or plumes of relatively high pollutant concentration flowing from some point source. The exchange for such speed of response is an increase in complexity, power drain and cost. The characteristics, merits and drawbacks of active sampling are discussed in Section 2.2.

2.1 Passive Sampling

Transport of vapor species through ambient air occurs through natural convection and diffusion. The speeds of transport for these two mechanisms are vastly different, and because of the variability of convective transport with prevailing weather conditions, the "supply" of a particular pollutant from a particular source to some point where a standard observer is located may fluctuate widely. Two modes of passive sampling will be assessed, the "flat plate" and the diffusion tube, in the light of such fluctuations.

2.1.1 Flat Plate Absorbers

It will be assumed that a specific (for a given pollutant), totally absorbing material coats an appropriate substrate and is carried in a holder that permits a well-defined, flat area, A, to be exposed for some specified period of time, T_D, to ambient air. Unless a very high velocity air stream is directed to impinge normally on this flat surface, there will exist a layer of stagnant air—a boundary layer—between the surface of the absorber and the ambient air through which the pollutant must diffuse to be collected. The thickness of this layer, δ, will depend upon the incident velocity of the air and the size of the body to which area A is attached. This is illustrated in Figures 2.1 and 2.2. In Figure 2.1, only the absorber area A is used to intercept the air stream, of initial velocity ν_0. Depending upon whether or not the air is incident from the front (absorber coating side) or back, the air flow pattern and, hence the boundary layer thickness will be different. An even greater effect is shown in Figure 2.2 where the absorber is carried on a much larger body that will appreciably alter the air flow pattern.

These are illustrations of size and orientation effects on the air flow geometry in the vicinity of the absorber. Size will vary from person to person, and orientation, given the same size absorber and carrier, may vary from minute to minute. Therefore, for a given pollutant concentration, C_0, in the ambient air stream incident on the carrier, there may be a large variation in the actual transport rate of pollutant by diffusion, due primarily to the alteration of the stagnant layer geometry. Consequently, it is very difficult to quantitate the dosage as a concentration time product.

This difficulty is sidestepped in part by the diffusion tube sampler which will be considered next.

2.1.2 Diffusion Tube Dosimeter

The diffusion tube dosimeter is a simple device for measuring the exposure to a particular gas in ambient air. It consists of a tube of fixed length and area with one end open to the air and the other end ending in a collecting medium. The collecting medium is assumed to be specific for the gas to be sampled, and, ideally, will absorb all of the particular gas that reaches it.

Experimental work on diffusion samplers has been done by Palmes and Gunnison[2] and Gunnison, Gunnison, and Palmes[3] for water vapor, SO_2, and NO_2. The results have encouraged further development of the technique.

The analysis of the behavior of the diffusion tube is simplest in the steady state. It is assumed that the concentration of the component

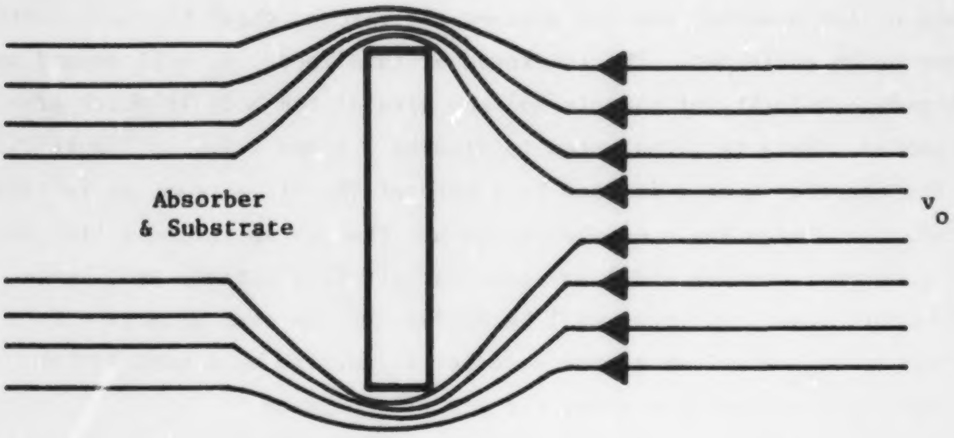
Absorber
& Substrate
v_o

Figure 2.1. Air Incident upon Absorber and Substrate Only.

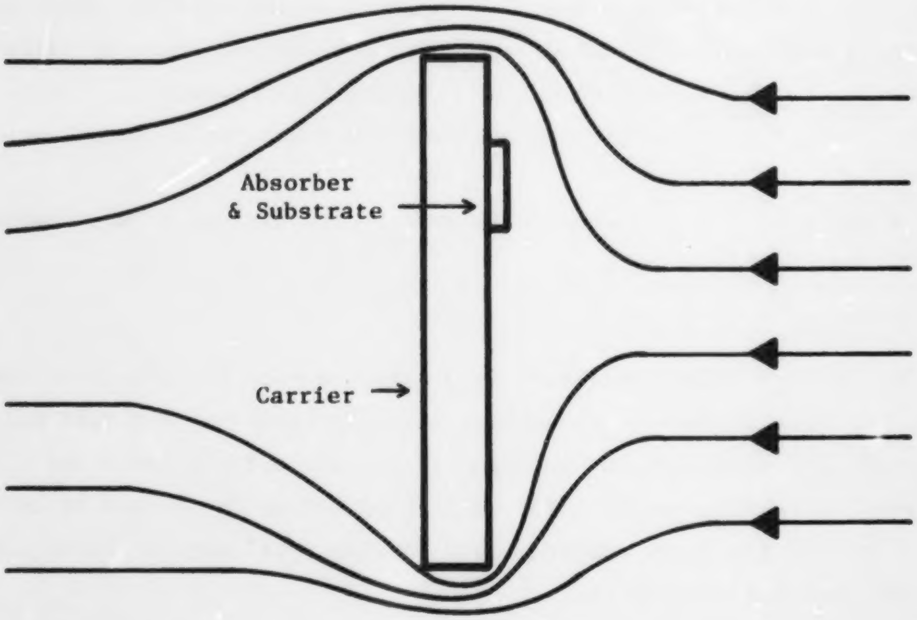
Absorber
& Substrate
Carrier

Figure 2.2. Air Incident upon Absorber and Substrate Mounted on Larger Area Carrier.

in the air being sampled is given by C_0, that the concentration in air at the surface of the absorber is zero, and that the temperature is held constant.

The equation describing diffusion in this case is

$$J = -D \frac{\partial C}{\partial x} , \tag{2.1}$$

where J is the flux of mass (mole/cm^2/sec); D is the diffusion constant; and C the concentration as a function of position within the tube. The total mass transferred in time t is

$$Q = JAt = D \cdot A \cdot \frac{C_0 t}{L} , \tag{2.2}$$

where A is the area of the tube and L is its length.

The gas which is collected for a time t is analyzed by means appropriate to the medium and the average exposure (ppm/hr) can be calculated.

Experimental verification of Equation 2.1 in small diffusion tube samplers indicates that it is correct over a range of about 3 to 1 in $\frac{A}{L}$. The overall accuracy of the collected sample is roughly 90 ± 20%, that is to say, there is a fairly large scatter among various tube sizes. This may be due to unaccounted for effects of tube geometry or it may simply represent a certain variability of the collection and analysis process.

The experimental work has generally been done at constant pressure and temperature. In real life sampling, these variables will not be controlled and it is necessary to assess their effects on the collected samples.

The temperature dependence of the diffusion constant D is T^n, where n is between 1.5 and 2.0 for various theoretical models (T is absolute temperature). For a temperature range of 0°F to 100°F, this gives a range of D from .76 to 1.13 of the value at 68°F (assuming T^2 dependence).

Similarly the pressure dependence of the diffusion constant is P^{-1}. However, ambient air pressure will rarely change ± 5 cm.Hg. from the standard value (76 cm.Hg.), and this amounts to a variation of $\pm 6.6\%$ in D.

It might be expected that air turbulence would seriously affect the amount of material collected. However, wind tunnel studies have demonstrated that wind velocities at 140 and 440 ft/min have essentially no effect at most angles of incidence, with perhaps a small (20%) increase of material captured at 45°-60°.

Thus, the contributions of these three effects--temperature, pressure and turbulence--are generally less than the variations of the collection and analysis process. Of these, temperature has the greatest effect because the person wearing the sampler can easily be exposed to the extremes used in the calculations. If the average temperature is higher than 68°F, then the sampler will overestimate the integrated exposure of the wearer. If the average temperature is less than 68°F, then the sampler will underestimate the exposure. However, if the average temperature is known, a correction can be estimated for the exposure which will reduce the error due to temperature well below the error level of the sampling process.

In general, the diffusion tube sampler will collect 90% of the material entering its port, with a scatter of $\pm 20\%$. By standardizing a particular tube geometry, it is estimated that the statistical errors can be reduced to about $\pm 10\%$ with all effects included.

To be realistic the response of a diffusion tube exposed to concentrations that vary with time should be considered. The equation describing this reponse is, for a one dimensional model,

$$\frac{\partial C}{\partial t} = D \frac{\partial^2 C}{\partial x^2} . \qquad (2.3)$$

It will be assumed that a step change in concentration occurs at the tube inlet, which can be described by the following boundary conditions:

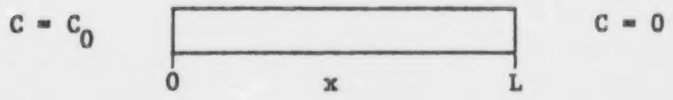

at t = 0: $C(x = 0) = 0 \quad C(L) = 0$
at t = ∞: $C(x = 0) = C_0 \quad C(L) = 0$

The partial differential equation (2.3) is separable and leads to a solution of the form:

$$C(x,t) = C_0\left[\left(1 - \frac{x}{L}\right) - \frac{8}{\pi^2} \sum_{n=1,3,5\ldots} \frac{1}{n^2} \cos\frac{n\pi x}{2L}\, e^{-n^2\left(\frac{\pi}{2L}\right)^2 Dt}\right] . \qquad (2.4)$$

The term in parentheses is the steady state solution of Equation (2.1).

Figure 2.3 shows the concentration as a function of position along the tube for various times after the step change in concentration.

Evaluation of the current $J(x,t)$ can be obtained by differentiating Equation (2.4) term by term. Thus,

$$J(x,t) = \frac{C_0 D}{L}\left[1 - \frac{4}{\pi} \sum_{n=1,3,5\ldots} \frac{1}{n} \sin\frac{n\pi x}{2L}\, e^{-n^2\left(\frac{\pi}{2L}\right)^2 Dt}\right] . \qquad (2.5)$$

Again, the first term corresponds to the steady state solution. Here it is useful to note the behavior of the Fourier components. Because the exponential factor depends on n^2, and because n is restricted to odd values, by the time $\left(\frac{\pi}{2L}\right)^2 Dt = 1$, most of the contribution is from the $n = 1$ term.

An effective time constant, τ, can be defined by the relation

$$J(L,\tau) = .63\, J(L,\infty) \qquad (2.6)$$

which gives

$$\tau = \frac{1.25}{\left(\frac{\pi}{2L}\right)^2 D} . \qquad (2.7)$$

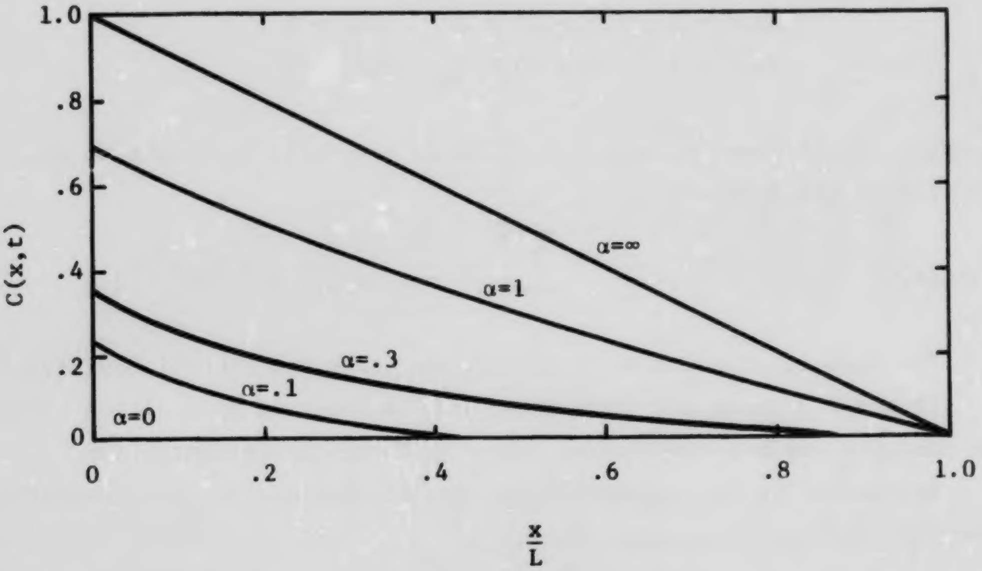

Figure 2.3 Normalized concentration in the diffusion tube as a function of position along the tube for various times after a step change in concentration. $\alpha = (\frac{\pi}{2L})^2 Dt$

The behavior of J for t > τ is essentially exponential in its approach to the limiting value.

Figure 2.4 shows the current, J, as a function of position along the tube for various times.

Since the main interest is in the integrated quantity of material collected, this quantity will be calculated by

$$Q = \int_0^t J \cdot dt$$

$$= \frac{C_0 Dt}{L} \left[1 - \frac{4}{\pi}\frac{1}{\alpha} \sum_{n=1,3,5\ldots} \frac{1}{n^3} \sin \frac{n\pi x}{2L} \left(1 - e^{-n^2\alpha}\right)\right] \qquad (2.8)$$

where $\alpha = (\frac{\pi}{2L})^2 Dt$.

Again, the first term gives the steady state response. The effect of the Fourier components is to delay the effective collection of material. Collection for a time $t \gg \tau$ will give $Q(t) \approx Q_0(t-\tau)$, where Q_0 is the amount of material passing through the open end of the tube.

To visualize the size of the numbers, assume a tube about 6.4 cm long and a diffusion constant of .144 cm^2/sec (NO_2 at 68°F). These parameter values give a τ of 140 seconds.

For all practical purposes steady state is reached in 3τ (95% response) or 420 seconds. If the concentration in ambient were to go to zero at time t_1, then the amount of material collected would be essentially constant at t_1 + 420 seconds.

Figure 2.5 shows the amount of material passing the inlet (x = 0) and the amount of material collected at x = L as a function of time after the step change in concentration. The amount continuously increases with time, and eventually the material is collected at the same rate at x = L as passes through the inlet. Then the amount collected at any time is equal to the amount which had passed through the inlet τ seconds earlier. Another way of describing the result is that an amount of material equal to J·τ is between the inlet and collection area once the steady state is reached.

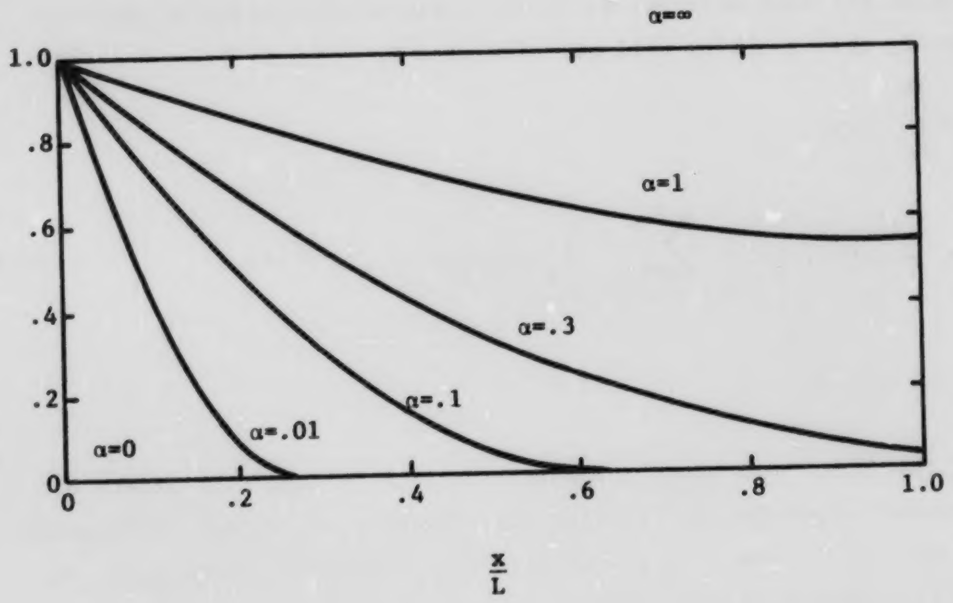

Figure 2.4. Normalized Current in the Diffusion Tube as a Function of Position and Time. $\alpha = (\frac{\pi}{2L})^2$ Dt.

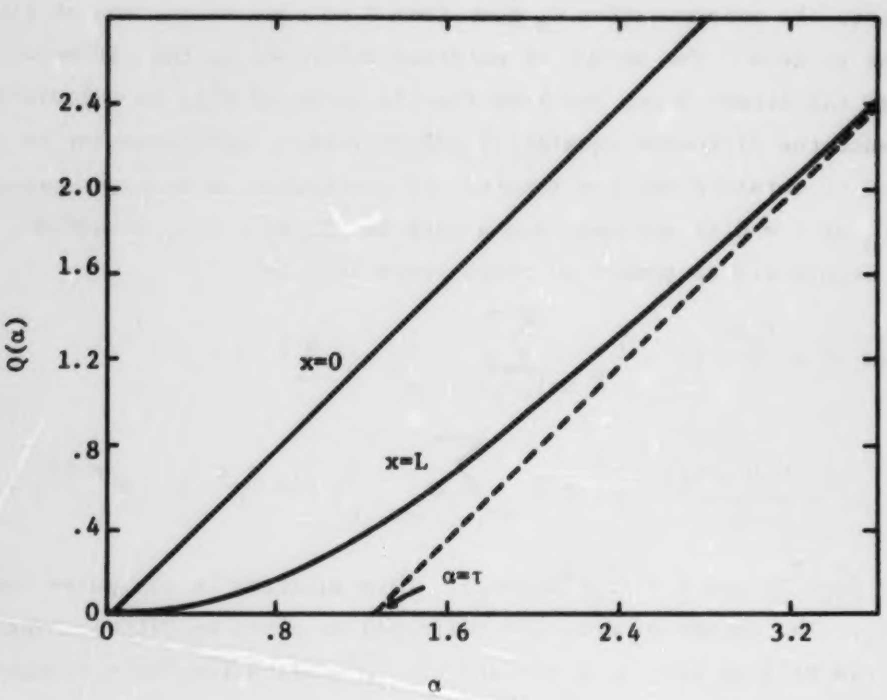

Figure 3. Normalized amount of material passing the inlet of the diffusion tube (x=0) and being collected (x=L) as a function of time. $\alpha = (\frac{\pi}{2L})^2 Dt$. The dashed line is the limiting amount of material being collected; it extrapolates backward to zero at $\alpha \simeq \tau$.

As a final step in the analysis, the effect of wafting will be estimated by analyzing response to a pulsed input of pollutant. Suppose at time zero the concentration C_0 goes from 0 to some value, and at time t_1 returns to zero. The amount of material collected in the diffusion tube after the steady state has been finally obtained will be calculated.

Because the diffusion equation (2.3) is linear, solutions may be superposed to obtain a desired result. In particular, a step to concentration C_0 at $t = 0$ is assumed, and a step to $-C_0$ at $t = t_1$ is added.

The superposed responses to these steps lead to

$$Q(N,t) = \frac{C_0 Dt}{L}\left[1 - \frac{4}{\pi}\frac{1}{\alpha}\sum_{n=1,3,5\ldots}\frac{1}{n^3}\sin\frac{n\pi x}{2L}\left(1 - e^{-n^2\alpha}\right)\right]$$

$$- \frac{C_0 D(t-t_1)}{L}\left[1 - \frac{4}{\pi}\frac{1}{\beta}\sum_{n=1,3,5\ldots}\frac{1}{n^3}\sin\frac{n\pi x}{2L}\left(1 - e^{-n^2\beta}\right)\right] , \qquad (2.9)$$

where $\alpha = (\frac{\pi}{2L})^2 Dt$ and $\beta = (\frac{\pi}{2L})^2 D(t-t_1)$. This equation is the pulse response for $t > t_1$. The amount of material collected is given by $Q(L,\infty)$. The exponentials will be zero at $t = \infty$ and $\sin\frac{n\pi x}{2L}$ will alternate ± 1 depending on n at $x=L$. Therefore,

$$Q(L,\infty) = \frac{C_0 Dt}{L}\left[1 - \frac{4}{\pi}\frac{1}{(\frac{\pi}{2L})^2 Dt}\sum_{n\ \mathrm{odd}}\frac{1}{n^3}\sin\frac{n\pi}{2}\right]$$

$$- \frac{C_0 D}{L}(t-t_1)\left[1 - \frac{4}{\pi}\frac{1}{(\frac{\pi}{2L})^2 D(t-t_1)}\sum_{n\ \mathrm{odd}}\frac{1}{n^3}\sin\frac{n\pi}{2}\right] \qquad (2.10)$$

$$Q(L,\infty) = \frac{C_0 D}{L} t_1 .$$

This result is independent of the length of time t_1 in comparison with τ, provided the sampling continues several time constants beyond the end of the pulse. In fact, if the product $C_0 t_1$ is held constant as the pulse length varies, then the same integrated dosage will be measured. This is important, because any random pulse shape can be approximated with a number of small rectangular pulses. Figure 2.6 shows the amount of material collected after a rectangular pulse as a function of time.

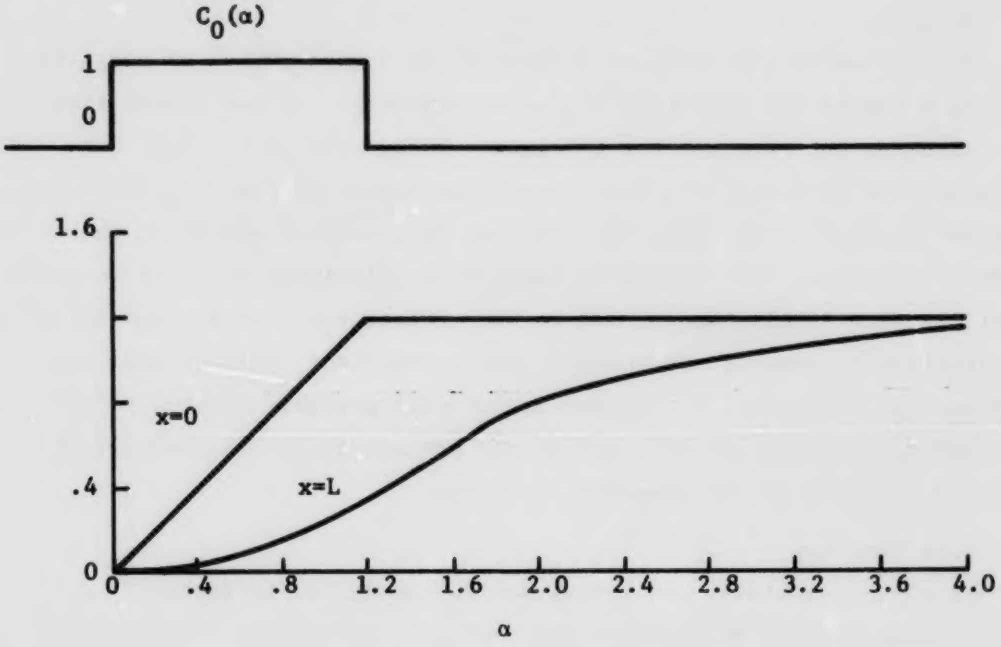

Figure 4. Normalized response of the diffusion tube sampler to a pulse input, with the amount of material passing the inlet (x=0), as a function of time $\alpha = (\frac{\pi}{2L})^2 Dt$.

2.1.3 Summary

The diffusion tube sampler appears to be a good method of passively acquiring a sample for measuring pollutant exposure. It has a slow transient response, but measures the integrated dosage reliably. The characteristic time constant is a function of the length of the tube and the diffusion constant of the gas, but does not enter significantly in the integrated response. The diffusion sampler is relatively insensitive to ambient pressure level changes, and to wind velocities. It is somewhat more sensitive to temperature changes, but corrections could be applied fairly easily. Comparable or larger errors will probably occur due to non-specificity of the absorber and in the preparation of the absorbtion medium for analysis of the absorbed pollutant.

2.2 Active Sampling

Many of the continual monitoring methods discussed in Section 4.0 of this report require acquisition and presentation of either a pulsed or steady air stream to the sensor. This has the advantages of metering a fairly precisely known quantity of air during the measurement and of responding to changes in the ambient concentration due to the continual supply of fresh sample to the sensor. These advantages are countered by the increased cost, complexity and, usually, the necessity for a portable electrical power source.

Because of the increasingly stringent requirements for occupational and environmental monitoring, many miniaturized air pumps have been developed which are capable of operating from a battery supply for periods of typically 8 to 10 hours, at air sample flow rates of anywhere from 20 mℓ/min to several liters per minute. A representative list of such commercially available pumps is given in Table 2.1.

Design of the sample air flow system should minimize obstructions to flow in order to keep the pressure drop, ΔP, within that rated for the pump. Otherwise the flow rate will be decreased below the design level. For some measurement methods--e.g., those in which the sample air stream is flowed over a sensor and not appreciably depleted by sorption in the process--this will not be critical. However, for methods

Table 2.1. Characteristics of Commercially Available Sampling Pumps

Mfr.-Model	Volts	Amp Hours	Duration in use(hr)	ΔP in H_2O	Rated Flow mℓ/min	Wt(g)	Size(mm)	Remarks
Micronair (Unico)	3.75	1.0	8-10	4.0	2000	510	156x83x64	Adjustable 1.5-2.5 ℓ/min
Micronair (Telmatic)	8.4	0.5	5	12.0	2800	1000	185x120x100	Adjustable 1-5 ℓ/min
Casella Mk II	6.4	0.9	8-10	17.7	2000	600	127x79x57	Adjustable to 3000 mℓ/min
Misco	---	0.5	6-10	1.4 25.0	2800 2000	570	110x90x30	
SKC	3.0	---	8	---	200	1000	165x89x45	Adjustable 40-200 mℓ/min
Unico C115	6.0	2.0	14 8	4.0 12.0	2000 2800	1360	165x140x63	Adjustable to 3.5 ℓ/min
Sipin SP-1	---	---	8	2.5	200	1670	130x64x38	Adjustable 50-200 mℓ/min
Monitair	6.0	---	4 8	12.0 ---	2800 2000	540 740	107x102x51	Revised model
Spectrex AS-100,120	6.0	.32A		4.0	1400	170	51x51x51	Pump only

in which essentially all of the pollutant is removed by sorption as the sample air is moved through the instrument, change in sample flow rate can cause a proportionate error in measurement.

SECTION 3

3.0 SORPTION METHODS

Most methods of pollutant measurement rely on extraction of the gas phase pollutant from ambient air by contract with either an absorbing solid or liquid phase or an absorbing liquid phase. The physical and chemical nature of these methods is such that the adsorption methods can be predominantly or partially reversible in nature, but the absorption method is predominantly irreversible under normal conditions of temperature and pressure.

3.1 Sorption Mechanisms

It is well known that surfaces of high specific surface (area/unit mass) are capable of adsorbing gas and vapor phase molecules. The extent of adsorption (and degree of reversibility) depends upon the chemical nature of the solid and the physical nature of the solid. The chemical nature of the solid surface is dependent on the nature of the unsatisfied chemical bonds of the surface atoms and may also be dependent upon the general electronic properties of the bulk material. This is exemplified by many semiconductor materials and transition metals used for heterogeneous catalysis. The physical nature of the solid surface, particularly its surface area and porosity, also have a large effect.

3.1.1 Reversible Sorption

When adsorption occurs predominantly due to Van der Waals' force of attraction between the adsorbate gas molecules and the adsorbent substrate, the resulting adsorption is termed "physical" adsorption.[4] It is to a large extent reversible. Because all molecules can exhibit the fluctuating induced dipole moments that lead to Van der Waals attraction, this type of adsorption is not specific. However, because some molecules exhibit permanent dipole moments, they are more susceptible to physical adsorption on most substrates; and if the gas phase concentration is high enough and the temperature low enough, condensation may occur. A notorious example is water vapor which is a strong competitor for adsorption sites on many surfaces.

The Langmuir and BET isotherms, which describe the quantity of gas adsorbed on a given material at constant temperature as a function of the partial pressure of the gas,[5] are usually derived theoretically and determined experimentally for only one type of gas present over the sorbent substrate. A far more complicated situation arises when several gas and vapor species are present simultaneously. Although it is conceptually possible to set up a mathematical model describing such a situation, as has been done to derive the Langmuir isotherm for the case when two gases are being absorbed,[6] the number of unknown parameter values in such a theoretical model makes the application to a real situation impractical, if not impossible. At present, one must rely on an empirical approach when applying most sorbents in a measurement scheme, particularly when trying to assess interference effects and the effect of temperature on the amount of a particular gas adsorbed relative to its partial pressure in the gas mixture in contact with the sorbent.

Another method of obtaining reversible sorption is to coat a solid phase with a suitable liquid which can take the vapor or gas species into solution at some temperature, T_1, and release it back into the vapor phase at some higher temperature, T_2, or back into the vapor phase when the vapor phase concentration has been reduced to a lower value or zero. The operative principles are diffusive transport from the "bulk" gas phase across a stagnant boundary layer followed by adsorption at the surface of the liquid phase and then, usually, absorption into the bulk liquid.[7] The equilibrium relation between the partial pressure, P_i, of the species in the gas phase being sorbed and the concentration of this species in solution, C_i, is given by Henry's law

$$P_i = HC_i \ . \tag{3.1}$$

For small values of P_i, H is independent of C_i, but is a function of temperature.

Equation (3.1) is an equilibrium relation, and time is required for diffusive processes in the gas and liquid phase to establish this relation. Typically, gas phase diffusion constants are in the range of 0.1 to 1 cm^2/sec at 300°K and vary as the 1.5 power of temperature and inversely with total gas pressure.[8] The boundary layer is not large, being on the order of 0.1 cm. In contrast, the diffusion constant in liquids is typically 10^{-4} to $10^{-5} cm^2/sec$. Even if a high surface/volume ratio is obtained for an absorbing liquid there will still be an appreciable time lag between the establishment of a given partial pressure, P_1, over the liquid and the attainment of the corresponding equilibrium concentration given by (3.1).

The situation can be greatly improved by introducing convective transport through turbulence in both the gas and liquid phases.[9] The resulting eddy-diffusion enables a much higher mass transfer rate. For a discussion of the theory and practice of eddy-diffusive transport the reader is referred to Reference 9.

3.1.2 Irreversible Sorption

It is possible for gas and vapor phase species to be irreversibly (or quasi-irreversibly) taken up by both solids and liquids. Such irreversible sorption can be due to a combination of both physical and chemical factors. On micro-porous solids, capillary condensation can lead to a marked hysteresis of the isotherm. An example, taken from Reference 4, is shown in Figure 3.1. Here, water vapor adsorbed on titania gel exhibits a complicated isotherm which is dependent upon the history of exposure. Even if condensation does not occur it is possible that very fine pores or intergranular seams can reduce the diffusion coefficient of gas species. The relationship between diffusion coefficient and pore size is shown schematically in Figure 3.2, taken from Reference 4. Although not strictly irreversible, such physical mechanisms can lead to quasi-irreversible behavior that severely limits the dynamic response of measurement methods which depend on such sorbents.

Another method through which sorption can be made irreversible is through chemical reactions of the sorbed species with the sorbent to chemically bind the sorbed material. Although the chemical reactions through which this occurs may be strictly reversible, in practice the reaction rates for the inverse reaction are negligible with respect to the forward reaction rates. This can occur both in the chemisorption of gas species on solid surfaces and in the chemical conversion of gas species in solutions.

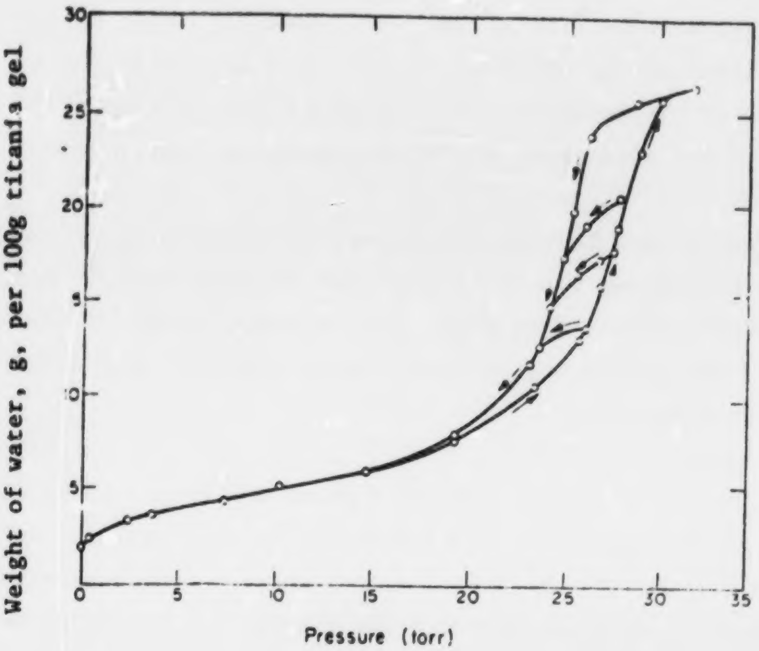

Figure 3.1 Adsorption Hysteresis for Water Vapor in Titania Gel.

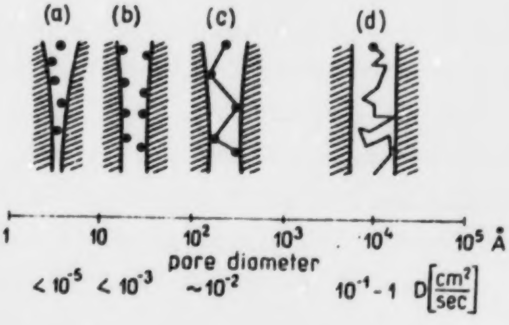
(a)
(b)
(c)
(d)
1
10
10^2
10^3
10^4
10^5 Å
pore diameter
$< 10^{-5}$
$< 10^{-3}$
$\sim 10^{-2}$
$10^{-1} - 1$
$D\left[\frac{cm^2}{sec}\right]$

Figure 3.2. Relation between Pore Size and Diffusion Coefficient. (a) Solid diffusion; (b) surface or Volmer diffusion; (c) Knudsen diffusion; (d) free or molecular diffusion.

3.2 Sorbents for Sulfur Dioxide

Sulfur dioxide, as indicated in Figure 3.3, may be regarded as a tetrafunctional reagent; that is, it may undergo four modes of reaction.

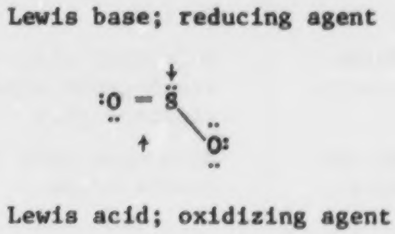

Figure 3.3. Sulfur Dioxide Reaction Mechanisms.

In the Lewis acid-base system, an acid-base reaction consists of the donation of a pair of electrons from the base to the acid. In the sulfur dioxide molecule, the double bond between the sulfur and oxygen atoms enables this molecule to accept a pair of electrons and, therefore, act as a Lewis acid. Furthermore, the ability to accept an electron pair enables sulfur dioxide to undergo an oxidation-reduction reaction by accepting a pair of electrons from a reducing agent. Likewise, the unshared pair of electrons on the sulfur atoms enables sulfur dioxide to function as a Lewis base by donating an electron pair or to act as a reducing agent in an oxidation-reduction reaction.

The chemisorption of sulfur dioxide is determined by these possible reaction mechanisms. Table 3.1 summarizes the types of species that would be expected to exhibit Lewis acidity or basicity. Some examples of Lewis bases, which will be utilized further in the discussion, are organic amines, $R-NH_2$ (R = organic group), and amine-modified silica gels,

$$\sigma - CH_2CH_2CH_2NH_2$$

where σ represents a silicon atom at the surface of silica gel. Another common Lewis base used as a sorbent is the tetrachloromercurate anion.

Table 3.1. Species with Lewis-Acid-Base Character

Lewis Acids	Lewis Bases
Anion	Cations
Molecules with double bonds (except carbon-carbon double bonds)	Molecules containing fifth- or sixth-group atoms with an unshared electron pair
Halides in which the central atom may exceed its ocetet	Molecules with carbon-carbon double bonds

Considering more specific examples of species, a representative list of materials used as chemical and physical absorbents of sulfur dioxide is presented in Table 3.2.

Table 3.2. Typical Chemical and Physical Sulfur Dioxide Adsorbents

Chemisorbents
Vanadium Oxide[11] (V_2O_5)
Gold[13]
Gold-Nickel Alloy[13]
Pyridine Benzene Copolymers[14]
Lead Oxide (PbO_2)
Hydrogen Peroxide[15]
Tetrachloromercurate ($HgCl_4^{=}$) Solutions[15]
Organic Amines[16]
Physical Adsorbents
Molecular Sieves (Silica Gel)
Activated Carbon[10]
Zeolite[10] ($Al_2O_3 \cdot nSiO_2 \cdot xH_2O$ or $Na_2O \cdot Al_2O_3 \cdot nSiO_2 \cdot xH_2O$)
Dawsonite[10]
Polystyrene Foam Fibers Containing Activated Carbon[12]
Nylon Foam Fibers Containing Activated Carbon[12]

Of these materials the most promising appears to be the amines because they can be selected "as is" or modified to control the specificity and reversability of the adsorbate-adsorbent reaction.

Amine modification for selectivity or specificity can be demonstrated by considering several examples. Silica gel, chemically modified by conversion into

$$\sigma - CH_2CH_2CH_2NH_2$$

where σ represents a silicon atom at the surface of the silica gel, selectivity adsorbs SO_2 and CO_2 in a Lewis acid-base reaction at 25°.[17] The carbon dioxide is liberated by temperature programmed desorption at about 100°, but the sulfur dioxide is not released. If this gel is converted to $\sigma\text{-}CH_2CH_2CH_2NH_3^+Br^-$, a selective and reversible adsorbent for sulfur dioxide results. This hydrobromide gel adsorbs sulfur dioxide at 25° and releases it by temperature programmed desorption peaking around 92°. Moreover, carbon dioxide is not adsorbed by the amine hydrobromide gel nor is nitrogen, oxygen, carbon monoxide, ethylene, ethane, nitric oxide or nitrogen dioxide.

The amine hydroiodide gel $\sigma\text{-}CH_2CH_2CH_2NH_3^+I^-$ adsorbs sulfur dioxide less strongly, but the adsorption can be increased by methylating the hydroiodide gel to give $\sigma\text{-}CH_2CH_2NH_2CH_3^+I^-$. The addition of alkyl groups, for example, the methyl group, increases the electron donor capacity of the amine group by a positive inductive effect or releasing electrons to the nitrogen. Hence, this alkylation should strengthen the Lewis acid-base reaction and, as shown, increase the adsorption of sulfur dioxide relative to the unalkylated amine hydroiodide gel.

The amine hydroiodide gel binds sulfur dioxide with a strength intermediate between that of the hydrobromide and the hydroiodide gels while the amine hydrofluoride gel does not absorb sulfur dioxide under the same conditions.

The amine modified silica gels exemplify the specificity, reversibility and modification potential of amines for pollutant dosimeters.

In addition to silica gel amines, various organic amines have been investigated for SO_2 sorption. The adsorption capacity for sulfur dioxide of the following amine copolymers decreased in the order of 4-vinylpyridine divinylbenzene, 2-methyl-5-vinylpyridine divinylbenzene, 2-vinylpyridine divinylbenzene and 5-ethyl-2-vinylpyridine divinylbenzene.[14] The copolymer with the vinyl group in the number 4 position would be expected to be the strongest Lewis base and, as seen, should adsorb more sulfur dioxide in a Lewis acid-base reaction than the similar copolymers.

A comparison of the relative adsorption of several different amines and several non-amine adsorbents for SO_2 is given in Table 3.3. The relative response is given in terms of resonant frequency change ΔF of a quartz piezoelectric crystal when coated with each of the materials and allowed to adsorb SO_2 under the same conditions. This measurement technique is described in detail in Section 4.5 of this report. Two different cell volumes were used, Cell 1 of 2 cm^3 internal volume and Cell 2 of 0.1 cm^3 volume. For Cell 1, all the coatings except for the two asterisked ones, are amines. The first non-amine is an ethylene oxide homopolymer terminated at one end with an alkylphenol and at the other end with ethanol. Cellobiose units, shown in Figure 3.4, constitute the matrix of the other non-amine.

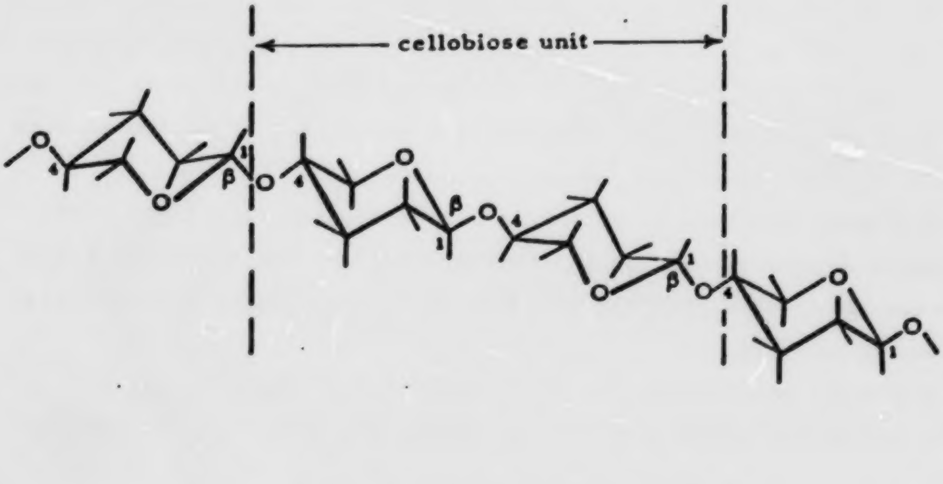

Figure 3.4 Cellulose Nitrate Matrix.

Table 3.3. Relative Response of Amines and Non-Amines[16]

Cell 1 (2 cm^3 volume)	ΔF
Tridodecylamine	160.
Diallylamine	70.
*Alkylphenoxy Poly (ethylene oxy)- Ethanol (Igepal CO-880-Appl. Sci. Lab.)	69.
*Cellulose Nitrate	35.
Diallyl Melamine	24.
Melamine	4.
Cell 2 (0.1 cm^3 volume)	
Tripropylamine	225.
Styrene-Dimethylaminopropyl Maleimide (SDM-Uniroyal)	195.
Polyvinyl Pyridine (PP-2040-Ionic Chem. Co.)	190.
Phenyldiethanolamine	150.
Quaternary Aliphatic Polyamine (PE-100-Ionac Chem. Co.)	68.
*Polyamide (Versamid 900)	50.
*Vinyl methyl Silicone (UC-W98-Appl. Sci. Lab.)	45.
*2,2-(m-tolylimino)diethanol	3.

For Cell 2 the best adsorbing amines, as with Cell 1, are alkylated; the first one, by three propyl groups and the second one by two methyl groups. As expected, of the amines listed, these should be the strongest Lewis bases and, hence, adsorb more sulfur dioxide.

From this, organic amines appear as promising candidates for a sulfur dioxide adsorbent which exhibit (1) a large sulfur dioxide adsorption coefficient, (2) specificity, (3) reversibility and (4) ease of modification to enhance adsorption capacity, specificity and reversibility.

An irreversible SO$_2$ uptake is provided by conversion of SO$_2$ to a sulfate. Such a method is used in the well known "lead candle" method for SO$_2$ measurement[18-20] to obtain a solid phase sulfate. As far as can be determined, no analysis has been made of the detailed mechanism for the transport of SO_2 from the gas phase to an adsorbed species which is subsequently converted to sulfate; and therefore, a theretical relationship between gas phase SO_2 concentration and solid phase sulfate weight as a function of exposure history has not been worked out.

This method is sensitive to SO_2 concentrations up to 700 ppm, but in general is not a quantitative method. The basic reaction depends upon a number of factors which influence its completeness: wind velocity, thickness of the lead dioxide, its wetness, the particle size, and purity. Candles made from the same batch of lead dioxide by the same technique should give reliable relative exposures.

Aside from the positive interferences mentioned, methyl mercaptan reduces the sulfation rate of reaction, although quantitative data is not available.

Because of the importance of liquid absorbents in several accepted methods of SO_2 measurement from ambient air samples, many studies of asborption efficiency have been made. Boström[21] used an isotopic tracer method to determine the collection efficiency of TCM and hydrogen peroxide solutions. Both were found to have about 99% efficiency at flow rates of 1.2 ℓ/min in the range from 0.9 pphm to about 10 pphm when the sample air was bubbled through a solution column of at least 3 cm. A similar study of hydrogen peroxide solution, carried out in essentially the same manner[22] also found about 99% collection efficiency.

3.3 Sorbents for Nitrogen Dioxide

The nitrogen dioxide molecule contains an unpaired electron and, therefore, is paramagnetic. Moreover, this unpaired electron accounts for the strongly electrophilic, oxidizing, and Lewis acid properties of this molecule. Nitrogen dioxide is an electron or free radical scavenger with an electron affinity of 3.99 eV[23] and can be expected to react with electron rich species such as Lewis bases or basic species. The nitrogen dioxide molecule has a dipole moment of 0.58 Debye.[24]

Likely candidate sorbents, then, would be materials containing electron rich species such as the phenolate oxygen atom in p-cresol, or polar species, such as a molecular sieve.

A study of various absorption liquids for collecting NO_2 has been reported by Nash.[25] He operated on the hypothesis that since NO_2 is such a good electron acceptor, electron-donor charge transfer type solutions should provide fast response time and high absorption capacity. He tested the following groups of sorbents:

a) inorganic salts with reducing or polarizable ions

b) alkaline solutions of phenols and ß-diketones

c) aromatic amines

d) some "control" compounds, e.g. alkali, sulfamic acid and unionized phenols.

Table 3.4 contains the results of this work and, in addition, pK and E° values. The terminology C(50) and C(90) represents the concentrations, in millimoles, at which 50% and 90% more NO_2 was collected than a control of either plain water or water with alkali added to match the pH of the test absorber. The terminology pK represents the negative logarithm of the equilibrium dissociation constant of an acid or base in aqueous solution. E° is the standard oxidation potential in volts, V. The gas sampling flow rates, 1 ℓ/min, and concentration of NO_2, 3 ppm in air, were the same for test solution and control solution. By comparison, water with 0.1 N alkali was 14% efficient. A solution of alkaline guaiacol (O-methoxy phenol (0.05%) in 0.1 N alkali) was 97% efficient.

Examination of the four classes of liquid sorbents listed in Table 3.4 reveals that the nitrogen dioxide sorption efficiency of the phenols is superior to the other classes represented.

For the first class of sorbents listed in Table 3.4, the phenols, a study of the relationship between the sorption of nitrogen dioxide and the basicity of the phenols is instructive. The pK values listed for the phenols in Table 3.4 are the negative logarithms of the acid dissociation constants. As seen in the table, p-cresol is more basic than phenol. Thymol could be expected to dissociate less than p-cresol because the isopropyl group ortho to the hydroxyl should sterically hinder the dissociation of the hydroxyl proton. Similarly, o-methoxy phenol would be expected to dissociate less than phenol because a hydrogen bond can form between the hydroxyl proton and the methoxy oxygen. The electrostatic interaction or

Table 3.4 Liquid Sorbents for Nitrogen Dioxide

Concentrations (mM) Required to Collect 50% More and 90% More NO_2 Than Control Solution[25]			pK Values[24]	E°, V[24]
	alkali	(pH = 13)		
	C(50)	C(90)		
Phenols				
Phenol	5	100	9.89	
p-Cresol	0.7	8	10.17	
Thymol	0.1	1		
o-methoxy phenol	0.07	0.7		
β-Diketones				
Barbituric Acid	30	---	4.01	
Acetylacetone	4	40	9[4]	
	Neutral	Solutions		
	C(50)	C(90)		
Amines				
Aniline	45		9.42	
p-Anisidine	3		9.71	
Inorganic Salts				
Azide	1800	---		
Thiosulfate	1250	---		-0.09
Sulfanilate	1000	---		
Iodide	125			-0.535
Sulfite	13			-0.6
Ferrocyanide	13			-0.56[5]

---Blanks indicate 90% collection not obtained for saturated solution.

hydrogen bonding in guaiacol should be stronger than the steric hinderance in thymol. Consequently, guaiacol should be more basic than thymol. It appears that for the phenols, the basicity increases in going from the top to bottom of the list in Table 3.4. Furthermore, as seen in this table the sorption of the phenols increases as their basicities increase. Therefore, it is recommended that if a researcher is investigating alkaline solutions of various phenols for nitrogen dioxide sorption, he study phenol derivatives with more basic properties than phenol.

The next sorbents listed are the β-diketones. It is seen from the pK values of these two acids that the acetylacetone is more basic than barbituric acid. Again, the nitrogen dioxide sorption of these β-diketones increases as their basicity increases. Therefore, it is recommended that if one is searching for alkaline solutions of β-diketones for nitrogen dioxide sorption, he investigate β-diketones which are more basic than acetylacetone.

The next class of sorbents listed in Table 3.4 are the amines. The dissociation of amines in aqueous medium is illustrated in the following equation,

$$\phi\text{-NH}_2 + H_2O \quad \phi\text{-NH}_3^{+} + OH^{-} .$$

As shown by this equation, the more basic or electron rich amine specie would be the undissociated amine, $\phi\text{-NH}_2$. Consequently, of two amines, the amine with the larger pK value would represent the lesser dissociated molecule or the more electron rich specie. Using this criterion as the measure of the availability of electrons, p-anisidine is more basic than aniline and would be expected to sorb more nitrogen dioxide as seen in Table 3.4. Again, using the principle that the correlation between the pK values and the sorption of nitrogen dioxide suggests that the same factors should govern both properties, it is recommended that if solutions of amines are investigated for sorption properties, the amines with the higher pK values of dissociation of the base should be chosen.

The next group of sorbents listed in the table are the inorganic salts. Comparison of the sorption concentrations of these salts with the standard oxidation potentials shows that a relationship exists between these two properties. As the oxidation potential of the salts decrease, their sorption capabilities increase. By this correlation, it is suggested that the same factors should govern both properties and that if neutral solutions of salts are investigated as sorbents, the anions with the lower oxidation potential should be chosen.

Sorption of nitrogen dioxide on solids will now be considered. In particular, sorption by molecular sieves will be discussed.

Molecular sieves, a group of adsorptive desiccants developed by Linde, are crystalline aluminosilicate materials, chemically similar to many clays and feldspars and belonging to a class of minerals known as zeolites. The outstanding characteristic of these zeolite materials is their ability to undergo dehydration with little or no change in crystal structure. The dehydrated crystals are interlaced with regularly spaced channels of molecular dimensions. This network of uniform pores comprises almost 50 percent of the total volume of crystals.

The general chemical formula for Type 4A is $0.96 \pm 0.04\ Na_2O \cdot 1.00\ Al_2O_3 \cdot 1.92 \pm 0.09\ SiO_2 \cdot xH_2O$. Type 5A is produced from Type 4A through ion exchange of about 75% of the sodium ions by calcium ions. The general chemical formula for faujasite Type 13X is $0.83 \pm 0.05\ Na_2O \cdot 1.00\ Al_2O_3 \cdot 2.48 \pm 0.03\ SiO_2 \cdot xH_2O$. Molecular sieves have a pH of approximately 10 and are stable in the 5 to 12 pH range.

An important distinction between the faujasite type zeolites and the type 5A is the interiors of the small pore system. In faujasite type zeolite, the interiors of the small pore system coincide with the interiors of the sodalite units or cages, while in the type 5A zeolite pores contain calcium as well as sodium cations.

Molecular Sieves Type 4A, 5A, and 13X absorb only those molecules that are small enough to enter their pore system. Type 4A has a port opening that will permit only molecules smaller than about 4 Angstroms to enter the cavities and be absorbed. Type 5A has a slightly larger pore opening which will admit molecules up to about 5 Angstroms in diameter. Type 13X has a still larger pore opening which will admit molecules up to 10 Angstroms in diameter.

Ma and Mancel[26] have performed diffusion studies of nitrogen dioxide on molecular sieve zeolites by gas chromatography. In this study, they measured the effective diffusion coefficient of nitrogen dioxide in type 5A and faujasite sieves. They reported that the effective diffusion coefficient is approximately the same in both sieve materials. For a given gas, the pore size of the sieve is normally regarded as an important factor which affects the diffusional resistance. Since the pore diameter in the faujasite sieve is twice as large as the type 5A, the fact that the effective diffusion coefficients were approximately the same can be interpreted as a larger diffusional resistance for the faujasite zeolite. Recalling that the faujasite pores contained only sodium cations, while the type 5A contained sodium and calcium, it is postulated that the increased diffusional resistance is due to a specific interaction between nitrogen dioxide and sodium cations in the interiors of the pores. Therefore, it is recommended that if molecular sieves are investigated as sorbents for nitrogen dioxide, molecular sieves containing pores lined with sodium cations should be studied.

3.4 Sorbents for Ozone

Ozone is a strong oxidant. This fact complicates its specific sorption because ozone decomposition is catalyzed by surface contact. An idea of the extent of the non-specificity of this material can be realized by studying the investigations of Altshuller.[27] He reported that of the various materials studied he found that only glass or teflon did not catalyze ozone decomposition.

The oxidizing ability of ozone has been utilized as the basis of selecting sorbents for its collection. Unfortunately, by the nature of its sorption mechanism, ozone sorption for the most part is irreversible. Let us evaluate and compare several different ozone sorbents.

The classic sorbent is a neutral or alkaline solution of potassium iodide. The reaction of alkaline potassium iodide with ozone is $2KI + O_3 + H_2O \rightarrow I_2 + O_2 + 2KOH$. This sorbent is sensitive to peroxides as well as nitrogen dioxide and sulfur dioxide.

Another ozone sorbent is reduced phenolphthalein.[28] This sorption is based on the oxidation of reduced phenolphthalein to phenolphthalein. The limitation of this sorbent is its sensitivity to any oxidant.

The redox indicator diphenylaminesulfonate is a sorbent superior to iodometric sorbents in two respects.[29] The diphenylaminesulfonate yields a turquoise color with ozone, a violet color with gaseous chlorine and peroxides and a yellowish-green color with nitrogen dioxide. In addition to the different colors produced by interfering gases, the redox potential is better adjusted to ozone, i.e., 0.85 V instead of 0.59 V for the I_2 - KI reaction.

Fluorescein is an ozone sorbent which is oxidized to fluorescein.[30] Fluorescein is reported to exhibit excellent sensitivity.[30] The substance 4,4'-dimethoxystilbene sorbs ozone by cleavage of the double bond to form anisaldehyde.[31]

The collection efficiencies of the various sorbents have been reported. Table 3.5 summarizes these efficiencies determined at the recommended sampling rates.

Table 3.5. Apparent Sorption Efficiencies

Sorbent	Recommended Sampling Rate (liters/min)	% Sorption Efficiency at 3.0 ppm
Potassium Iodide	1.0	97.2
Phenolphthalein	0.9	92.0
Sodium Diphenylamine Sulfonate	2.83	91.7
4,4'-Dimethoxystilbene	0.1	97.7

Examination of Table 3.5 reveals that the sorption efficiency is greatest for 4,4'-dimethyloxystilbene.

The sensitivities of these sorbents can be evaluated by comparing their molar absorptivity values reported in Table 3.6.[32]

Table 3.6. Molar Absorptivities

Sorbent	Molar Absorptivity (absorbance $cm^2 mole^{-1}$)
Potassium Iodide	24,200
Phenolphthalein	26,900
Sodium Diphenylamine Sulfonate	2,500
4,4'-Dimethyoxystilbene	15,300

A simple, convenient, and useful sorbent is rubber.[33] Standardized strips of rubber are folded in the middle, and the ends are secured together to produce a reproducible tension. The ozone exposure time of these strips in minutes, times the ozone concentration in parts per minute, gives a constant that has excellent reproducibility under standard conditions.

The sorbents discussed so far sorb ozone irreversibly. Silica gels and orthosilic acid polymers have been investigated for reversible ozone adsorption. It has been shown that adsorption of ozone on silica gel from -117° to 20° with specific surface 360 $m^2 g^{-1}$ is of the type shown by low adsorption heat and complete reversibility.[34] No decomposition of ozone on the gel was observed by a spectrophotometer.[34]

The absorption mechanism of ozone adsorbed on silica gel has been investigated by infrared spectroscopy. It was found that the ozone is rendered comparatively unreactive as a result of strong hydrogen bond formation with the surface hydroxyl groups.[35]

Investigations revealed a temperature dependent correlation between ozone adsorption and silica gel structure.[36] In an independent study, Reimshuessel attained the same results.[37] He evaluated the adsorption of ozone at -80° on silica gel, that had been annealed at various temperatures, as a function of the thermal history of the gel by the application of the B.E.T. equation. At annealing temperatures of 105° to 108°, maximum values for the monolayer concentrations of ozone were observed for silica gel that had been annealed at 150°, indicating that the monolayer concentration is affected by the type as well as by the extent of surface hydration. Two surface silanol groups are involved in the adsorption of one molecule of ozone and a hydrogen bonding adsorbate-absorbent reaction is assumed. Annealing at less than or equal to 105° results in a reduction of ozone adsorption and in about a two-fold increase of monolayer concentration compared to the value obtained after annealing at 150°, suggesting that ozone is adsorbed only onto a water monolayer at these temperatures.

SECTION 4

4.0 METHODS FOR CONTINUAL MONITORING

This section surveys principles which have been applied for the measurement of SO_2, NO_2 and O_3 in ambient air. For each method, the prior use is reviewed to put into perspective the performance. Then the measurement principles are mathematically modeled to enable the calculation of projected performance from a miniaturized version. Logistical factors bearing on portable operation are surveyed and the type of dose rate information available is noted.

In order to place the utility of these methods in perspective, consideration must be given to the size and weight of a convenient instrument package. A "briefcase size" of about 12.7 cm x 30.5 cm x 45.7 cm (5 in x 12 in x 18 in) will have about 16,500 cm^3 of volume available. A weight of about 7.0 Kg (15.4 lbs) could be carried. These limits can be compared to the volume and weight requirements of the methods reviewed in this section.

Each of the methods requires active sampling. From the data of Table 2.1 a typical pump with its associated battery would be about 750 cm^3 volume with a weight of about 0.75 Kg. This would operate for up to 10 hours without recharge.

Many of the methods require liquid reagent, typically at a flow rate of about 1 ml/min, per pollutant channel. For 24 hour operation per channel, about 1500 cm^3 of solution storage will be required. An equal amount of storage is required for waste reagent, increasing the required volume to 3,000 cm^3 per channel. Some of the aqueous reagent will be lost due to evaporation upon mixing with the sample air stream. As an example, if sample air at 20% relative humidity and 25°C temperature flowing at 100 cm^3/min is contacted with aqueous reagent flowing at 1 cm^3/min, the water loss from the reagent is 4%. However, such loss will be dependent upon temperature and humidity of the sampled air. Practically speaking, the spent reagent volume storage must equal the supply volume.

Another major volume and weight contribution will be required for the electronic signal processing and data storage components and their associated battery supplies. These requirements will depend upon the design used. The size and power requirements for data storage systems are discussed in Section 5.0. The largest volume is taken up by a cassette-type digital tape recorder with its associated circuitry, about 3200 cm^3. The weight is about 1.36 Kg. Among the electronic components used in the methods discussed in this section, the largest volume would be occupied by a photomultiplier tube, about 200 cm^3 including a magnetic shield and its associated inverter-type high power supply, which would occupy about 250 cm^3. Power for the signal processing and data collection electronics will require at least two 12.2 volt Ni-Cd rechargeable batteries of 205 cm^3 volume, 570 g weight each.

All of the required support items must be added to the volume required for the basic measuring device itself in order to see whether or not the "briefcase size" ideal can be met.

4.1 Conductometric Analyzer

This measurement principle utilizes the increase in electrical conductance of an electrolyte solvent caused by the absorption of ionizable chemical species to develop a signal proportional to the liquid phase concentration of the ionized species. At low concentrations this concentration can be made to be proportional to the gas phase concentration of the ionizable species contacted with the absorbing electrolyte.

4.1.1 Prior Use

Conductance cells were among the first widely applied instruments for measuring SO_2 in ambient air. The instrumental construction is relatively simple, but numerous practical problems limit the credibility of the measurements obtained and the reliability of instruments used in the field. The most important problem areas are:

1. Susceptibility to interference by other gas or vapor species which can be absorbed and ionized in the electrolyte.
2. Temperature dependence of conductivity and gas absorption rate.
3. Establishment of good contact of ambient air sample with absorbing electrolyte.
4. Necessity for a continuous supply (and disposal means) of electrolyte of uniform (invariant with time) characteristics.

Similar remarks apply to the application of the conductance method to NO_2 measurement.

Ozone does not ionize in aqueous solution. However, its ability to oxidize halogens to produce ionic species in aqueous electrolytes can be used to produce conductivity changes proportional to ozone concentrations.

4.1.2 Model Detector

The model used is shown in Figure 4.1. A coaxial conductance cell defined by an inner electrode of radius r_1 and an outer electrode of radius r_2, both of length L, is filled with an electrolyte solution which flows through the annulus between the electrodes. A voltage source, E, is connected in series with a current measuring amplifier which provides an output voltage signal, e_o, proportional to current i through the cell. If care is taken to avoid polarization effects at the solution-electrode interfaces, the current is related to the supply voltage by

$$i = GE \qquad (4.1)$$

where G is the conductance of the electrolyte in the annular cylinder. The conductance is determined by the geometry of the cell and the conductivity, g, of the electrolyte as

$$G = g \; 2\pi L/\ln(r_2/r_1) \; . \qquad (4.2)$$

The geometric factors are constant for a given design.

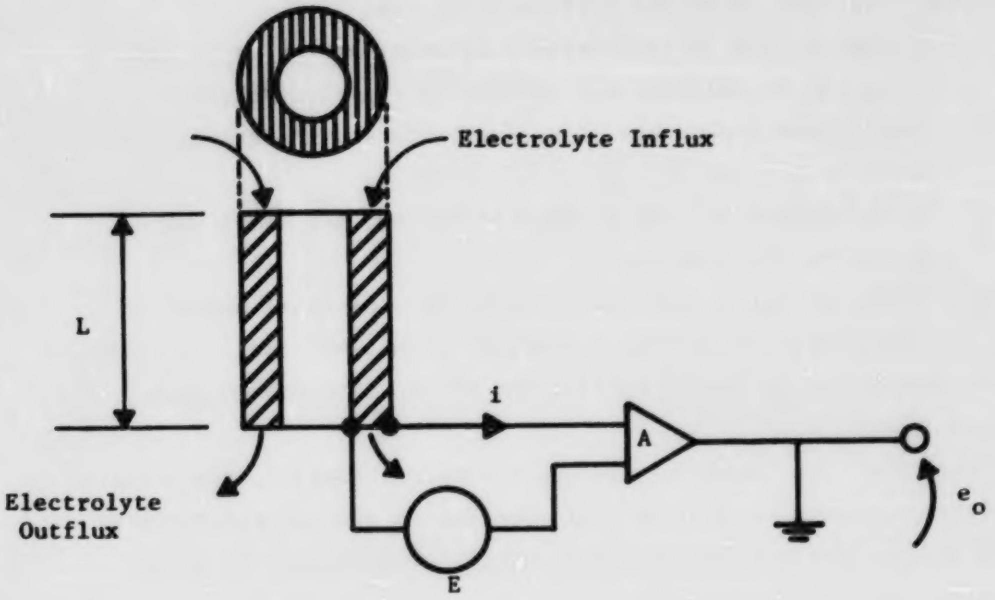
Electrolyte Influx
L
i
A
Electrolyte Outflux
E
e_o

Figure 4.1. Basic Conductance Cell Arrangement.

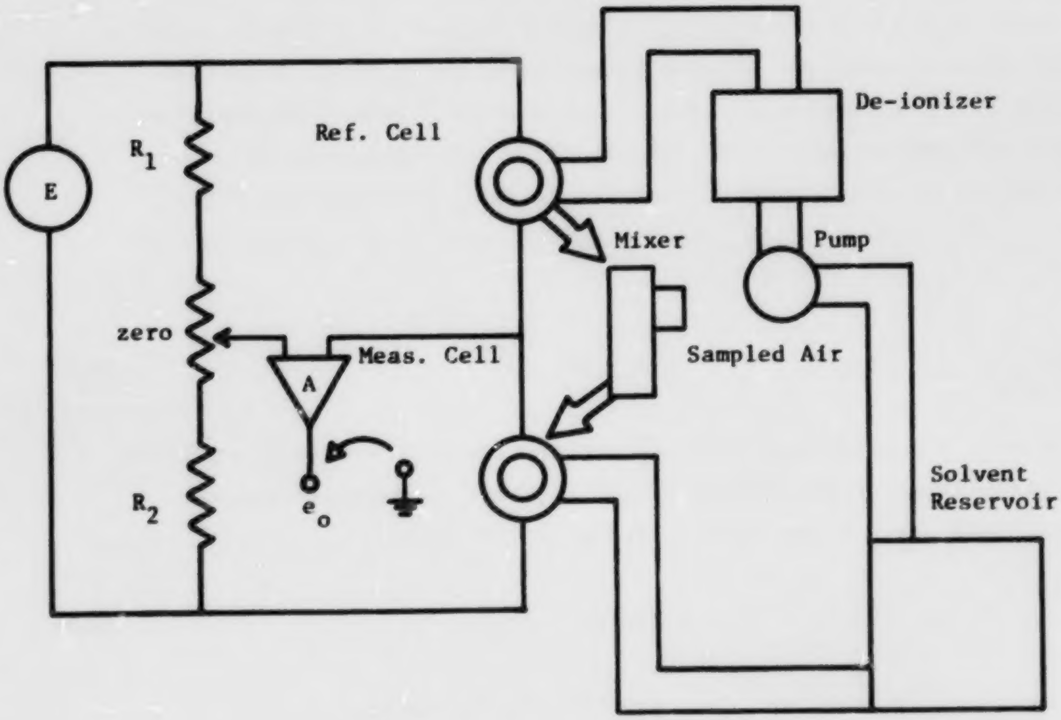
De-ionizer
Ref. Cell
E
R_1
Mixer
Pump
zero
Meas. Cell
A
Sampled Air
e_o
R_2
Solvent Reservoir

Figure 4.2. Bridge Arrangement for Conductance Cells.

The conductivity will depend upon the types of ions, their concentration, the type solvent used, and the temperature. These factors will be examined. It is convenient to express g in terms of the equivalent condutance, λ, and the concentration, c, of the ions in the electrolyte, or

$$g = c\lambda/1000 \tag{4.3}$$

where c is expressed in gram equivalents per liter of solution. When there is a mixture of ions,

$$c\lambda = \sum_i \lambda_i c_i \; . \tag{4.4}$$

Since λ_i is a function of both concentration, in a given solvent, and temperature, these factors must be examined. As a rule of thumb, the temperature coefficient is about 2% per degree Celsius.

If it is assumed that water is used as a solvent and the absorbed species concentrations are small enough to regard as infinite dilution, standard equivalent conductances can be used to make trial calculations of the sensitivity expected. Combining equations (4.1)-(4.4) gives

$$i = \frac{\pi L}{500 \; \ell n(r_2/r_1)} (\Sigma_i c_i \lambda_i) E \; . \tag{4.5}$$

For small changes due to fluctuations in temperature, T, or supply voltage, E,

$$(\Delta I)_N = \frac{\pi L}{500 \; \ell n(r_2 r_1)} \left(E \Sigma_i c_i \frac{\partial \lambda_i}{\partial I} \Delta T + \Sigma_i c_i \lambda_i \Delta E\right). \tag{4.6}$$

The fluctuations due to these sources will determine the minimum detectable change in current. The temperature changes may be compensated by measuring the solution temperature and adjusting the amplifer gain automatically with a feedback signal dependent upon the temperature signal. Alternatively the conductance cell can be thermostated or a bridge arrangement used, as sketched in Figure 4.2. It should be noted also that the temperature of the ambient air is also important since (assuming the ideal gas law)

$$x = \frac{n}{v} = P/RT \ . \tag{4.7}$$

If the partial pressure remains constant, the volumetric concentration will vary with temperature as

$$\frac{1}{x}\frac{dx}{dT} = -1/T$$

or

$$\frac{\Delta x}{x} = -\frac{\Delta T}{T} \ . \tag{4.8}$$

At T = 300°K, a 1°C change results in

$$\frac{\Delta x}{x} = -0.00333 \ . \tag{4.9}$$

The error due to this source must be compared to the error from other sources to determine whether or not it can be ignored.

Another important point in the design is the "mixer" indicated schematically in Figure 4.2. This functions to contact the sampled air stream with the absorbing solvent stream. The efficiency of this contact and its reliability--in terms of constancy of efficiency with respect to time and pollutant concentrations--is essential to the accuracy of the instrument. Denoting by η the mass fraction of pollutant absorbed into the solvent stream from the sampled air stream, the mass of pollutant taken in per unit time in the sample air stream is

$$\frac{dm_a}{dt} = xMQ_a \tag{4.10}$$

where M is the molecular weight of the pollutant and Q the sample air stream volumetric flow rate. The mass rate transferred to the liquid steam is, by definition of η,

$$\frac{dm_\ell}{dt} = \eta x M Q_a \; . \qquad (4.11)$$

The solvent volumetric flow rate, Q_ℓ, along with the mass transfer rate from the air, given by (4.11), determines the mass concentration in the liquid, and therefore the equivalent concentration

$$C = Z \eta x M Q_a / Q_\ell \qquad (4.12)$$

where Z is the number of equivalents per gram molecular weight. Use of this expression, along with equations (4.5) and (4.6), enables the calculation of current levels and fluctuations expected for certain situations.

For definiteness in modeling, the miniature conductivity cell and gas-liquid contactor design of Hall[38] will be used. These are shown in Figure 4.3. This cell operates with solvent flow rates of 0.1-1 cm^3/min and gas flow rates of 5-500 cm^3/min.

Neglecting (for purposes of calculation) the change in cell constant due to the presence of the liquid exit tube, the value is approximately

$$K_c = \frac{\pi L}{500 \; \ell n(r_2/r_1)} = \frac{\pi \times 0.794}{500 \; \ell n(0.10/0.082)} = 2.5 \times 10^{-2} \; . \qquad (4.13)$$

Assume flow rates of

$$Q_a = 100 \; cm^3/min$$

$$Q_\ell = 1 \; cm^3/min$$

with aqueous solvent containing sulfuric acid at a concentration of 5μM

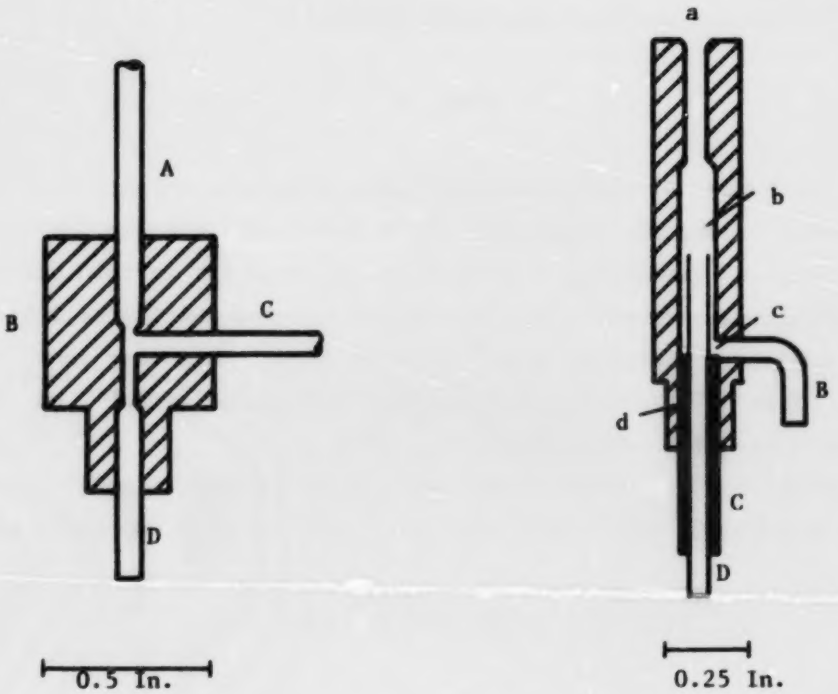
A
B
C
D
0.5 In.
a
b
c
B
d
C
D
0.25 In.

Figure 4.3. Conductivity Cell Design of Hall.[38]

(to suppress bicarbonate buffering) and hydrogen peroxide at 1%. An absorption efficiency of 97-99% can be expected[21,22] but η will be conservatively estimated at 0.95.

The species to be detected is SO_2, which will be assumed to be present at a level of 20 pphm in air at 300°K. Therefore,

$$M = 64 \text{ grams/mole}$$

$$x = 20 \times 10^{-8} \times 4.05 \times 10^{-2} \text{mole/liter}$$

and since the reaction in solution is

$$2H_2O + H_2O_2 + SO_2 \rightarrow 2H_3O^+ + SO_4^=$$

there will be 1 mole of negative charge per 32 grams of SO_2, or

$$Z = 2 \text{ equivalents/64 gm.}$$

The background conductance due to the H_2SO_4 and H_2O_2 in the water will be, at 25°C, approximately

$$g \simeq \frac{1}{1000} \Sigma_i c_i \lambda_i$$

$$\simeq 10^{-3}[10^{-5}\lambda^o_{H_3O^+} + 10^{-5}\lambda^\circ_{1/2SO_4^=}] = 4.29 \times 10^{-6} .$$

The cell conductance at 25°C will be approximately

$$G = 2.5 \times 10^{-2} \times 4.29 \times 10^{-6} = 1.07 \times 10^{-7} \text{mho} .$$

For a supply potential of 1 volt, the current due to the electrolyte solution is about 0.1 microampere.

Using the atmospheric concentration and parameters assumed above, the change in solution conductance will be

$$\Delta g = \Delta C(\overset{\circ}{\lambda}_{H_3O^+} + \overset{\circ}{\lambda}_{1/2SO_4^=}) \times 10^{-3}$$

or

$$\Delta g = 2 \times 0.95 \times 8.1 \times 10^{-9} \times 100(350 + 79) \times 10^{-3}$$

which represents a fractional change of

$$\frac{\Delta g}{g} = 6.6 \times 10^{-7}/4.3 \times 10^{-6} = 0.15$$

or 15%. This corresponds to a change in cell current of 16 nanoamperes. A plot of change in cell current, Δ_i, versus SO_2 concentration in air at 300°K for the assumed values in the model is shown in Figure 4.4.

The National Air Quality Standards for SO_2 (secondary standards) range from an annual arithmetic mean of 2 pphm to a three hour average of 50 pphm, which would correspond to a range of 1.6 nA to 40 nA current change in the model conductivity cell.

A similar calculation can be made for NO_2. Assuming an absorbing solution of water with 5% efficiency[25] the background conductance of the absorbing solution will be

$$g = 10^{-3}[10^{-7} \times 350 + 10^{-7} \times 199] = 5.5 \times 10^{-8} \text{ mho-cm}^2.$$

With the same air and solution flow rates assumed for the SO_2 calculation, the equivalent concentration in solution for an ambient air concentration of 20 pphm will be, from equation (4.12), 4.05×10^{-8} equivalents per liter. This will cause a change in conductance of 1.78×10^{-8} mho-cm^2, or a fractional change of

$$\frac{\Delta g}{g} = 1.78 \times 10^{-8}/5.5 \times 10^{-8} = 0.32 \; .$$

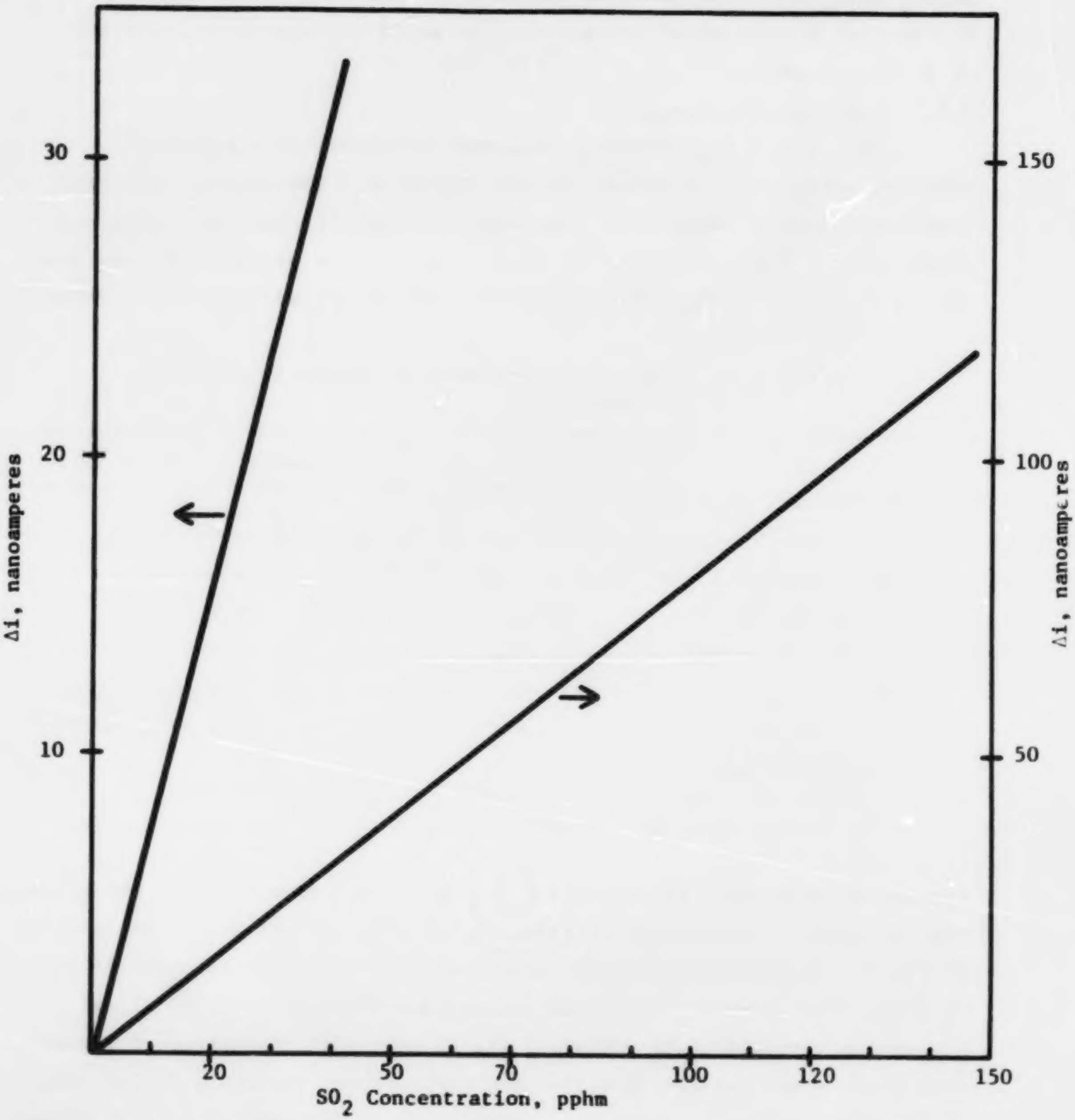

Figure 4.4. Change in Conductivity Cell Current for Various Concentrations of Sulfur Dioxide.

This represents, for a cell voltage of 1 volt, a current change of 0.445 nanoampere. Calculations for a range of ambient air concentrations of NO_2 give the curves shown in Figure 4.5. The National Air Quality Standard of 5 pphm annual arithmetic mean would correspond to a current of 0.106 nanoampere.

4.1.3 Projected Performance

The projected performance in terms of sensitivity (slope of response curve) and fractional current change at 5 ppb desired detection limit are shown in Table 4.1. The required stability and resolution are better than 0.5%. It is doubtful that this could be achieved in practice due to a variety of factors. In the case of the NO_2 solvent, pure water, scrupulous care would be required to prevent ionic impurities in the solvent supply system. Although an increase in the base current due to an increase in solvent conductivity could be zeroed out with each new batch of solvent, it would place greater demands on the current resolution of the signal processing circuitry. In addition, the 2% change in conductance per degree Centigrade would require sophisticated compensation circuitry. Also, there would be errors due to changes in temperature of the sampled air, as discussed previously.

Table 4.1. Projected Performance of Conductivity Cell Analyzers

Operational Parameters	Pollutant	
	NO_2	SO_2
Cell Voltage	1 volt	1 volt
Cell Constant	2.5×10^{-2}	2.5×10^{-2}
Absorber Efficiency	0.05	0.95
Base Current	1.37 nA	100 nA
Sensitivity	0.022 nA/pphm	0.8 nA/pphm
Fraction of base current at 5 ppb	0.008	0.004

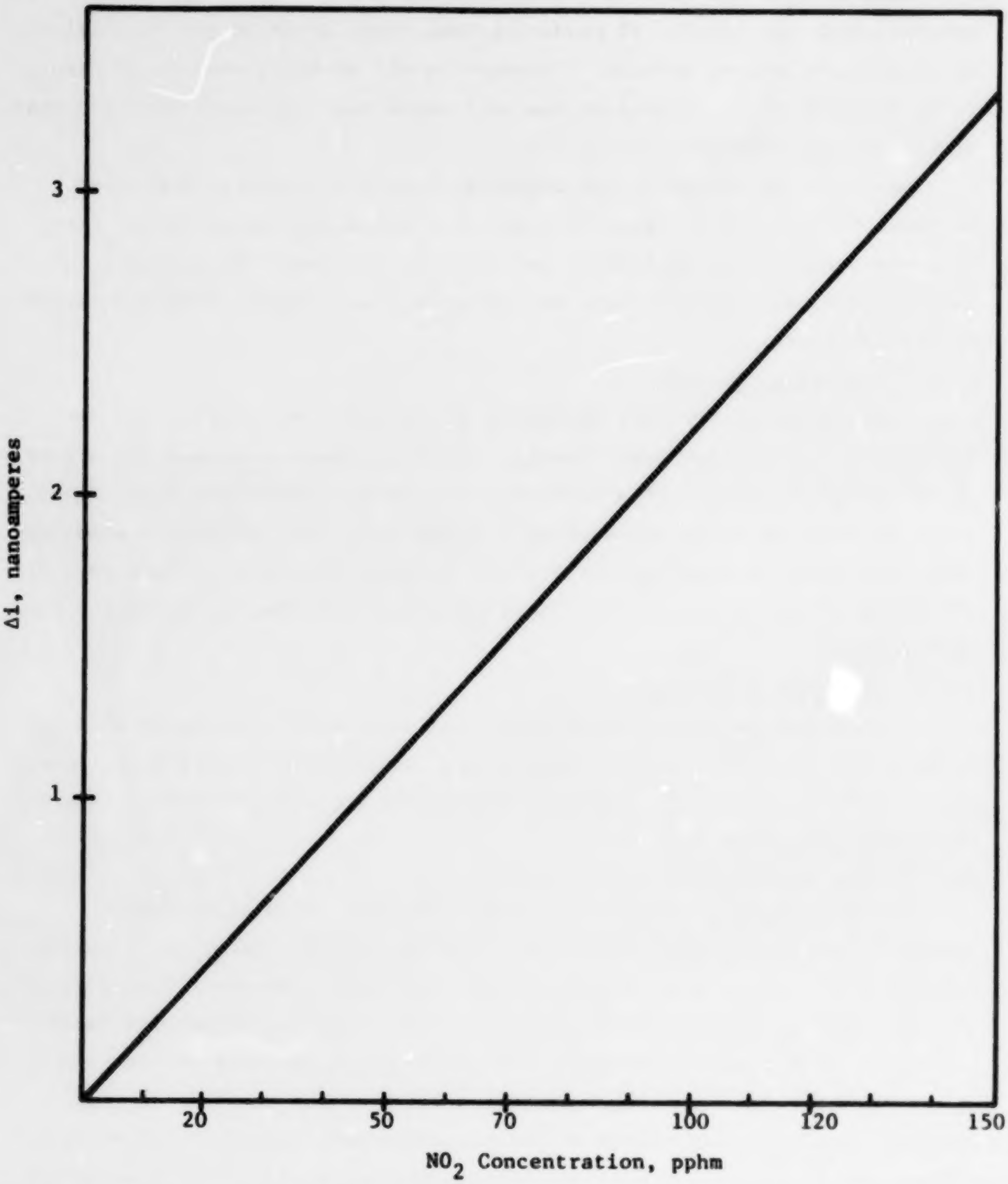

Figure 4.5. Change in Conductivity Cell Current for Various Concentrations of Nitrogen Dioxide.

More serious problems are created by the occurrence of other pollutant species which are capable of producing ions, many of which have equivalent or larger conductance effects. Considering all of these sources of error, it is doubtful that the conductance cell could meet the zero drift and span stability requirements in Table 1.1.

One possible design of the potential source and current amplifier is shown in Figure 4.6. This is based on a versatile, multi-range, fast response conductivity amplifier, described in Reference 39, designed to respond to conductivity changes occurring in times ranging from milliseconds to several hours.

4.1.4 Logistical Factors

The conductivity cell described can be made very compact and can be operated at very low power levels. However, there is a need for a supply of absorbing solution. At a flow rate of 1 mℓ/min continuous flow, about 1.5 ℓ of solution would be required for each cell. In addition a sampling pump capable of pulling ambient air through each cell at a minimum rate of 100 mℓ/min would be necessary. These have been described in Section 2.0 of this report.

4.1.5 Dose Rate Information

A continuous electrical signal, proportional to the conductance cell current and, therefore, to the ambient air concentration of pollutant would be available for periodic sampling; digitizing and storage techniques are described in Section 5.0.

4.2 Halogen/Halide Redox Amperometry

This instrumental method is based on the reduction of molecular halogen (X_2) at one platinum bright electrode and the oxidation of halide to trihalide at a second platinum bright electrode. An electrical circuit for measurement consists of the two electrodes immersed in alkalai halide solutions of different concentrations contained in separate cathode and amide chambers; an ion bridge connection which allows ionic conduction, but inhibits diffusive mixing of the two different electrolytic concentrations; and an external connection between the electrodes through a current monitor to measure the current generated by the reaction of pollutant species with electrolytic species. This current is dependent on the time rate of supply of pollutant (input molar flow rate).

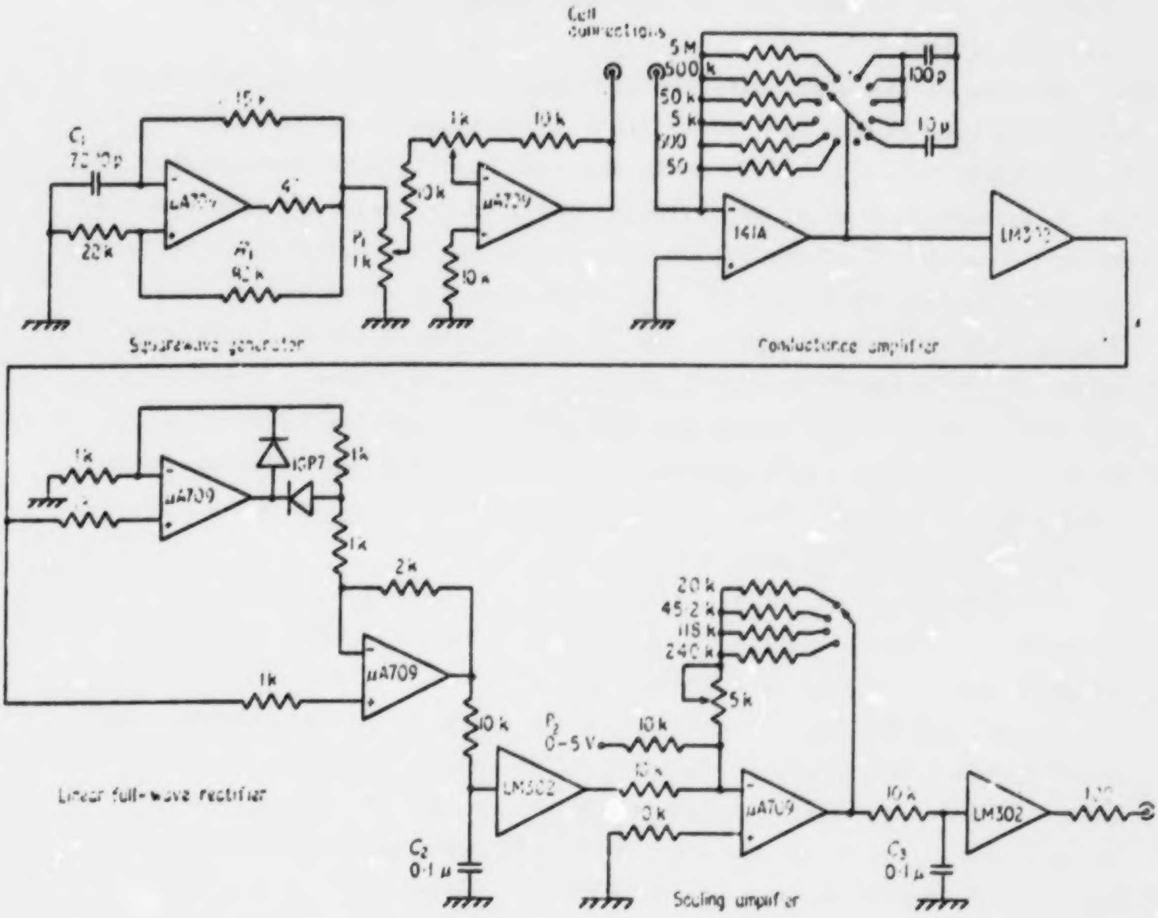
Cell connections
5 M
500 k
50 k
5 k
500
50
100 p
10 p
15 k
C1
7000 p
μA709
47
22 k
R1
40 k
1 k
10 k
10 k
P1
1 k
10 k
μA709
141A
LM302
Squarewave generator
Conductance amplifier
1 k
1k
μA709
1GP7
1 k
1 k
2 k
μA709
1 k
10 k
Linear full-wave rectifier
LM302
C2
0·1 μ
P2
0–5 V
10 k
10 k
10 k
20 k
45·2 k
115 k
240 k
5 k
μA709
10 k
C3
0·1 μ
LM302
100
Scaling amplifier

Figure 4.6. Schematic Diagram of Conductance Amplifier Circuit.[39] For Clarity the Standard Power Supply and Compensation Element Connections to the Operational Amplifiers Have Been Omitted.

Another variation of this method is to use the same electrolyte concentration of alkalai halide at both electrodes and to provide an external potential source of about 150 millivolts to drive the reaction by polarizing the electrodes. Trihalide ions produced by oxidant reaction with alkali halide reacts with hydrogen. Current flows in the external circuit to maintain the hydrogen concentration at equilibrium.

4.2.1 Prior Use

Because of its simplicity the KI solution with polarizing potential method has been widely applied in field instruments to measure ozone. It is subject to many interferences and must be calibrated dynamically.[40] The relationship of moles of triiodide produced per mole of ozone reacted depends upon the pH of the KI solution. Usually this solution is buffered to nearly neutral pH (6.8-7.0). The weight percent of KI used varies, ranging from 1%[41] to as high as 20%.[40] At a given KI concentration the amount of triiodide in solution, produced by a given input of ozone, can vary with time.[42] High concentrations give a maximum ion production immediately, whereas lower concentrations may require some time to achieve a maximum. Electrolyte evaporation can be a problem unless means are taken to replenish from a reservoir.

In addition to ozone, NO_2 and SO_2 can be detected. When NO_2 is absorbed into the KI electrolyte, it reacts in the same manner as ozone. Hence it can act either as a positive interferent, or if ozone has been eliminated from the input sample stream by suitable filters, the NO_2 can be monitored. For the KI concentrations and neutral pH solution normally employed, however, the absorption efficiency of the electrolyte for NO_2 is very poor, just a few percent. When SO_2 is absorbed into the KI electrolyte, it acts in an opposite manner to ozone or NO_2. The SO_2 is converted to sulfate ion and in the process produces electrons to reduce I_2 to iodide.

Kromhyr[43] has described a cell of the type shown schematically in Figure 4.7. For ozone the concentration in ambient air is related to current, i_m, and the sample air flow rate, Q_A, by

$$i_m = 3.87 \times 10^{-10} \left(\frac{PQ_A}{T}\right) \chi(O_3) \qquad (4.14)$$

where P is the sampling atmospheric pressure in millibars, Q_A the sample air flow rate in ml/min, T the air temperature in °K and $\chi(O_3)$ the ozone concentration in pphm. At 5 ppb ozone this corresponds to 65 nanoamperes. This cell exhibits a background current of about 200 nanoamperes when air with ozone removed is bubbled through it. In order to obtain a quantitative reading, this background must be subtracted out. If the background is not constant in time, the fluctuations may be interpreted as a signal unless they are dynamically corrected.

One method for doing this is to use two cathodes,[44] one of which is exposed to air from which the ozone has been removed, and one which is exposed to air in which the ozone remains. A schematic diagram of this instrument is shown in Figure 4.8. A filter of Cr_2O_3 and orthophosphoric acid on an inert substrate is used to remove interfering reducing agents from the inlets of both cathodes. For the reference side, aluminum foil maintained at 150°C was used to destroy ozone. Sample air is passed through a humidifier to minimize electrolyte evaporation. Iodine evaporation is apparently no problem either. The performance of this instrument, as reported in Reference 44, is summarized in Table 4.2. Field tests show excellent (0.999) correlation with chemiluminescent ozone measurements. Operation without electrolyte and reducing filter renewal for better than 1 year were demonstrated in field tests.

4.2.2 Model

The design features of the differential cell of Lindqvist appear to be the most suitable for this approach to a dosimeter. This reference reported that a study of the effect of flow rate, Q_n, and cathode length, L, on current, i_m, generated by the oxidation effect of ozone or the halide electrolyte showed that above 8 cm length the current is directly proportioned to the flow rate. A 10 cm cathode length can be accommodated in a briefcase sized sensor package.

Assuming KI electrolyte, ozone in the sample air produces iodine by the reaction

$$2KI + O_3 + H_2O \rightarrow 2\,KOH + I_2 + O_2\ . \qquad (4.15)$$

This iodine is reduced at the cathode by

$$I_2 + 2e \rightleftarrows 2I^-\ . \qquad (4.16)$$

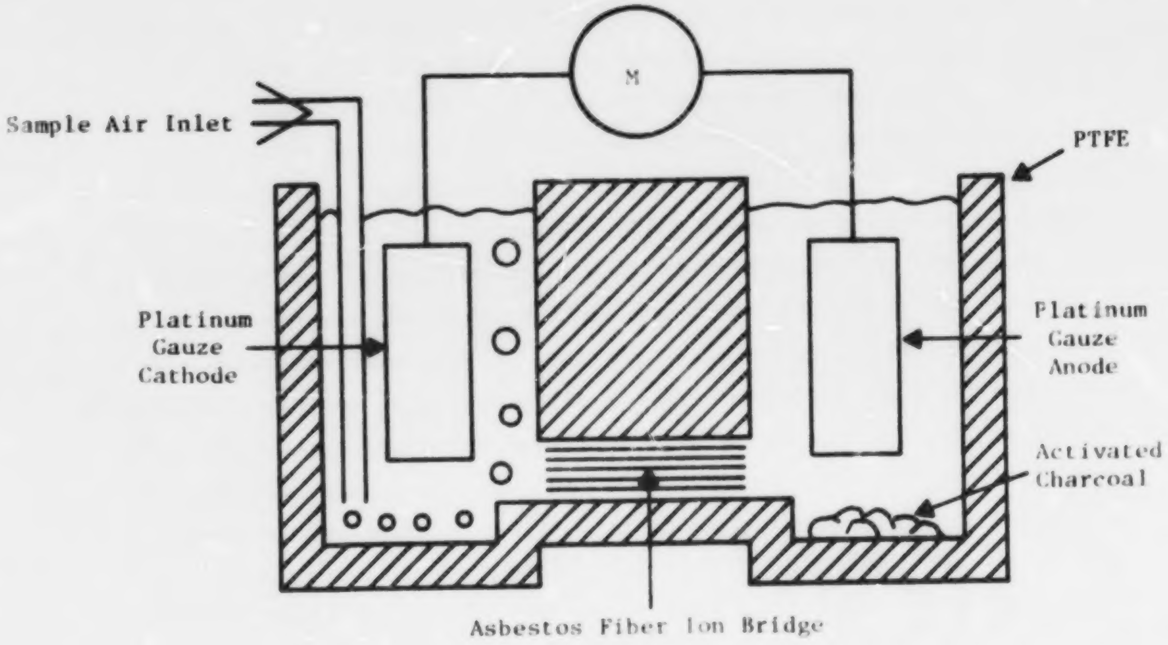
M
Sample Air Inlet
PTFE
Platinum
Gauze
Cathode
Platinum
Gauze
Anode
Activated
Charcoal
Asbestos Fiber Ion Bridge

Figure 4.7. Kromhyr Cell.

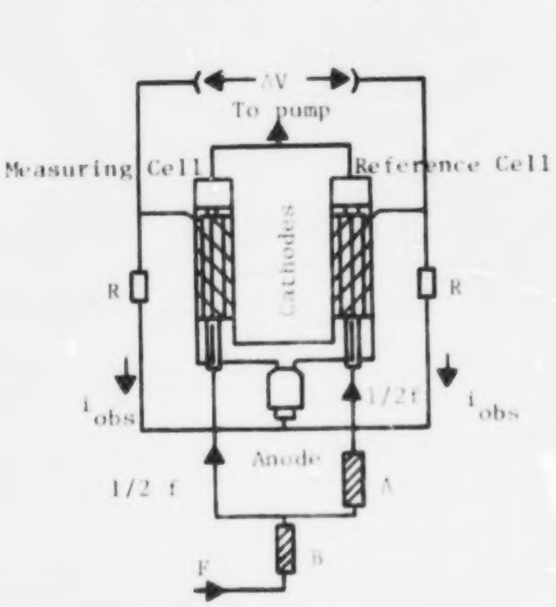
ΔV
To pump
Measuring Cell
Reference Cell
Cathodes
R
R
i_{obs}
i_{obs}
1/2f
Anode
1/2 f
A
B
F

Figure 4.8. Lindqvist Cell.

Table 4.2. Performance Summary for Differential Amperometric Method for Ozone Measurement

Flow rates	150 ml/min per cell
Span	0-400 µg/m^3 (0-200 ppb) ozone
Span Drift	5.5% in 22 hrs (possibly due to ozone generator drift)
Zero Drift	2.3 µg/m^3 (1.15 ppb) in 62 hours 6 µ/m^3 (3 ppb) in several weeks
Noise Equivalent	0.6 µg/m^3 (0.3 ppb)
Time Constant	40 seconds
Interferences	1. None for concentrations up to of SO_2 = 4350 µg/m^3 (1.5 ppm) H_2S = 2660 µg/m^3 (1.7 ppm) C_2H_4 = 3300 µg/m^3 (2.8 ppm) 1-butene = 8800 µg/m (3.8 ppm) 2. For NO_2 about 0.08 mole equivalent up to 2520 µg/m^3 (1.3 ppm) 3. For Cl_2 about 0.01 mole equivalent up to 2500 µg/m^3 (0.85 ppm). 4. For PAN about 0.12 mole equivalent up to 1240 µg/m^3 (0.24 ppm).

A complementary reaction occurs at the anode, which is made of activated carbon paste, where iodide ions are converted either to triode or to molecular iodine, depending upon the iodide concentration. Assuming that the latter is true, the pertinent equation is the inverse of equation (4.16) above. It should be noted, however, that the concentrations (or more properly, the activities) of I^- and I_2 can be very much different around the cathode and around the anode. Therefore, the Nernst equation for the potential difference will be

$$E = -0.0295 \left(\frac{T}{300}\right) \log \frac{a(I_2,A)}{a(I_2,C)} \frac{a^2(I^-,C)}{a^2(I^-, A)} \qquad (4.17)$$

where the a's denote activities for the species noted at the anode (A) and cathodes (C). If the external resistances, R, shown in the circuit diagram of Figure 4.8, are not too large, the current flow in the external circuits between the respective cathodes and the anodes will tend to equalize the forward and backward rates of equation (4.16), giving currents which are quantitative for the oxidation due to ozone (and other oxidizing species).

The necessity for using the resistors to develop a differential voltage signal is eliminated if a differential current measuring circuit, using standard electrometer design techniques, is employed. A schematic diagram of such an arrangement is shown in Figure 4.9. The electrometer amplifiers, A_1 and A_2, provide essentially zero resistance for the respective cell currents. Output voltages from these amplifiers are algebraically summed to provide a net output voltage signal, C_o, which is proportional to the pollutant concentration and sample air flow rates. If the latter are held constant, the signal will be proportional to pollutant concentration only.

Assuming total cancellation of the "background" current component by the reference cell, the net current from the differential cell is

$$2(O_3) = 3.87 \times 10^{-10} (PQ_A/T)\chi(O_3) \cdot \qquad (4.18)$$

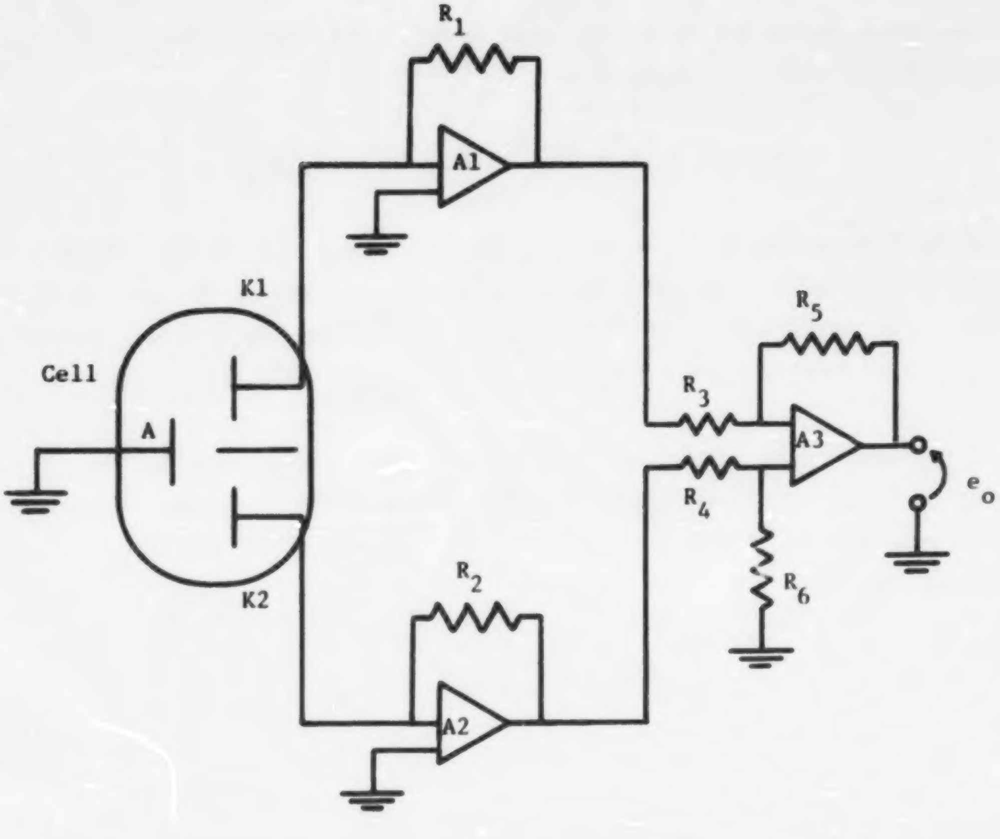
R1
A1
K1
Cell
A
K2
R2
A2
R5
R3
A3
R4
e0
R6

Figure 4.9. Signal Processor for Differential Current Measurements.

Note that this formula assumes total conversion of the incoming ozone, which assumption is verified experimentally.

Since NO_2 acts as an interferent, KI oxidizes according to the equation

$$NO_2 + 2KI + 2H^+ \rightarrow NO + I_2 + H_2O + 2K^+ \ . \qquad (4.19)$$

The electrode reactions of (4.16) will occur. The formula (4.18) for the current due to ozone is changed to

$$i(NO_2) = 3.87 \times 10^{-10} \ \eta(NO_2)(PQ_A/T)\chi(NO_2) \qquad (4.20)$$

where the concentration is in pphm of NO_2 and where the factor $\eta(NO_2)$ represents the efficiency of conversion of NO_2 to oxidant in the electrolyte. It should be noted that with dissolved oxygen in the electrolyte, NO can be cyclically converted back to NO_2, necessitating dynamic calibration of the system.

By inverting the order of the filters A and B in Figure 4.8 to eliminate ozone from both sample streams and then reducing agents--assumed to be primarily SO_2--from the reference stream, a monitor for SO_2 can be obtained. The reactions are

$$SO_2 + H_2O \rightarrow H_2SO_3 \qquad (4.21)$$

$$H_2SO_2 + H_2O \rightarrow SO_4^{=} + 4H^+ + 2e \qquad (4.22)$$

followed by reaction (4.16). Each molecule of SO_2 is capable of producing one molecule of I_2, reducing the background current in the sample cell. This produces a negative current (with respect to the polarity obtained for the ozone reaction) of magnitude

$$i(SO_2) = 3.87 \times 10^{-10} \ \eta(SO_2)(PQ_A/T)\chi(SO_2) \qquad (4.23)$$

where the concentrations of SO_2 is in pphm and the factor $\eta(SO_2)$ represents the efficiency of conversion of SO_2 to a reducing agent in the solution.

4.2.3 Projected Performance

The minimum detectable concentrations for these differential cells will depend upon the noise levels in the cells themselves. Using the figure reported by Lindqvist of 4 nanoamperes of background cell noise current, and requiring a noise ratio of 2, the minimum detectable pollutant concentrations are as shown in Table 4.3 along with the sensitivity figures. Both rely on the assumed absorption efficiencies shown in the table and assume that the sampled air is at atmospheric pressure and 25°C.

Table 4.3. Projected Performance of Differential Amperometric Cell Analyzers

Operating Parameter	Pollutant		
	O_3	NO_2	SO_2
Absorber Efficiency	1.0	0.05	0.95
Sample Flow Rate	100 cm^3/min	100 cm^3/min	100 cm^3/min
Sensitivity at 25°C and 1 atm total pressure	131 nA/pphm	6.6 nA/pphm	125 nA/pphm
Minimum Detectable Concentration	0.6 ppb	12 ppb	0.7 ppb

The calibration will change as the atmospheric temperature and pressure change, but presumably these parameters could be also monitored and compensated for in the signal processor. The sampling rate will also have to be maintained constant. Since the current signals are directly proportional to the sample flow rate, any variation in this will cause a corresponding sized error in the dose rate reading.

The time response reported by Lindqvist[44], about 40 sec, could be expected for this method.

4.2.4 Logistical Factors

Liquid pumping is not required. Makeup water for the electrolyte would be required, however. A sampling pump would be required for each cell. If all three pollutants were measured with individual dual cells, the required pumping of sample air would be 600 ml/min, which could be handled by most of the pumps listed in Table 2.1. As with the conductivity cell reviewed in Section 4.1, care would have to be taken to keep the instrument package vertical in order to avoid leaking and plugging problems.

4.2.5 Dose Rate Information

A continuous electrical signal, proportional to the ambient air concentration of pollutant (when compensated for pressure and temperature changes) would be available for periodic sampling, digitizing and storage by techniques described in Section 5.0.

4.3 Halogen Generation Amperometry

Another method of amperometric measurement is to automatically titrate a solution by generating halogen to restore an equilibrium concentration in an absorbing electrolyte. Alternatively, halogen can be generated at a constant rate and deviation from halogen/halide equilibrium concentrations due to pollutant species can be used to measure the pollutant concentration.

4.3.1 Prior Use

Several different instrumental methods using halogen generation have been reported. Among these are the following:

1. Absorb pollutant into an electrolyte containing KBr and Br_2. Change in the Br_2 concentration develops a potential difference according to the Nernst equation.[45] This potential is used to drive generating electrodes until the depleted species is replenished. This generating current is proportional to the rate at which the pollutant is supplied to the electrolytes, which--at constant air sampling rates--is proportional to the ambient air concentration of pollutant.[46]

2. A constant current source normally oxidizes halide at one platinum electrode and reduces halogen at a second electrode in an alkalai halide/halogen electrolyte solution. A third electrode acts as a sensor which normally does not carry any current until pollutant is absorbed into the solution to change the halide/halogen equilibrium point. Then the sensing electrode will conduct a current proportional to the concentration deviation and, therefore, proportional to the rate at which pollutant is supplied to the solution.[47]

3. **Alkalai halide reagent is supplied at a constant rate to a reservoir where a pair of electrodes generates halogen at a constant rate. This halide/halogen electrolyte is mixed with sampled air and allowed to collect in another reservoir where a pair of measuring electrodes offset in potential by a reference potential source in the range of several tens of millivolts magnitude. Reaction of pollutant with either the halogen or halide change the relative concentrations, causing a change in solution conductance. The unbalance generates current proportional to pollutant concentration, which can then be measured.[48] The alkalai halide reagent is filtered to remove halogen and is recycled.**

Because of its relative simplicity, the third method would probably be easier to implement in a reduced size model.

4.3.2 Model

The model cell is shown in Figure 4.10. Alkalai halide, for example NI, reagent is metered at a constant flow rate past a pair of platinum electrodes, G and G_2, where a constant current source, I_G generates iodine through the anode reaction

$$2I^- \rightarrow I_2 + 2e \qquad (4.24)$$

The solution concentration of I_2 depends upon the liquid flow rate Q_ℓ and the current magnitude. From Faraday's Law the molar concentration of I_2 is related to Q_ℓ and I_G by

$$[I_2] = 0.31\ I_G/Q_\ell \qquad (4.25)$$

where I_G is specified in amperes and Q_ℓ in ml/min.

Following I_2 generation the liquid stream is mixed with the sample air stream to absorb pollutant. From the analysis outlined in Section 4.1.2, the concentration of pollutant in solution will be given by

$$C = 1.20 \times 10^{-10}\ \eta\chi P Q_A/Q_\ell T \qquad (4.26)$$

where η is the absorption efficiency of the solution for the particular pollutant and χ is the concentration in pphm of pollutant in ambient air sampled at pressure P in millibars and temperature T. The sample air rate is Q_A ml/min and the liquid flow rate is Q_ℓ ml/min.

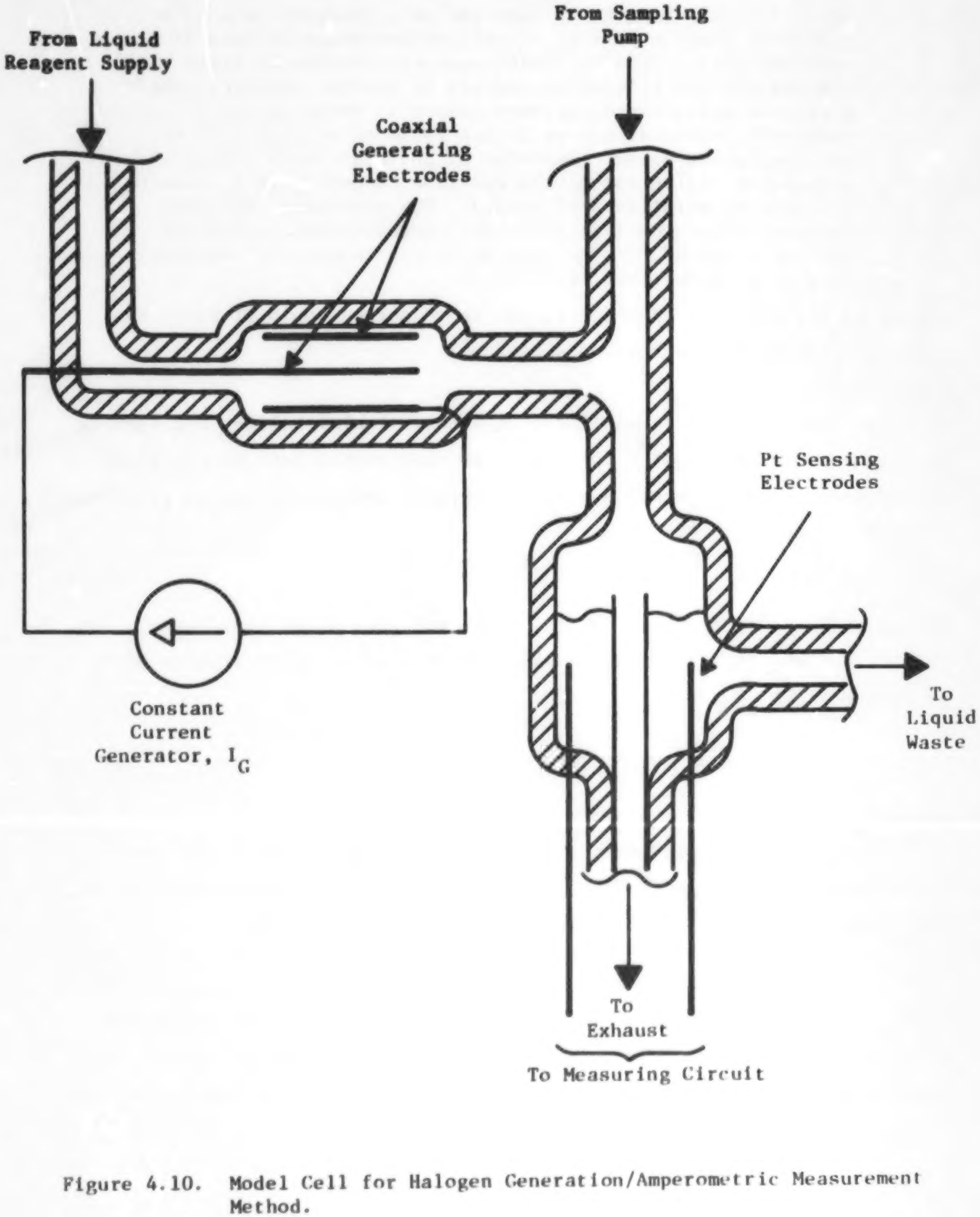
From Liquid Reagent Supply
From Sampling Pump
Coaxial Generating Electrodes
Pt Sensing Electrodes
To Liquid Waste
Constant Current Generator, I_G
To Exhaust
To Measuring Circuit

Figure 4.10. Model Cell for Halogen Generation/Amperometric Measurement Method.

It should be noted that evaporation of the electrolyte will occur in the mixing process. For example, for a sample air flow rate of 100 ml/min at 20% relative humidity, 25°C and at a nominal 1 atmosphere (1013 millibars) contacted with aqueous solution flowing at 1 ml/min, the water loss can be as high as 4% per pass. If the air sample is "bone dry" and at 35°C, the evaporation loss is almost 10% per pass.

One method of controlling this is to humidify the sample air. This can lead to more serious problems, however, when sampling for SO_2 since the loss of SO_2 on surfaces due to absorption from the gas phase is significantly increased with increasing relative humidity.[49] This has previously been discussed in connection with the analysis method of Section 4.2.

Designating the fraction of liquid volume lost by evaporation as ε, the concentration of pollutant and of iodine will both be increased by a fraction $(1-\varepsilon)^{-1}$.

Assuming perfect mixing and reaction rates high enough to totally react the absorbed pollutant, the reactions will lead either to an increase in I_2 concentration on a 1:1 mole basis for NO_2 and O_3 or to a decrease on a 1:1 mole basis for SO_2. Therefore, the change in I_2 concentration will be

$$\delta[I_2] = 1.2 \times 10^{-10}\ \eta\chi PQ_A/Q_{\ell T}\ (1-\varepsilon) \qquad (4.27)$$

and the fractional change will be

$$\frac{\delta[I_2]}{[I_2]} = 3.87 \times 10^{-10}\ \eta\chi PQ_A/I_G T \qquad (4.28)$$

Therefore, the fractional change in iodine concentration is independent of the concentration changes due to evaporation loss of water.

Schulze[48] has reported a linear relationship between conductance and iodine concentration for a constant value of bias voltage, E_B in Figure 4.10. The particular conductance levels will depend on the geometry of the platinum electrodes as well as the bias voltage and iodine concentration. Typically, the current levels involved are on the order of 1 μA full scale.

In order to assess the magnitude of the fractional changes in conductance predicted by (4.28), the following parameter values are assumed.

$\eta = 1.0$ $\qquad$ $Q_A = 100$ ml/min

$\chi = 100$ pphm $\qquad$ $I_G = 20\mu A$

$P = 1013$ millibar (1 atm) $\qquad$ $T = 300°K$

This gives a change of 65%. A concentration of 5 ppb corresponds to a 0.325% change in conductance. For 1 μA full scale current, the minimum detectable current change required is 3.25 nA.

For NO_2 the absorption efficiency of neutral KI solution is very low. At 5% efficiency the current change corresponding to 5 ppb NO_2 in ambient air would be about 0.16 nA. Measurements of currents at this level require careful circuit design.

As pointed out by Schulze, it is desirable to have steady, non-turbulent flow of electrolyte past the sensing electrodes, S_1 and S_2 in Figure 4.10. The mixing chamber should not introduce bubbles in the electrolyte, and the liquid flow system should be designed to eliminate plugging or any condition that would lead to slug flow.

4.3.3 Projected Performance

Based upon the model presented above, the projected performance of this method is shown in Table 4.4 below. No estimate of minimum detection table noise is given because there is no data on which to base a calculation.

Table 4.4 Projected Performance of Iodine Generator Amperometer

Operating Parameter	Pollutant O_3	Pollutant NO_2	Pollutant SO_2
Absorber efficiency	1.0	0.05	0.95
Sample air flow rate	100 cm^3/min	100 cm^3/min	100 cm^3/min
Sensitivity at 25°C and 1 atm total pressure	6.5 nA/pphm	0.325 nA/pphm	6 nA/pphm
Minimum Detectable Concentration	?	?	?

As is obvious from equation (4.28), the sampling air flow rate must be held constant. Any variation will cause a corresponding variation in signal (at constant χ). The total pressure and temperature of the air will also affect the calibration and should be accounted for if the results are to be interpreted in volumetric concentration terms.

The time response will depend on the flow rate of liquid and the hold up volume in the measuring cell. If the latter is 0.25 milliliter and the liquid flow rate is 1 ml/min the 90% response time will be about 35 to 40 seconds.

4.3.4 Logistical Factors

Liquid pumping as well as air pumping is required. Although the reagent is recycled, makeup water is required to take care of evaporation losses. Three separate cells, with appropriate filters to take out SO_2 and other reducing gases and ozone, are required. This brings total air pumping capacity to 300 ml/min, which can be easily handled by most of the pumps listed in Table 2.1.

4.3.5 Dose Rate Information

A continuous electrical signal from each cell, proportional to either pollutant mass concentration, or to pollutant volume concentration when temperature and pressure are compensated for, would be available for periodic sampling, digitizing and storage by techniques discussed in Section 5.0.

4.4 Membrane Amperometers

This method depends upon the diffusion of the species to be measured through a membrane chosen to selectively permeate this pollutant while discriminating against other, potentially competitive species as much as possible. Following the membrane diffusion, the species goes through a redox process at a sensing electrode to generate a current which is related to the gas phase concentration of the pollutant on the atmospheric side of the membrane. The membrane is used to minimize electrolyte evaporation as well as to provide some degree of selectivity.

4.4.1 Prior Use

Patents[50,51] for electrochemical transducers for SO_2 and NO_2 have been issued. Instruments based on these transducers are commercially available.[52] Table 4.5 shows operating parameter ranges for ambient air monitoring instruments and Table 4.6 shows manufacturer's data on interference equivalents of 1 ppm of the indicated species.[53]

Some of the operating advantages and disadvantages have been pointed out in a survey report by LBL.[53] These are listed in tabular form in Table 4.7. The temperature sensitivity must be either compensated for electronically or the device must be kept at a constant temperature.

Table 4.5. Features of ECT Analyzers

	Typical	Range
For ambient air monitoring:		
Sensitivity	0.01	0.005 to 0.02 ppm
Highest Range	5	1 to 10 ppm
Lag Time	10	---- to --- sec
Response Time		20 to 180 sec
Class	Portable	
Cost	2200	950 to 2300 $

Table 4.6. Model SS-310 Interference Data

Interferent	Response to 1 ppm
NO	< 0.001
NO_2	< 0.01
Aldehydes	< 0.001
Hydrocarbons	< 0.0001
CO	< 0.0001
CO_2	$< 10^{-8}$

Table 4.7 **Advantages and Disadvantages of ECT Analyzers**[53]

Advantages	Disadvantages
1. Fast response	1. Periodic electrolyte replacement required due to volatilization
2. Low maintainance	2. Membrane can be separated from thin film electrolyte by simple pump suction.
3. Small, light weight	3. Accumulation of adhering material in sample airstream may eventually block membrane
4. Low power consumption	4. Temperature sensitive
5. Continuous reagent supply not necessary	

4.4.2 Model

The model used for analysis is shown schematically in Figure 4.11. A membrane of thickness dm and area A is exposed to air containing the pollutant to be sensed--e.g., NO_2 with a gas phase partial pressure P_g. The membrane will have a permeability, P, for this species which is dependent upon its solubility, S_m, in the membrane material and its diffusion coefficient, D_m, in the membrane material according to

$$P = S_m D_m \ . \qquad (4.29)$$

At the back side of the membrane the diffused gas will have a gas phase partial pressure p_m. The flow rate of pollutant through the membrane will be given by

$$q = \frac{PA}{d_m} (p_g - p_m) = \frac{S_m D_m A}{d_m} (p_g - p_m) \ . \qquad (4.30)$$

As long as the concentration is small, the relationship between p_m, at the back face, and the concentration of pollutant at the surface of the thin

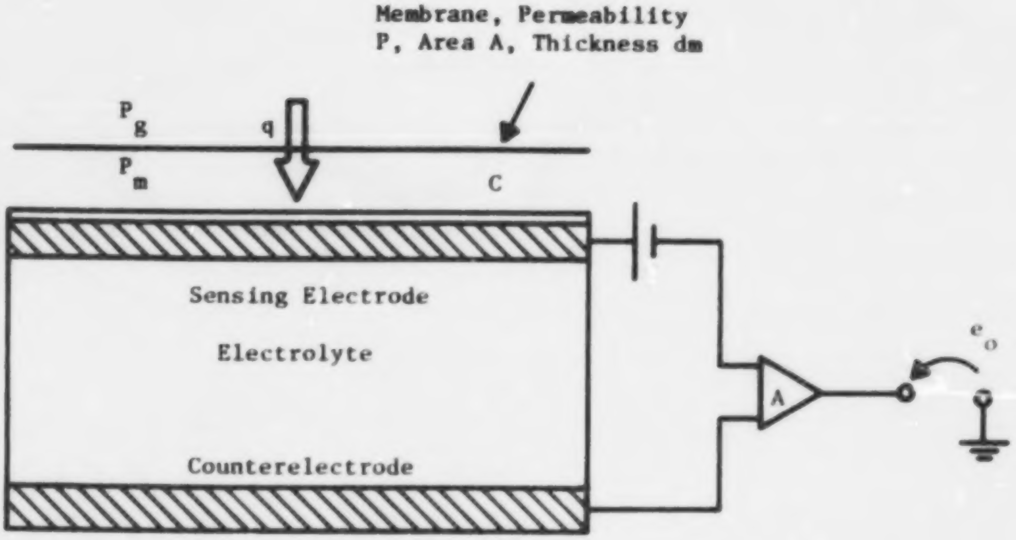
Membrane, Permeability
P, Area A, Thickness dm
P_g
q
P_m
C
Sensing Electrode
Electrolyte
Counterelectrode
A
e_o

Figure 4.11. Model Membrane Amperometer.

electrolyte layer between the membrane and the sensing electrode, c, will be given by

$$c = S_E p_m \ . \tag{4.31}$$

The diffusive flux of pollutant through the electrolyte of thickness d_E and diffusion coefficient D_E is given by

$$J = -D_E \ c/d_E \tag{4.32}$$

if it is assumed that the concentration of pollutant at the electrode surface is zero. That is, the pollutant species is consumed (transformed into another species) by the redox process.

It should be noted that equations (4.29)-(4.32) are steady state equations. For transient analysis, Fick's second law equation must be applied.

Equating the flow rate through the membrane with the diffusive flow rate through the electrolyte (also of area A) leads to the following expression for flow rate of pollutant to the electrode:

$$Q_p = K\left(\frac{D_E S_E}{d_E}\right)\left(\frac{P/d_m}{\frac{D_E S_E}{d_E} + P/d_m}\right) A\ p_g \quad \frac{\text{moles}}{\text{sec}} \tag{4.33}$$

where K is a proportionality constant included to convert the expression to a molar flow rate. The current generated at the sensing electrode is

$$I = \left(\frac{\#\text{moles}}{\text{sec}}\right) \times \left(\frac{\#\text{ equivalent}}{\text{sec}}\right) \times \left(\frac{\#\text{ Coulombs}}{\text{equivalent}}\right)$$

or

$$I = nFQ_p . \tag{4.34}$$

The solubility and diffusion parameters of the membrane and electrolyte will be dependent upon temperature as

$$P = P_o \exp\left(-E_p/RT\right) \frac{\text{cm}^3(\text{STP})}{\text{sec}} \cdot \frac{\text{cm}}{\text{cm}^2 \cdot \text{atm}} \tag{4.35}$$

$$D = D_o \exp\left(-E_D/RT\right) \text{cm}^2/\text{sec} \tag{4.36}$$

$$S = S_o \exp\left(-\Delta H_s/RT\right) \text{cm}^3(\text{STP})/\text{cm}^3 \cdot \text{atm} \tag{4.37}$$

where E_D is the activation energy for diffusion, ΔH_s is the heat of solution for the pollutant species in the medium, R is the gas constant and, for a given medium

$$E_p = E_D + \Delta H_s . \tag{4.38}$$

Values of these parameters are shown in Table 4.8 for the case of NO_2 permeation in Teflon.[54] Table 4.9 shows the relative permeation of several different membrane materials for SO_2, NO, and NO_2.[53] These data give some idea of the mass flow rate magnitudes obtainable with membranes.

Table 4.8 Parameter Values for Permeation of NO_2 in Teflon[54] at 25°C

$P = 1.57 \times 10^{-9}$

$D = 3.7 \times 10^{-9}$

$S = 0.43$

$E_p = 10.67$ kJ/mole

$E_p = 58.6$ kJ/mole

$\Delta H_s = 47.7$ kJ/mole

Rate of change of permeability with temperature, about 1.4%/°K at 300°K

Table 4.9 Relative Permeation of NO, NO_2 and SO_2 in Various Materials[53]

Membranes	Permeation Ratios		
	SO_2	NO	NO_2
Teflon, 1/4 mil	0.83	0.73	1.0
Polyethylene, 1.2 mils	1.00	0.08	0.03
Polyethylene, 0.3 mils	1.00	0.08	0.0
Polyvinylchloride, 1.5 mils	1.00	0.0	0.0
Pellicon, 0.5 mil	0.94	0.0	1.0
Zitex 12-137B, 2 mils	1.00	0.30	0.69
Cellophane, 1 mil	1.00	0.0	0.0
Polyethylene and Pelicon Double Membrane, 1.5 mils	1.00	0.0	0.0

The electrolyte used will determine the values of solubility, S_E, and diffusion constant , D_E. The patents[50,51] on this basic method used 1N sulfuric acid as the example electrolyte for both NO_2 and SO_2 models and claimed the use of aqueous acid electrolytes. This obviously places NO_2 at a disadvantage because of its low solubility in acid solution relative to SO_2. Other electrolytes have been investigated and found more sensitive and selective for NO_2.[55]

The type electrolyte used will determine the bias potential, E_B in Figure 4.11, which is used to promote the devised reaction while suppressing competing reactions which occur at higher potentials. However, reactions which occur at lower potentials can still interfere. The cited patents[50,51] discuss the factors involved in the choice of counter electrode materials.

For a quantitative estimate of the current obtainable from this transducer, it will be assumed that in (4.33) the membrane and solution permeation factors are such that

$$D_E S_E / d_E >> P/d_m \ .$$

Then

$$Q_p = 4.46 \times 10^{-13} \left(\frac{PA}{d_m}\right) x \text{ moles/sec} \qquad (4.39)$$

where x is the pollutant concentration in pphm. With typical values for NO_2 in teflon, with a 5 cm diameter teflon membrane, 1/4 mil thick (6×10^{-4} cm), and a reaction that gives 2 equivalents per mole, the current is related to concentration by

$$I = 8.5 \times 10^{-11} x \text{ amperes} \qquad (4.40)$$

This can be improved somewhat by increasing the area of the membrane or by finding a membrane material of higher permeability. Either course will probably also increase the evaporative loss of electrolyte by "reverse" permeation through the membrane. It appears that a practically sized sensor will have a sensitivity of the order of 0.1 nA/pphm.

The method has no counterpart for ozone.

4.4.3 Projected Performance

Based upon the discussion in the previous section, the projected performance of these sensors for NO_2 and SO_2 is as shown in Table 4.10 below.

Table 4.10 Projected Performance of Membrane Amperometers.

Operating Parameters	Values
Membrane Area	20 cm^2
Membrane Thickness	6×10^{-4} cm
Sensitivity	0.1 nA/pphm
Minimum Detectable Concentrations	10 ppb

4.4.4 Logistical Factors

In contrast to the previous methods discussed, this transducer does not require forced air flow although it can be used. Because of the sensitivity to temperature of permeation rates through the membrane and electrolyte, the temperature of the device should be controlled.

4.4.5 Dose Rate Information

A continuous electrical signal proportional to pollutant concentration in ambient air is available for periodic sampling, digitizing, and storage by techniques discussed in Section 5.0.

4.5 Colorimetric Methods

These methods of detection and measurement are based upon the reaction of the pollutant species with a regent dye to give a characteristic color. It is convenient to divide these methods into two categories, namely, surface detection and volume detection. In surface detection, the dye is coated on a solid substrate such as filter paper or silica gel and the concentration of the pollutant is determined from the intensity of the characteristic color reflected when the surface is illuminated with white light. In volume detection a decolorized dye is converted to a colored species and the amount of light absorbed at the characteristic color is measured.

4.5.1 Prior Use

Many methods have been reported which use surface colorimetric reactions for SO_2 detection and measurement.[56] Crude applications have been in the form of indicator papers. Litmus paper has been used as has congo red paper. Filter paper coated with starch-potassium iodate-potassium iodide-glycerol, sodium nitroprusside/sodium carbonate, p-phenyl anediamine, zinc nitroprusside/ammonium sulfite, among other reagents, have been used to indicate the presence of sulfur dioxide. Generally, these indicator paper methods have required a relatively large concentration, relative to ambient air standards, in order to develop a color detectable by the human eye.

The primary application of surface colorimetric reactions has been in the area of "detector tubes" designed for occupational environmental monitoring. The Draeger, Kitagawa and MSA commercial series include stain indicator tubes for sulfur dioxide. The use, characteristics and limitations of stain indicators has been reviewed by Saltzman[57] and Linch.[58] The support material for the indicator dye is usually silica gel. Various inorganic and organic color producing species are used to coat the substrate. Many of these have been reviewed in Reference 56. As with paper indicators the usual read-out of these indicator tubes is by the human eye, observing the length of stained section colored by drawing in a well defined volume of sample air. However, at least one technique has been devised in which a photocell is used to compare the developed colors with a standard set.[59]

Volumetric detection is usually accomplished as a two step process. The first step requires absorption from the gas phase into a suitable liquid, and conversion to a sulfite or sulfate ion. Then this solution is reacted with a suitable reagent to develop a colored species in the mixtures for analysis via photometric absorption.

Various methods have been used to contact the sampled air stream with absorbing (or "scrubbing") solution. The simplest is to flow the air stream across the surface and rely upon diffusion through the boundary layer from the gas phase to the liquid phase. Alternatively, the air stream may be directed toward the liquid surface (or "impinged"). The collection efficiency of these methods is highly dependent upon flow rate, temperature and solution chemistry.

Various studies have been made of the collection efficiency of bubbler systems to contact a sample air stream with absorbing solution.[60] Sulfur dioxide at 25 to 700 $\mu g/m^3$ in air at a sampling rate of 1.4 ℓ/min has been collected at 98.5 to 99.2% efficiency in 50 mℓ of 1% H_2O_2 solution. At lower concentrations collection efficiency drops to about 95%. Another study[61] of bubbler efficiency at flow rates of 1.2-6ℓ/min with SO_2 concentrations up to 17 pphm (440 $\mu g/m^3$) indicated collection efficiency of better than 97% in 1% H_2O_2, tetrachloromercurate solution and water at pH 5. Efficiency was found to increase with decreasing flow rate and increasing SO_2 concentration. One of the problems with bubblers is the increased chance of NO_2 interference due to physically entrained air bubbles in the absorbing solution.

A more complicated method has been devised by Lyshkow,[62] who used a countercurrent of sample air stream with a scrubbing solution stream and enhanced contact by using rotating discs. This method decreases physical entrainment of bubbles. A countercurrent absorption method has also been used to absorb SO_2 directly into a color producing reagent--a starch-iodine aqueous solution--in a portable SO_2 monitor.[63]

A wide variety of color producing chemical reagents has been studied for sulfur dioxide measurement. Many of these have been reviewed in Reference 56. The most widely used is the standard West-Gaeke method modified to eliminate NO_x and ozone interferences. The procedure, now the Federal Standard Reference method for determining atmospheric SO_2, is described in detail in Reference 64.

Several other dyes have been used or proposed for use in colorimetric SO_2 detection. These have been reviewed and compared with pararosaniline in a recent survey of monitoring methods.[65]

One of the major problems with colorimetric reactions is the length of time required to develop a color. This is due to several factors. The absorption and mixing step both require some time, and if a sequence of reactions is used, the mixing and equilibration time of each adds to the total analysis time. The kinetics of the reactions depend upon the concentrations. At lower concentrations of reactant more time is required to reach the end point on color development. The response time can range from a few minutes to a half-hour.

Many methods have been reported which use surface colorimetric reactions for NO_2 detection and measurement.[66] Filter paper has been impregnated with sulfanilic acid, α-naphthyl amine, alcoholic diphenylamine, p-anisidine, starch-iodide solution, and acidic pyramidone among other substances. As with most colorimetric reagents, stability is a problem and shelf life is very limited. Blue litmus paper has also been used for NO_2 detection as has cellophane coated with various dye mixtures. Silica gel has been coated with diphenylamine/NaCℓ solution, O-tolidine chloride, p-aminobenzoic acid/nickelous chloride solution, antipyrine, dimethylaniline and sulfanilic acid/N-(1-naphthyl) ethylene diamine dihydrogen chloride solutions, among others, to obtain response to NO_2. As with the filter paper coatings stability and shelf life are usually limited. Also there are generally many interfering substances which will also develop the characteristic color of the indicator dye species.

Reagent dye solutions used for NO_2 detection by volumetric methods have included acidified diphenylamine, sulfanilic acid/α-naphthylamine/acetic acid, phenoldisulfonic acid, indigosol in dilute sulfuric acid solution, and NEDA/sulfanilamide with phosphoric or tartaric acid.

Detection of ozone through surface colorimetric reactions has been ported[67] which use filter paper coated with tetramethyl-p-diamidodiphenylamine, benzidine, KI/starch, thallnium hydroxide, ferric oxide/potassium thiocyanate, and 4,4'-tetramethyldiamino diphenylamine. Others have used silica gel coated with liminol/NaOH, fluorescein/KOH, and fuchsin. Many of these systems are also responsive to other oxidants.

Volumetric colorimetric detection reagents for ozone have included m-phenylenediamine hydrochloride, fluorescein, indigo/sulfuric acid and sodium diphenylamine sulfonate/perchloric acid. One of the most widely used colorimetric reagents for ozone is aqueous potassium iodide. The Federal Reference method for calibration of ozone instruments uses 1% (by weight) KI buffered to a pH of 6.8 and assumes a unity conversion ratio of ozone to the triiodide ion colored species. This has been disputed.[68] Higher weight percentages of KI have been used, but there is evidence that the effect of NO_2 interference increases with increasing KI concentration.[69] To counter this, however, there is evidence that higher concentrations of neutral buffered KI give higher absorbances than lower concentration solutions in response to the same O_3 concentration, particularly at low O_3 concentrations.[70] In addition, the amount of KI used apparently affects the time required to develop maximum color at 352 nm.

From the point of view of portable instruments for the field the surface detection reagents are limited by their stability, i.e., by becoming de-colored or discolored "on the shelf", and the volumetric reagents present a logistics problem of continual supply and waste removal, as well as stability problems in many cases. Another problem is that the response times are relatively long. For "surface" reaction reagents, this is due to the necessity for the pollutant to penetrate by diffusion into the reagent to develop color to a sufficient depth to become detectable. For volumetric reactions there is the necessity to contact the sample stream with the reagent, following which diffusion must also occur to allow the reaction to take place in over a volume that will lead to a detectable quantity of colored species. In the cases where the absorbing reagent and the color-producing reagent are different, there is also an additional time penalty for mixing of the two.

4.5.2 Model Detectors

Several possible model volumetric detectors are shown in Figure 4.12. It is assumed that mixing of the air stream has occurred prior to entry into the analysis cell of each combination. The scheme of Figure 4.12A could be termed the conventional approach wherein linear

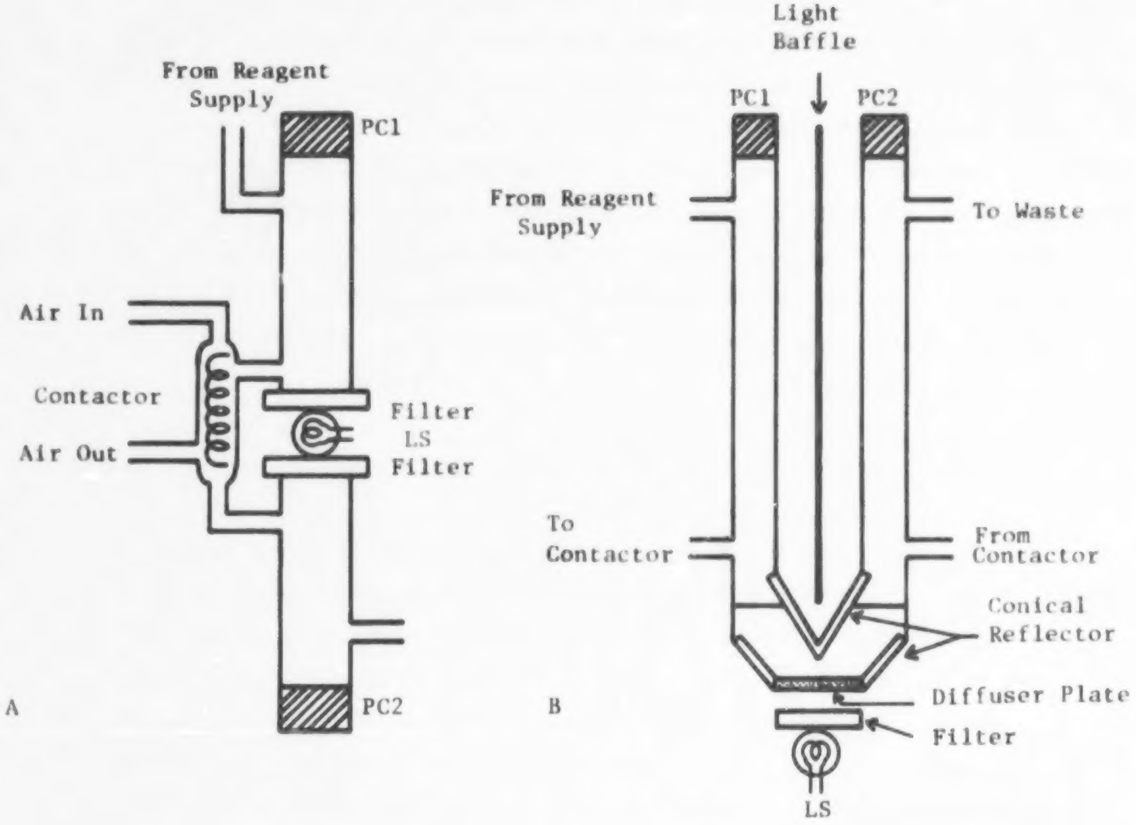
From Reagent Supply
PC1
Air In
Contactor
Air Out
Filter
LS
Filter
A
PC2
Light Baffle
PC1
PC2
From Reagent Supply
To Waste
To Contactor
From Contactor
Conical Reflector
B
Diffuser Plate
Filter
LS

Figure 4.12. Model Colorimeter Detectors.

cells are used with a sequential liquid reagent feed in order to eliminate a pump for this loop. For increased sensitivity the cell length L is made as long as practicable, since according to the Beer-Lambert relation

$$I/I_0T_L = 10^{-\epsilon CL} \qquad (4.41)$$

where I is the light intensity at the photodetector, I_0 the light intensity at the source, ϵ the molar absorption coefficient, C the molar concentration of absorbing species, and L is the path length. The factor T_L is the transmission factor for the liquid in the absence of colored species developed by the pollutant. The practical limit is the maximum allowable vertical dimension of the container for the instrument. For a briefcase sized package, a practical cell length would be about 10 cm at the most. With a molar absorptivity of the developed colored species of about $10^4(\text{M-cm})^{-1}$ the intensity ratio is related to the concentration by

$$C = -10^{-5}\log_{10}(I/I_0T_L)\text{mole/liter} \ . \qquad (4.42)$$

The detection limit is set by the minimum detectable intensity ratio change. This is determined by the ability of the signal processor to discriminate a change which is sufficiently larger--say by a factor of two--that the normal fluctuations due to photocell detector, amplifier "noise", light source fluctuations, refractive index fluctuations in the liquid and liquid absorbance fluctuations. If it is assumed that the dual chamber/photocell arrangement effectively cancels out light source fluctuations and that the sample air/colorimetric reagent liquid mixing is thoroughly done to eliminate absorbance fluctuations but in a manner that does not generate scintillations due to bubbles, the sensitivity limit is set by the system electrical noise. A practical value for this is about 1 part in 10^3. This corresponds to a concentration change of about 8×10^{-9} mole/liter.

Using an analysis similar to that given is Section 4.1.3 to determine the amount of material transferred from the sampled air stream to the liquid, the concentration of colored species will be given by

$$C = 4.46 \times 10^{-10} \left(\frac{273}{T}\right) \beta\eta\, x\, Q_a/Q_\ell \text{ moles/liter} \tag{4.43}$$

where T is the air temperature, β is the efficiency for converting one molecule of pollutant species to one molecule of colored species, η is the absorption efficiency of the liquid for the pollutant species, x is the volume ratio of pollutant species in the sampled air (in pphm), Q_a the air sampling flow rate, and Q_ℓ the reagent liquid flow rate.

Assuming the following values for these parameters

$T = 300°K$ $\qquad$ $Q_a = 100\ cm^3/min$

$\beta = 0.1$ $\qquad$ $Q_\ell = 1\ cm^3/min$

$\eta = 0.1$

the minimum detectable air concentration is about 0.2 ppm. In order to achieve the desired detection limit of 0.005 ppm, both the conversion and absorption efficiency would have to be increased until their product is 40 times the value obtained from those assumed above. Another possibility is that a colored species could be found which would have a higher molar extinction coefficient than the value of 10^4 assumed for this calculation.

The arrangement sketched in Figure 4.12B could use longer cells, but not more than a factor of two. A multipass arrangement such as the internal reflection scheme sketched in Figure 4.12C could be used to obtain longer effective path lengths. The ratio of path length per pass to cell length is sec θ, where θ is the angle of incidence and reflection. The number of passes, N, is determined by this angle and by the width dimension of the cell, W, from

$$N = (W/2L')\cot\theta \;. \qquad \text{[illegible]}$$

For a specular reflectance, R, assumed constant over both reflecting surfaces the light intensity at the exit slit, I, is related to that at the entrance slit, I_0, by

$$I/I_0 = R^N 10^{-\varepsilon CNL'\sec\theta} . \qquad (4.45)$$

As long as the reflectance remains constant in a time period long compared to the measurement time, the effect of reflectance changes can be taken into account by occasional instrument "zero" adjustments.

The major trade-off for the multipass arrangement is in response time and loss of time resolution versus increased sensitivity for the dose rate measurement. The larger volume requires more time to fill. For practical logistical reasons the reagent flow rate cannot be too large. One mℓ/min is equivalent to 1.440 liters (about 1.5 quarts), which quantity must not only be stored in supply, but also in waste. Assuming an entrance angle of 2.5° and 12 passes, the width required for the cell is about 11 cm if the cell length, L', is assumed to be 10 cm. For a cell thickness of 0.5 cm, the volume is 55 cm^3. At a flow rate of 1 cm^3/min, almost three hours would be required to achieve 95% response to a step change in input concentration. This can be compared a single pass cell, used in the methods shown in Figures A and B, with the same length, 10 cm, and with a diameter of 0.5 cm. The volume for this cell is only about 2 cm^3. At the same flow rate of liquid, 95% response to a step change would require only about 6 minutes. The sensitivity gained due to increased path length is about a factor of 12, versus a factor of 27.5 increase in response time.

Some of the response time could be regained by using a zig-zag chamber with reflecting surfaces at the "elbows". This method would reduce the volume and hence the response time, but only by the same factor as the increase in path length.

One possible model measuring device using surface colorimetric reactions is represented in Figure 4.13. The method depicted in Figure 4.13 uses a transparent film for transporting the reagent past a nozzle

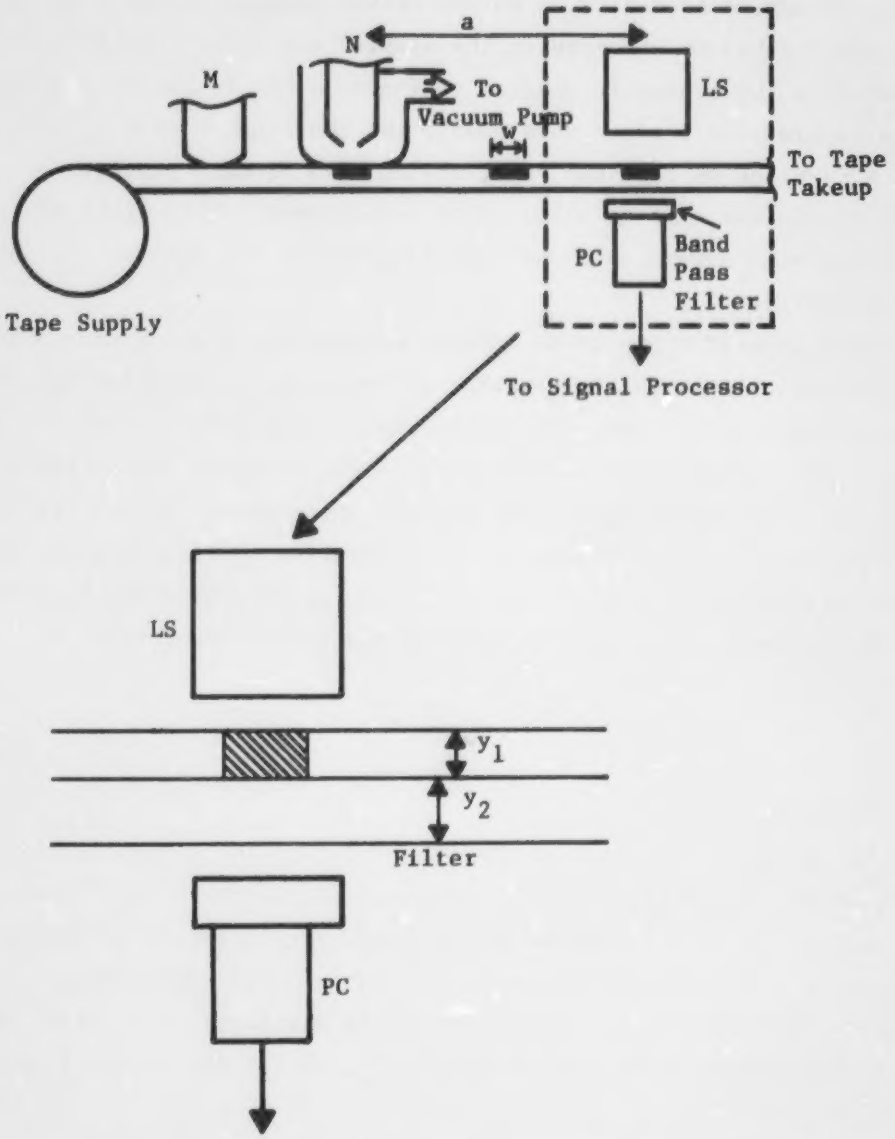
a
N
M
To
Vacuum Pump
w
LS
To Tape
Takeup
PC
Band
Pass
Filter
Tape Supply
To Signal Processor
LS
y_1
y_2
Filter
PC

Figure 4.13. Transparent Film Substrate Colorimetric Detector.

where sample air is impinged intermittently to provide alternating exposed, unexposed strips. Because of reagent stability problems upon exposure to air, and/or the necessity to provide moisture to enhance colorimetric reactions, it may be necessary to supply either reagent or water to the tape immediately before exposure to the sampled air. The applicator, designated M in the schematic diagram of Figure 4.13, is for this purpose. Spacing a is provided between this nozzle and the light source (LS)/ detector (PC) plane so that the tape, moving with linear velocity υ, will have sufficient time to allow color development. This width of the exposed strip will depend upon the "on" time of the air stream, t_s, and the tape velocity.

When the exposed strip is positioned between the light source (LS) and the photocell (PC), the development of color due to reaction between the reagent and the pollutant will attenuate the light in a given frequency band. A band pass filter can be used to reduce the incoming light to only those wavelengths near maximum absorption. It may (or may not) be necessary to add a heater in the separation space a in order to speed up the color development. The absorbing species will be distributed in the reagent layer, thickness y_1 with an integrated absorbance of

$$A_1 = \int_o^{y_1} \varepsilon c(y)dy = \varepsilon\bar{c}y_1 \; . \tag{4.46}$$

In addition to this there will be absorbance due to the supporting film of thickness y_2, characterized by an absorption coefficient α_2. The reagent film which is not exposed to the pollutant will have an absorption coefficient α_1. The filter, if used, will have a peak transmission, T_F, at the analyzing wavelength. Therefore in the absence of coloration the light intensity measured by the photocell, I_r, is related to the incident intensity, I_o, by

$$\log_{10} \frac{I_r}{I_o} = \log_{10} T_f - [\alpha_1 y_1 + \alpha_2 y_2] \; . \tag{4.47}$$

When all of the factors except the colored species concentration are constant, the ratio of intensities is

$$\log_{10}\left(\frac{I_s}{I_r}\right) = -\varepsilon \bar{c} y_1 \; . \qquad (4.48)$$

Spatial variations of thickness or absorption coefficient of either the reagent or the support film can occur. From equation (4.47), the intensity fluctuation will depend on these variations as

$$\frac{\delta I}{I} = -2.303[\alpha_1(\delta y_1) + (\delta\alpha)y_1 + \alpha_2(\delta y_2) + (\delta\alpha_2)y_2] \qquad (4.49)$$

where the δ( ) quantities represent small deviations from nominal values. If the length (in the direction of transport) of these is enough to spread them over at least one measurement-background cycle, they will be balanced out. If they are shorter, however, they can introduce error either through addition to or subtraction from the net absorption signal. Generally, the reagent depth, y_1, will be small compared to tape thickness, y_2. Also, if the applied reagent has uniformly wetted the tape surface there should be relatively few short term fluctuations in the reagent absorption coefficient. This leaves only fluctuations in tape thickness and absorption coefficient as possible major sources of error.

A more complex system for analysis is the model shown in Figure 4.14, The applied reagent--whether applied immediately before measurement by dispenser M or applied long before during tape manufacture or preparation prior to loading--is coated on the surface of the fibers that make up the tape. As shown in the sketch, a light beam coming from the light source will, more often than not, have to follow a tortuous path through the tape, undergoing multiple reflections from the fiber surfaces. Each reflection is through a thin layer of reagent coated onto the surface. If the reagent has been applied by M there may be an appreciable amount of liquid filling the interstices, even though sample air has been drawn through the tape to allow pollutant to develop the color. The multiple reflections greatly increase the path length and give much higher sensitivity than the transparent tape scheme previously discussed.

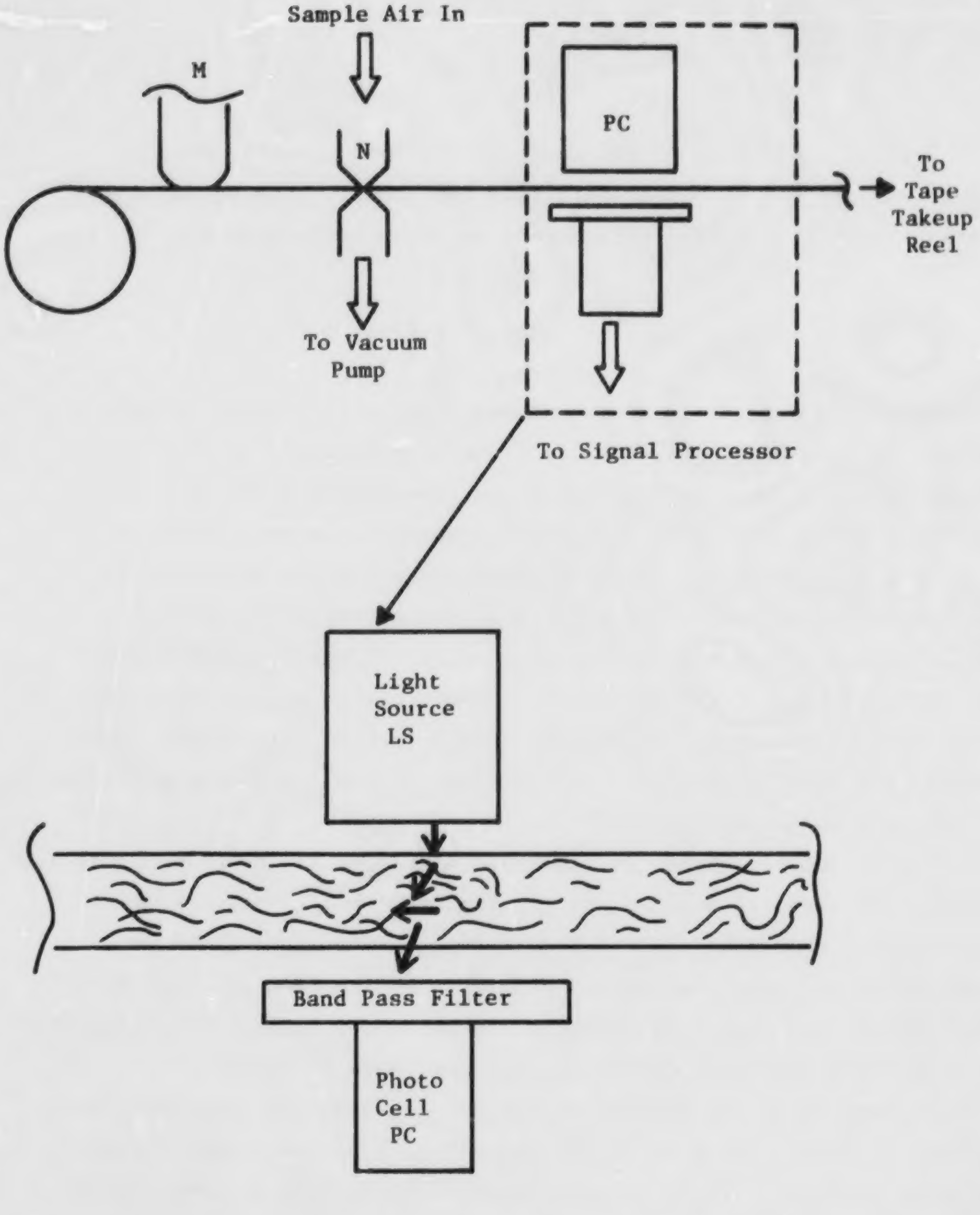
Sample Air In
M
N
PC
To Tape Takeup Reel
To Vacuum Pump
To Signal Processor
Light Source LS
Band Pass Filter
Photo Cell PC

Figure 4.14. Tape System Using Fibrous Tape.

A third method of measurement using surface colorimetric reactions is sketched in Figure 4.15. The multiple reflectance scheme discussed above also can lead to a large amount of backscattered radiation. This diffuse reflectance has been long used as an analytical technique. One particularly sensitive method is to use plane polarized radiation and select fiber or grain diameters in the diffuse reflecting surface to optimize the absorption at a particular wavelength. This has been discussed by Kortum[71] and an example is shown in Figure 4.16 to illustrate. In addition to polarization and particle or fiber size, the angle of observation, θ, for the detecting photocell, both measured with respect to normal incidence, can be selected to enhance the effect of absorption. This is illustrated in Figure 4.17, also taken from Kortum, where the reflectance as a function of θ is shown for various α values at two different wavelengths, one in the absorption range (550 nm) and one outside the absorption range (650 nm) for rhodamin dye coated on a paper substrate. For example, at $\alpha = 60°$, $\theta = 50°$ the fraction of reflected linearly polarized light has increased from 0.25 to 0.75 due to the absorption, a factor of 3, whereas for $\alpha = 0°$ and $\theta = 50°$, there has been a factor of 12 increase, although the intensity is lower than with the large angle of incidence.

A quantitative estimate based on a model of the diffuse reflectance mode of operation is difficult to obtain. For weakly absorbing powders the Kubelka-Munk theory[71] relates diffuse reflectance to concentration by the formula

$$c = S(1-r)^2/2\varepsilon r \qquad (4.50)$$

where c is the concentration (M) of absorbing species, S(cm^{-1}) a scattering coefficient, ε the molar absorptivity $(\text{M-cm})^{-1}$, and r is the ratio of diffuse reflectance with absorber to that without absorber. The value of S for very fine particles (1 to 4 μm) for the visible region is about 100 to 400 cm^{-1}. Assuming that a 1% change in reflectance is detectable, and that the colored species has an ε value of 10^4, the minimum detectable concentration change is, for $S = 200\ \text{cm}^{-1}$, 1×10^{-6}M. If these particles are silica with a specific surface of 1 M^2 per gram, packed with a porosity of 0.5, and the material converted to colored species has a depth of 0.1 μm

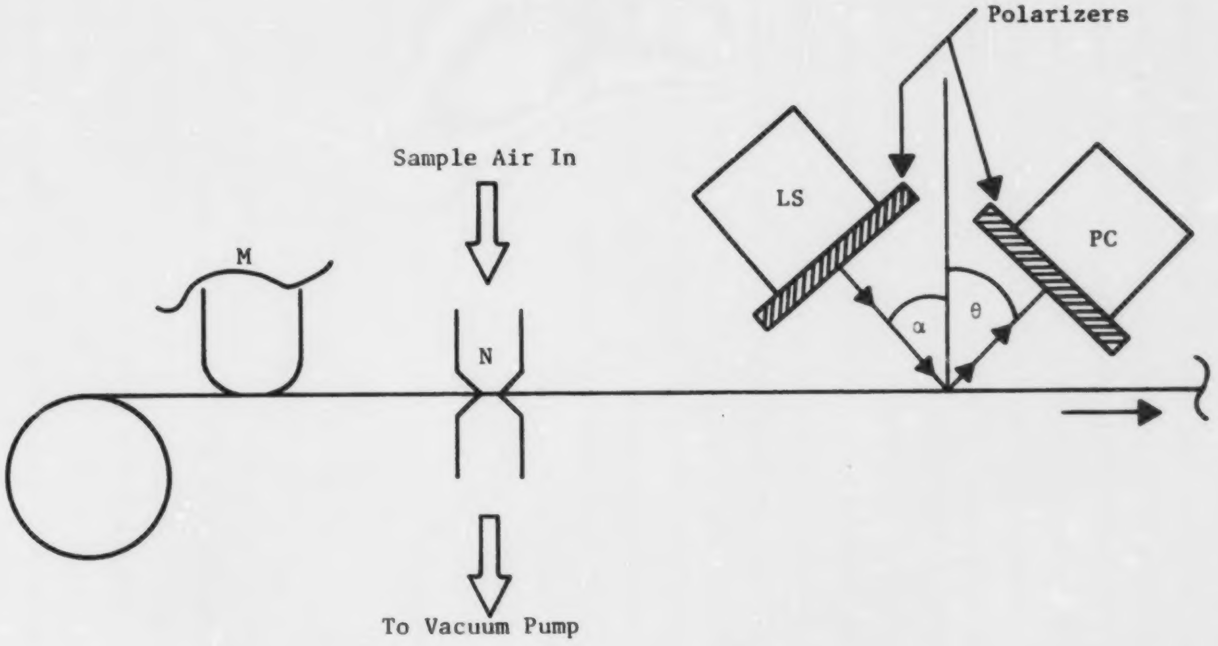
Polarizers
Sample Air In
M
LS
PC
α
θ
N
To Vacuum Pump

Figure 4.15. Measurement Using Surface Reflectance Change Due to Pollutant Exposure.

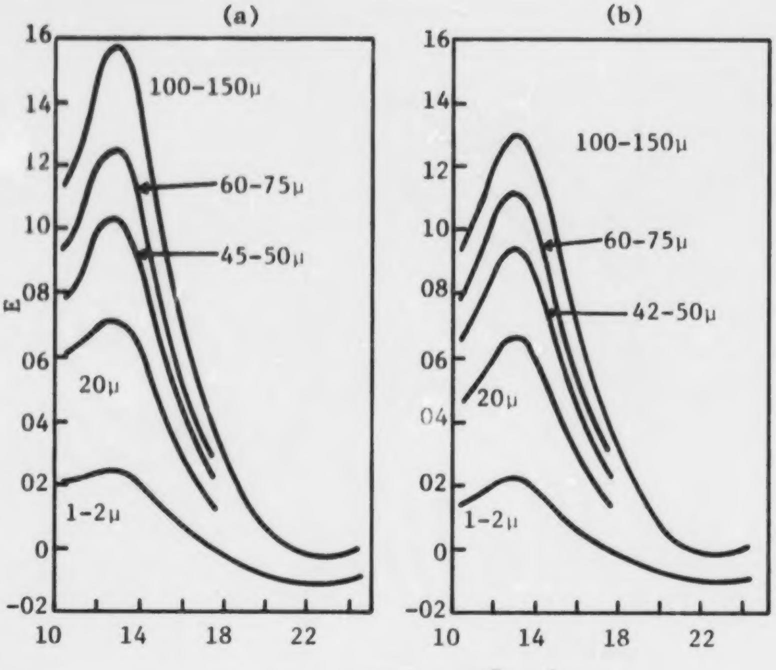

Figure 4.16. Remission Spectra of Pure $CuSO_4 \cdot 5H_2O$ at Five Different Crystal Sizes, Measured Against the White Standard of Zeiss; a) Taken with Polarized Radiation; b) Taken with Natural Radiation.

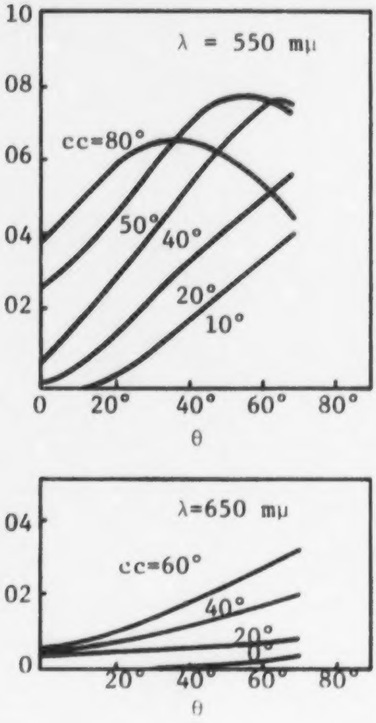

Figure 4.17. Fraction R of Linearly Polarized Light After the Reflection on Paper Dye with Rhodamin, for Various Angles of Incidence α as Parameter and Dependent on the Observation Angle θ. Lower Part: $\lambda = 650$ mμ; Upper Part: $\lambda = 550$ mμ (in the Absorption Range).

on the surface of each particle, distributed on particles in a volume defined by a 5 mm diameter spot to a depth of 10 μm, the quantity of colored material will be about 2×10^{-13} moles.

If it is assumed that the efficiency for converting pollutant to colored species is 1% and the quantity adsorbed represents that obtained from 100 cm^3 of sample (i.e., a sample air flow rate of 100 mℓ/min for 1 minute), the minimum detectable change corresponds to a pollutant concentration in ambient air of about 5 ppb.

This optimistic estimate depends upon the existence of a reagent which will develop colored species with a molar absorptivity of at least 10^4 $(M\text{-}cm)^{-1}$ and a reasonable value of the particle scattering coefficient S. If ε is smaller or S larger (or both), there will be corresponding factors of increase of the minimum detectable concentration of pollutant.

4.5.3 Projected Performance

Using a volumetric absorption technique similar to those analyzed in the preceding section, except with considerably shorter cells, Lyshkow has claimed a sensitivity of 5 ppb for both NO_2 and SO_2.[72] The detectors used were photoresistive. The Lyshkow method used reagent dyes which developed higher molar absorbance than the 10^4 $(M\text{-}cm)^{-1}$ assumed in the foregoing analysis. The absorbing solutions also had a higher value than the 10% efficiency assumed for the model calculation.

Of the three surface absorption techniques reviewed the use of reflected polarized light appears to be the most sensitive. If stable dyes can be obtained, the method should be capable of reaching the 5 ppb detection limit desired.

Sample and zero stability will be difficult to maintain in the dual sample cell-dual photodetector volumetric method because of differences in the individual photodetectors. An alternate arrangement is to use a single photodetector with a mechanical chopper to alternate transmitted light from the "signal cell" and the "reference cell" onto the detector. This increases design complexity but has an additional advantage of enabling the use of synchronous a-c signal processing techniques which can improve both stability and sensitivity.

Such a system is already inherent in the reflective surface adsorption technique. Alternation of exposed-unexposed (to sample intake air) surfaces provides a dynamic reference. However, the tape transport will be relatively slow, so that for all pratical purposes the photodetector signal will be d-c amplified unless some mechanical chopping arrangement is used to enable use of synchronous a-c detection.

For both methods the dynamic range is limited by the background coloration of the reagent dyes due to factors other than exposure to the particular pollutant to be detected.

4.5.4 Logistical Factors

The volumetric method requires a liquid supply of about 1.5 liter of reagent solution per pollutant per 24 hours and an equivalent amount of waste disposal volume. Sample air pumping requirements are minimal, easily handled by most of the pumps listed in Table 2.1. Although gravity feed could be used, it would probably be better to also pump the dye solutions. Signal processing electronics could be easily accommodated on a battery supply.

4.5.5 Dose Rate Information

After analog conversion from non-linear forms inherent in light transmission measurements, a continuous electrical signal proportional to pollutant concentration in ambient air is available for periodic sampling, digitizing, and storage by techniques discussed in Section 5.0.

4.6 Gas Phase Luminescence

Gas phase luminescence methods rely on the creation of an excited state (non-equilibrium energy state) of the pollutant or one of its reaction products. Spontaneous emission of a photon occurs when the excited molecule relaxes back to an equilibrium energy state. The wavelength distribution is characteristic of the molecule (specificity) and the emitted intensity is proportional to the pollutant concentration in the gas phase. Creation of the excited state can occur through chemical reaction (chemiluminescence), direct excitation by light (fluorescence/phosphorescence), or indirect excitation. In the latter case light excites a metastable state of some intermediate gas the excited gas molecules of which are capable of energy transfer upon collision with a pollutant molecule. Following this collisional transfer, the pollutant molecule can emit radiation via fluorescence.

4.6.1 Prior Use

Detection of ozone by chemiluminescence from gas phase reactions has been based primarily on the ozone-ethylene reaction first used by Nederbragt[73] and then improved by Warren and Babcock.[74] The method, used in conjunction with the wet chemical KI verification of the ozone output from a calibration ozonator.[75] Hodgeson, et al[76] have determined the spectral characteristics of the reaction and compared the performance characteristics of this instrumental technique to those of instruments based on the ozone-NO gas phase reaction and the ozone-Rhodamine B heterogeneous reaction.

The ozone-NO reaction has been studied in detail by a number of workers. Clyne and Thrush[77] and their coworkers have reported on the spectral characteristics and kinetics of the reaction. Fontijn[78] has been issued a patent on one configuration that uses the reaction for ozone detection, which is essentially the instrument compared by Hodgeson et al[76] to the ozone-ethylene instrument. Turning the reaction around and using ozone as a reagent, the method of Fontijn has been developed as an NO detector[79] and with the addition of an appropriate catalytic reduction surface to change NO_2 to NO[80] the instrument has been modified to some extent and developed for field use by several commercial firms. It has been reported that commercial NO_x monitors which rely on reduction of NO_2 to NO are non-specific but also convert PAN and other volatile organic nitrates to NO.[81]

Both the ozone-ethylene instrument and the O_3-NO instrument require a constant supply of gas reagent. In addition, the effluent from the reaction, excess ethylene or excess NO along with NO_2, must be scrubbed to prevent the production of pollutants.

In addition to the use of the gas phase chemiluminescent reaction between NO and ozone to detect NO and NO_x, and ozone-ethylene to detect ozone, the reaction between atomic oxygen and NO or SO has been used by Wooten et al to detect NO_x and SO_2.[82] Another patent[83] claims the use of the NO + O reaction to detect many nitrogen containing compounds.

The kinetics, energetics and spectral emission of reactions

$$O + NO \rightarrow NO_2^* \rightarrow NO_2 + h\nu$$

$$O + SO \rightarrow SO_2^* \rightarrow SO_2 + h\nu$$

have been studied and reported in a long series of papers by Thrush and his co-workers.[84-86] The O + NO reaction has been proposed as a standard for determining rate constants for other chemiluminescent reactions.[87] The method used by Thrush et al to produce these species was to break up SO_2 and NO_2 into SO, NO and atomic oxygen in a microwave discharge cavity and then study the recombination emission downstream of the cavity (afterglow). The method of Wooten et al[82] is to generate atomic oxygen separately with a pulsed (1-10 pps) electrical discharge. They use a reduced pressure of 0.5 to 5 torr in the reaction chamber. In this range there are no third body quenching effects[88] in contrast to the $NO + O_3$ and $SO + O_3$ reactions.

Sulfur dioxide has been detected down to a level of about 10 ppb in air by a fluorescent method.[89] Although the method has moved from the laboratory prototype stage to commercial instruments, it is not yet as well established as the ozone, NO_x chemiluminescence methods. Water vapor quenches the fluorescence, probably both in conventional gas phase collisional deactivation and by reactions of SO_2 with adsorbed water vapor on vessel walls. Collisions with many other types of gas molecules can also quench the fluorescence. These quenching effects greatly reduce the excitation efficiency making the emitted light intensity very weak. The sophisticated detection circuitry required for such low light is not readily reduced to miniature size. Table 4.11 taken from Reference 88 indicates the quenching effect of various vapor phase species normally found in ambient air on fluorescent emission by NO_2^* and SO_2^*.

4.6.2 Model

The reaction of SO and NO with ozone give emission intensities of[90,91]

$$I = \frac{K_1 K_2 [A] [O_3]}{K_2 + \Sigma_m K_{sm} [M]} \tag{4.51}$$

where [A] represents the concentration of either NO or SO and [M] is the concentration of third body species which contribute to quenching through collision with excited AO species. Since chemiluminescence is intimately related to the fluorescence properties of the AO species,[75] some idea of the effect of oxygen and nitrogen on quenching of cheiluminescence is gained by consideration of their quenching effect on fluorescence of NO_2 and SO_2. This has been studied and reported by Metee.[38] The kinetic studies of References 73 and 74 used argon as the third body. The data of Table 4.11 indicates that the quenching probability per collision is not drastically different for either NO_2 or SO_2 in their collisions with Ar, O_2 or N_2. Thus, the rate constants obtained in References 73 and 74 should be representative when air is the background gas rather than Ar or Ar/O_2. When pressures in the order of a torr or larger are used, $\Sigma_m K_{3m} [M] >> K_2$ and the emission intensity is given by

$$I = I_o [A][O_3]/[M] . \tag{4.52}$$

This gives the emission intensity in einsteins per second per liter when the concentrations are specified in moles/liter.

Table 4.11 SO_2 Emission Quenching Data[88]

Collision Partner	Collision Diameter (nm)	Polarizability ($10^{-30} m^3$)	Probability for Fluorescence Quenching per collision	
			SO_2	NO_2
N_2	0.386	1.76	0.28	0.10
O_2	0.369	1.60	0.27	0.13
CO_2	0.494	2.65	0.63	0.27
A	0.360	1.63	0.21	0.08
Ne	0.254	0.392	0.14	----

The effect of pressure and flow rate on emissions intensity has been studied by Steffenson and Steadman[92] for two different mixing arrangements and reactor configurations. The Fontijn spherical geometry reactor[79] has been analyzed by Harrison and Spangler.[93] Both analyses lead to an equation for the emission intensity of the form.

$$I_{eff} = \xi \, I_o \, \frac{[O_3]\,[NO]_o}{[M]} \, \frac{Q_A}{V_r} \, \tau_R \qquad (4.53)$$

where ξ = optical collection efficiency
$[NO]_o$ = initial NO concentration injected into the reactor
Q_A = gas flow rate
V_r = reactor volume
τ_R = lifetime of NO species due to reactions with ozone in the reaction volume.

Since the hydrodynamic time constant is V_r/Q (assuming perfect mixing), it can be seen that the emission intensity is related to the ratio of the reaction lifetime to the hydrodynamic residence time in the reaction chamber. The collection efficiency of the integrating sphere of Fontijn's geometry is on the order of 20% whereas the more cylindrical geometries used in the evaluation of Reference 92 would be expected to be somewhat lower. Most commercial instruments are designed to give as high detection (PM cathode) area to volume ratio as possible in order to approximate 2 π collection geometry.

As shown in Reference 93, the filter spectral response, photodetector spectral response and emission spectral characteristic can be combined to determine an average detector current per unit photon rate, which will be symbolized as G. This factor will include the photomultiplier gain factor if a PM tube is used. The signal current due to emission throughout the reaction volume V_R will be, when τ_R is approximated by $(k_1[O_3])^{-1}$, where k_1 is the rate constant for non-radiative reactions of NO and O_3,

$$i_s = 10^{-8} \, \frac{\xi G Q_A}{k_1} \, I_o \, \chi \, . \qquad (4.54)$$

A similar expression obtains for [SO]. Depending upon the type detector used and the type of signal processing (e.g., direct amplification or chopped light with a.c. amplification), the minimum detectable signal level will be set by dark current fluctuations or shot noise of the signal.

Comparison of the intensity factor, I_o, for the NO/O_3 and SO/O_3 reactions indicates a factor of about 4 higher intensity for the latter. This is counterbalanced by the fact that k_1 for the SO/O_3 reaction is about 5 times larger than that of the NO/O_3 reaction. However, the emitted light for the SO/O_3 reaction is in the 300-450 nm wavelength region[73] where photomultiplier cathode efficiencies are much higher than in $\lambda > 610$ nm region for the NO/O_3 reaction. These factors indicate that if some practical method is found to reduce SO_2 to SO in an analogous manner to that used for the $NO_2 \rightarrow NO$ reduction, a gas phase chemiluminescent detector based on SO/O_3 would be practicable.

The ozone-ethylene reaction is well known and has already been incorporated into portable instruments capable of monitoring ozone down to the ppb level.

Because of the low light levels available at low concentrations, a photomultiplier would have to be used. Presently available commercial silicon photodiode detectors have a sensitivity of about 0.2 Ampere/watt of radiant power in the 400 nm region. The sensitivity improves in the red and near infrared region, where the NO_2^* emission occurs, to 0.3 to 0.5 A/watt. This should be compared to the sensitivity of typically 15,000 A/watt available from a photomultiplier in the 400 nm region. Even though electronic amplification could be used to boost the dynamic signal from a silicon photodiode, careful design would have to be employed in a dark current suppression circuit to achieve proper temperature tracking.

4.6.3 Projected Performance

Presently available portable instruments for NO_x and ozone monitoring have the specifications shown in Table 4.12. Similar specifications could probably be obtained in a composite instrument package.

Table 4.12 Performance Values for Chemiluminescent Monitors

Parameter	Pollutant O_3	 NO_x
Span	100 pphm	100 pphm
Detection Time	0.1 pphm	1 pphm
Zero Drift	----	< 1 pphm/day
Span Drift	----	< 1 pphm/day
Sample Flow	1ℓ/min	1ℓ/minute
Response Time	20 seconds	1.1 minute

4.6.4 Logistical Factors

The data of Table 4.12 indicates that both instruments require relatively high flow rates. Equation (4.54) shows that the detector signal current should be directly proportional to the volumetric flow rate, Q_A, through the instrument. The air sampling pumps used must be capable of maintaining these flow rates at a constant value in order to minimize signal variations that could be construed as pollutant concentration variations. Several of the pumps listed in Table 2.1 are capable of 2 to 3 liters per minute, but at relatively low pressure drops. Stabilizing the sample air flows would be a problem. The high-flow rate pumps also use more power and limit the battery operation time to about 8 hours at the most. For the ozone monitor a source of ethylene is required. This can be supplied from a lecture bottle sized tank, but the continuous operating time will be limited to about 8 hours.

4.6.5 Dose Rate Information

A continuous electrical signal proportional to pollutant concentrators in ambient air is available for periodic sampling, digitizing, and storage by techniques discussed in Section 5.0.

4.7 Gas/Liquid Phase Luminescence

This method is based upon chemical reactions in a liquid medium containing a chemical reagent which is capable of emitting light when it reacts with species contained in an air stream which is contacted with the liquid.

4.7.1 Prior Use

The chemiluminescent reaction between ozone and a large number of organic dyes has been reported by Bowman and Alexander.[94] These reactions consume the organic species, producing reaction products which are generally incapable of any further useful emission. Life of the dye can be improved by using excitation transfer reactions[95] in a scheme symbolized by

$$A + B \rightarrow C^*; \; C^* + D \rightarrow C + D^*; \; D^* \rightarrow D + h\nu,$$

where A is the species to be detected (pollutant), B is an intermediate reacting species capable of combining with A to produce C in an excited state which can transfer its excess energy to a suitable chosen dye species D, creating an excited molecule which is capable of relaxing back to the ground state via emission of photon hν. This method was used by Bersis and Vassilious[96] to obtain chemiluminescent emission from Rhodamine B dye in a solution also containing gallic acid. The gallic acid was oxidized by ozone to create an excited species which tranferred energy to the Rhodamine B, which then emitted light.

Another approach is to use the pollutant species to catalyze a chemiluminescent reaction. Such a principle has been used to develop an instrument which monitors O_3, NO_2 and SO_2 via a catalyzed H_2O_2/luminol (5-amine-2,3-dihydro-1,4-phthalazine dione) reaction.[97] Detection limits in the range of 1-3 ppb are claimed for the method. Selected filters are used to absorb out various combinations of pollutants which are routed to different "microreactors" where they are mixed with the H_2O_2/luminol reagent to produce chemiluminescence. All of these "microreactors" are closely spaced in front of a two inch diameter PM tube. A rotating shelter sequentially exposes each reactor to allow the chemiluminescence from each pollutant to be monitored. The stored signals are compared to a zero air signal and stored calibration signals to obtain a quantitative readout.

A recent Russian patent[98] also uses luminol, modified by a copper-amine catalyst, flow through a porous disc to provide a continually fresh surface for exposure to ozone to obtain chemiluminescence.

4.7.2 Model

The miniature microreaction cells used in Reference 97 for the pollutant catalyzed H_2O_2/luminol chemiluminescent reaction employ very low reactant flow rates, ranging from 0.1 to 0.5 ml/min and high air flow rates, typically 2 ℓ/min. The cells are 0.635 cm (0.25 inch) I.D., resulting in a high air velocity which forces the liquid reagent into a thin film moving along the walls of the reactor tube. Light is emitted in the thin sheath of the liquid along the wall.

The geometry could be improved to enhance light collection and reduce the flow rate requirements. The use of a small amount of detergent to enhance uniform wetting of a glass surface by the liquid reagents would enable a flat surfaced cell with a mirror backing to be used in order to obtain as large a viewing angle as possible for the photodetector. In addition such mirroring could be used to isolate adjacent reaction cells to prevent "crosstalk" from the light generated by the filter-isolated pollutant/air streams flowing through each cell.

For a quantitative estimate of performance the mechanisms of the light generation reactions must be known in detail. From the data presented in Reference 97, it appears that for the reagent concentrations used--0.25 mg/ml luminol in 0.05N NaOH and 0.6% H_2O_2--the reactions are first order with respect to pollutant concentration. As shown in previous sections, the pollutant concentration, C, in an absorbing solution is related to the gas phase concentration, χ (in pphm), by

$$C = 4.46 \times 10^{-10} \, \eta Q_A \chi / Q_\ell \text{ mole/liter} \qquad (4.55)$$

where η is the absorption efficiency of the solution for the pollutant.

If κ is the rate efficiency for converting a pollutant species absorbed into solution into a photon emission, the emission rate will be

$$I = 4.45 \times 10^{-10} \kappa \eta Q_A \chi / Q_\ell \text{ einsteins/liter-sec.} \tag{4.56}$$

The detailed form for κ will depend upon the rates of reaction which cause or compete with (quenching) the emission.

The ratio of responses per pphm of pollutant for the reactant concentrations given above and for a Q_A of 2000 ml/min and Q_ℓ of about 1 ml/min are

$$(I/\chi)_{O_3} : (I/\chi)_{SO_2} : (I/\chi)_{NO_2} :: 1.0 : 0.2 : 0.04 .$$

Some of this difference is probably due to the difference in absorption efficiency. Both of the oxidants O_3 and NO_2 are capable of causing emission when only luminol (without H_2O_2) is used, but SO_2 gives no response.

The light emitted at the rate given by equation (4.56) will be emitted throughout a volume, V_R, determined by the thickness, δ, of the liquid film and the viewing aperture area, A. Use of reflective surfaces opposite the photodetector can improve the collection efficiency, as can close-spacing of the liquid film to the detector aperture. Taking these factors into account, the light rate to the photodetectors is

$$\phi = 4.46 \times 10^{-10} \xi V_R \kappa \eta Q_A / Q_\ell \chi \text{ photons/sec .} \tag{4.57}$$

Since the emitted light distribution is centered about 430 nm, this flux corresponds to a light power rate of

$$w = 2 \times 10^{-25} \xi \, V_R \kappa \eta Q_A \chi / Q_\ell \text{ watts} \tag{4.58}$$

where ξ is the light collection efficiency for the reaction cell/detector geometry, V_R the reaction volume, and the other symbols have been previously defined.

Of the parameters involved in equation (4.58) the emission rate κ is the one most difficult to quantitate. An estimate of the order of magnitude can be obtained from the data given in Reference 99. The EMI 9558 photodetector in that application is operated at about 1.5×10^4 A/watt at 430 nm. The response to ozone at 1 pphm, 17.9 v (across an anode load resistor of unspecified size) ratioed to the 0.5 v noise level, taken to correspond to 10^{-8} A, gives an estimated light power rate of 2.4×10^{-11} watt.

Assuming the following parameter values:

$\xi = 0.25$ $\eta = 1.0$ $Q_\ell = 1$ ml/min

$V_R = 1.2 \times 10^{-4}\ell$ $Q_A = 2000$ ml/min

gives a value for κ of 2×10^{15} photons/sec at 300°K.

In order to see whether or not a simpler photodetector can be used, i.e., a silicon photodiode rather than a photomultiplier, the estimated light power at 430 nm for 1 pphm of ozone, 2.4×10^{-11} watts can be used with a typical sensitivity figure for a commercial silicon photodiode of 0.2 Amperes/watt at 430 nm.[99] The photodiode would generate about 5 picoamps. This is well below the nanoampere dark current level typical in these devices. For a 1 Hertz bandwidth of the signal processing system, the shot noise corresponding to this dark current is calculated from

$$i_N = \sqrt{2eI_D\Delta f} \qquad (4.59)$$

where e is the magnitude of the electronic charge, I_D the dark current level and Δf the bandwidth, as 1.8×10^{-14} amperes. This is about 2 orders of magnitude less than the signal current. The dark current is very sensitive to temperature, doubling with every 10°C change. It could probably be zeroed out at a given temperature, but sophisticated circuit design would be required to make the zero track the dark current as temperature varied. A signal current level of 5 picoamperes (for ozone, for which the luminescence is highest) would require a carefully designed electrometer system, which would be difficult to keep operating properly, even in a laboratory environment.

Therefore, it appears that a photomultiplier must be used. Several commercial domestic and foreign firms make 1.27 cm or 1.9 cm diameter miniature PM tubes that would have sufficient sensitivity for this measurement scheme.

The patented method for the H_2O_2/luminol measurement technique uses a 5 cm diameter tube with a rotating shutter which sequentially exposes microreactors for viewing through 1.27 cm apertures. Another possible arrangement is to have a single reactor cell facing a single 1.27 cm diameter end-on PM tube and sequentially valving in a sample air stream which has been sequentially diverted through appropriate filters. Another possible arrangement is to use a rotating lens/prism system to sequentially reflect light from separate reactor cells to a commonly used PM tube. The third alternative is to use separate PM tubes. Not only would this be expensive in terms of power supply energy, weight and initial cost, but the different aging characteristics of different tubes would probably require frequent recalibration.

4.7.3 Projected Performance

The H_2O_2/luminol method appears to be promising in terms of sensitivity, detection limits and dynamic range. Assuming that a scaled down version can approach the performance of the patent prototype, the desired detection limit will be about 10 ppb. A dynamic range of 400 can be expected. Response time will depend upon the configuration used, but will probably be about 1 minute if a sequential sampling method is used.

4.7.4 Logistical Factors

Miniature photomultipliers are now being routinely used in portable equipment. Power demands are moderate, about 1.0 watt, which can easily be supplied from battery sources. Operating times of 10 to 12 hours on battery power should be possible. Reagent reservoirs of about 1ℓ each would be required for the luminol solution and the H_2O_2 solution. An equal amount of waste storage volume would be required for the spent reagent. Both solutions are apparently stable for a few days if stored under low light level exposure. Battery power would also be required for the air sampling pump and the liquid reagent pumps. An additional power demand would be imposed if a thermoelectric coder were used to stabilize the PM tube.

4.7.5 Dose Rate Information

Following PM tube signal processing, the integrated dose signal per pollutant, per cycle would be available for digitizing and storage by techniques discussed in Section 5.0.

4.8 Gas/Solid Luminescence

In this method the gas phase pollutant reacts with a reagent layer coated on a solid substrate to produce a chemiluminescent emission which can be measured by a photodetector and related to pollutant concentration.

4.8.1 Prior Use

In addition to experiments with chemiluminescence of liquid phase organic dyes exposed to ozone, Bowman and Alexander[94] also used dyes deposited on high area, dry subtrates, such as silica gel. Somewhat earlier Regener[100] had reported the use of Rhodamine B on silica gel for atmospheric ozone measurements.

Rhodamine B on silica gel has been used for the measurement of ozone in ambient air in an instrument prototype developed by RTI for EPA.[101] The operating characteristics of this instrument have been evaluated and described in detail by Hodgeson et al.[102] These authors have reported the use of a silicone resin to coat the silica gel substrate in order to minimize the adsorption of water vapor, which can have a large effect on both the time response and sensitivity of the chemiluminescent emission. Another problem, the gradual reduction with time of emission intensity at constant ozone input, is compensated in the instrument design of Reference 101 by periodic zero and calibration steps included with a measurement step in the operational cycle.

Guicherit[103] has reported that the use of gallic acid mixed with Rhodamine B prior to deposition on a silica gel surface precoated with a hydrophobic material produces very stable emission over a long period of time. As with the instrument described in Reference 101, Guicherit's instrument requires periodic exposure to ozone-free air. The sample-zero cycle time is relatively short, one minute, with 10 to 15 seconds allotted to sample measurement. The ozone-free air is prehumidified to provide a moisture content comparable to the sampled air. This prevents the transient response variation reported by Hodgeson, et al, who cycled dry zero air versus moist sample air. Because of the stability of the surface no internal calibration step was required, reducing both cycle time and instrument complexity. The instrument response was reported to be linear over the range 20-2000 μg/m^3 (0.01 to 1 ppm ozone). Normal ambient levels of NO, NO_2 and SO_2 were reported to have no effect. Testing up to 2 ppm with these as well as H_2S, Cl_2, NH_3, HCl, HF and H_2O_2 produced no interference. However, at much higher concentrations, up to 100 ppm, NO_2, Cl_2 and SO_2 were found to attack the chemiluminescent material. In field evaluations the calibration of the instrument remained stable over several weeks of continuous monitoring and showed close agreement with an electrochemical (galvanic) method.

The use of gallic acid with Rhodamine B by Guicherit in a dry form was based on a report of the same mixture used in solution form by Bersis and Vassilious.[96] It is one example of a general class of excitation transfer reactions which have been discussed above in Section 4.7.1.

One of the problems of chemiluminescent methods of detection is to get adequate mixing of the reagents. For example, the instrument of Reference 101 uses a spiral pattern of airflow across the RhB/silica gel disc to establish contact. With this arrangement at constant O_3 concentration the light output is proportional to flow rate for low flows (less than 200 mℓ/min) but tends to saturate at higher flows, indicating that an increasing proportion of material is going through unreacted.[102] The same phenomena is reported in Reference 103. Lyshkow has recently obtained a patent[104] on a device for producing turbulence in the analysis gas stream by close spacing in the reaction volume exposed to the detector PM tube. He claims that this is suitable for both gas phase, e.g., O_3-ethylene, or gas-solid, e.g., NO_2-sulfanilimide, or O_3-Al, chemiluminescent reactions.

4.8.2 Model

Miniaturization of an ozone analyzer appears to be a straightforward application of existing design such as that of Guicherit. Extensive research would be required to develop methods of extending the techniques to NO_2 and SO_2.

4.8.3 Projected Performance

A dynamic range of 0.01 to 1 ppm can probably be achieved with the reduced version. The 1 minute cycle time required for period zero air/sample air cycling limits the response time.

4.8.4 Logistical Factors

A sampling pump, an inverter for obtaining high voltage from the PM tube, and the signal processing electronics would all require battery power. Switching streams in the alternate zero air/sample air rhythm would require battery power also.

4.8.5 Dose Rate Information

A digital signal representing the ambient air ozone concentration would be available once a minute for electronic storage by techniques discussed in Section 5.0.

4.9 Ionization and Electrophoresis

The ionization detector[105] and electron capture detector[106] are examples of devices which ionize gaseous species and then drift them in an electric field to obtain a current which can be related to the concentration of the ionized species. The main problem with these simple devices is their lack of specificity. Many substances can be ionized by electron extraction or proton extraction, or proton capture or electron capture. Substances can be ranked in their ability to participate in such charge exchange or ion-molecule reactions.[107,108] However, some separation method such as a gas chromatographic column must generally be employed to supply only a known species to such a detector in a given time interval in order to develop a quantitative signal. Another method is to use the differences in mobility (velocity per unit electric field) between different ions to separate out a desired species.

4.9.1 Prior Use

Electrophoretic techniques, using the difference in mobility of ionic species to separate different species in a drift field (electrical field) while known to physicists for many years,[109] have been employed only recently for analytical purposes. The most prominent commercial example is the Plasma Chromatograph.[110] This instrument uses a beta emitter, Nickel-63, to produce primary ions which are capable of transferring charge, or participating in ion-molecule reactions, with molecular species to be analyzed. Identification of species is by means of characteristic drift times of different species, periodically gated into a gaseous drift field. While a great deal of theoretical work has been done on ion mobility,[111] practical measurements must rely on instrument calibration with known species under well defined operating conditions, just as gas chromatography is practiced. This instrument operates at ambient pressure, making atmospheric sampling much easier than with any other analytical instruments.

Vree and Fontijn[112] have disclosed an electrophoretic device in which chemionization is used to produce primary ions which are then reacted with gaseous molecular species to produce ions. These are pulled at a given stream velocity through a transverse electrical field. A schematic diagram is shown in Figure 4.18. This is a modification of an old technique known as the "Erickson air blast method".[109] Those ions with a mobility larger than some limiting value , K_o, are collected by the electrodes before being swept downstream. This method serves as an integral device, giving the number of ions of mobility greater than K_o, in contrast to the Plasma Chromatograph which serves as a differential device, giving the mobility distribution.

Another variation of this approach is to use a radioactive foil to create ions and then direct these through a series of baffles with potentials maintained on adjacent electrodes of such a magnitude that only those ions with mobilities in a narrow range, ΔK, about some central value R can be deflected along the tortuous path through the baffles without being discharged at some intermediate electrode and survive to be collected as a signal current. Devices built on this principle have been employed as detectors for chemical agents in ambient air by both the U.S. Army and Air Force.[113]

Lovelock[114] has obtained a British patent on the use of the electron capture detector to quantify the product of reactions which convert SO_2, NO_x and other pollutants (but not ozone) to electron capturing species.

Nov. 17, 1970 P. H. VREE ET AL **3,540,851**

METHOD OF DETERMINING TRACE AMOUNTS OF GASES

Filed Aug. 25, 1967

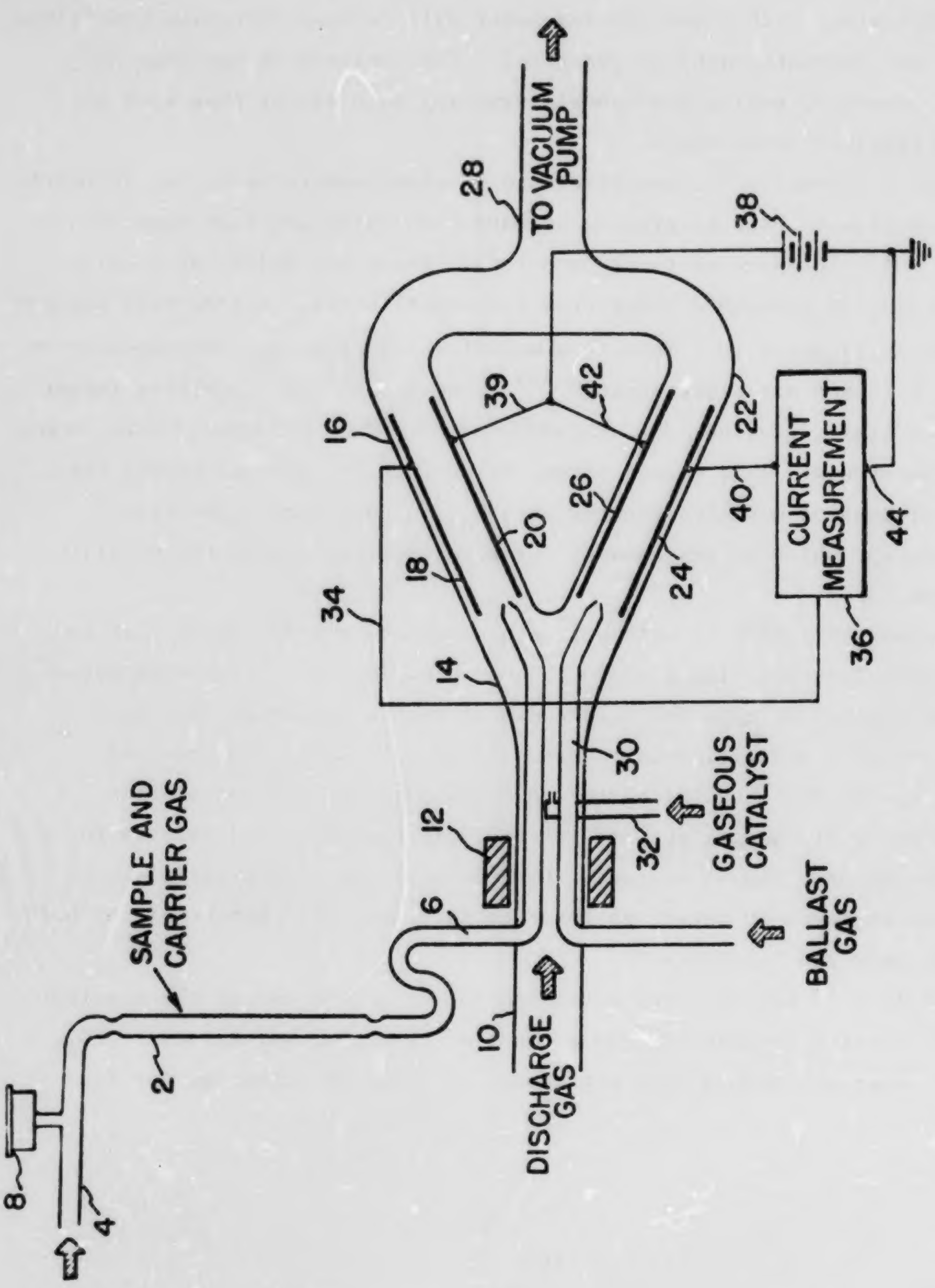
SAMPLE AND CARRIER GAS
8
4
2
6
10
DISCHARGE GAS
12
32
GASEOUS CATALYST
BALLAST GAS
30
14
34
18
20
16
39
42
26
22
24
28
TO VACUUM PUMP
38
40
CURRENT MEASUREMENT
44
36

Figure 4.18 Ionization/Electrophoresis Apparatus of Vree and Fontijn.[112]

4.9.2 Model

These brief considerations of ionization/electrophoresis suggest that a compact instrument could be designed based on the operating principles shown schematically in Figure 4.19. The sample air stream would be diverted sequentially to selective filters F_1, F_2, F_3 to pass only those components to be analyzed to the beta foil analyzer. A polarizing voltage source, V_A, would determine the polarity synchronized with that of V_A and would impose a transverse drift velocity $V_T = K E_r$ over length L. Only those ions with a mobility, K, such that their longitudinal velocity, u, and their transverse velocity transported them to collection electrode, C, would be registered as a current detected by an electrometer. The air stream could be moisture conditioned to maintain a constant hydration of the ionic species generated.

The hydration factor is important. To illustrate this, Figure 4.20 , taken from Reference 115, shows the distribution of hydrated protons as a function of temperature and water vapor partial pressure, when the hydrated ions are of the form $H^+(H_2O)_n$. This hydration can affect the mobility in two ways-by increasing the mass and by changing the collision cross-section. The effect on mobility of these parameters can be seen by considering the theoretical formula for mobility[111]

$$K = \frac{2.02 \times 10^{-8}}{N\sigma} \sqrt{\frac{(M_P + M_D)}{TM_PM_D}} \tag{4.60}$$

where N is the molecular density (m^{-3}) of the gas through which the ion drifts, σ is the collision cross section (m^2), M_P and M_D are molecular masses (kg) of the pollutant and drift gases, respectively, and T is the gas temperature. It is also obvious that a change in either gas pressure (i.e., N) or temperature can also affect the mobility. If the method is to be used as a measuring device compensation for changes in these parameters must be provided.

If it is assumed that the effect of adding one H_2O molecule is to increase the pollutant molecular diameter by one H_2O diameter and that subsequent hydration does not appreciably change the collision cross-section,

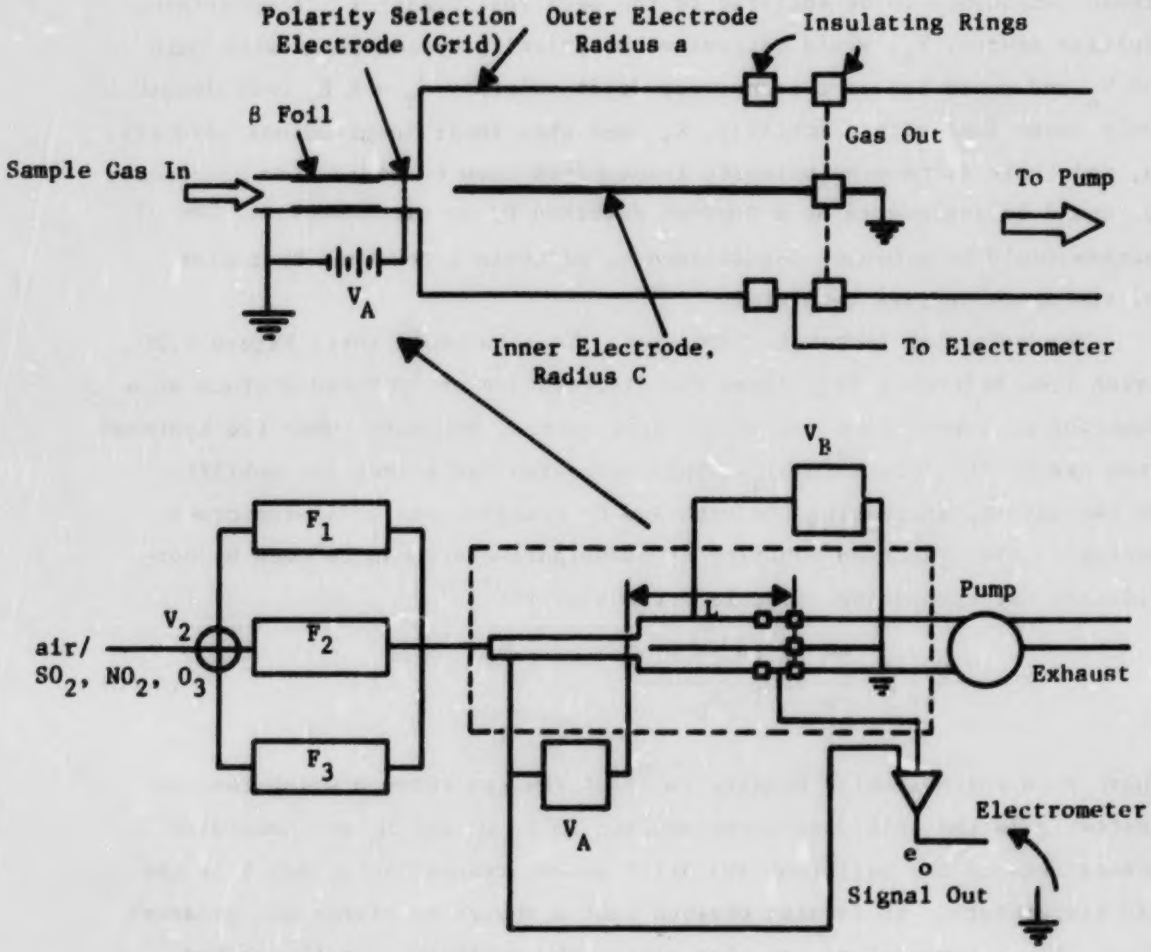
Polarity Selection
Electrode (Grid)
Outer Electrode
Radius a
Insulating Rings
β Foil
Gas Out
Sample Gas In
To Pump
V_A
Inner Electrode,
Radius C
To Electrometer
V_B
F_1
L
Pump
V_2
air/
SO_2, NO_2, O_3
F_2
Exhaust
F_3
V_A
Electrometer
e_o
Signal Out

Figure 4.19. Ionization/Electrophoresis Detector.

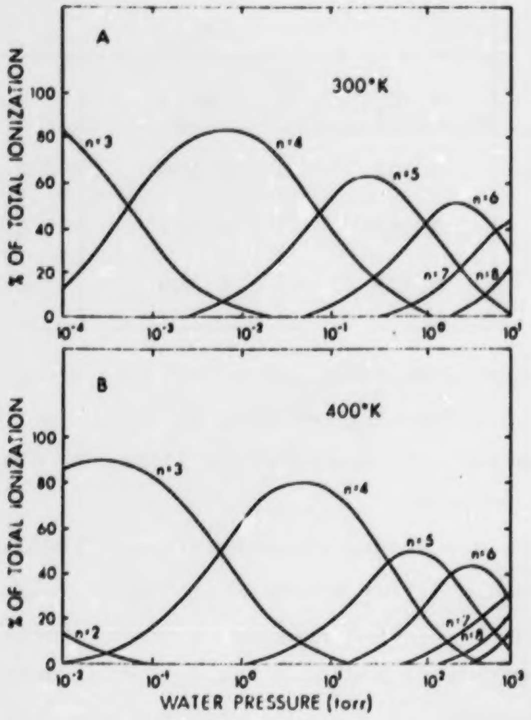

Figure 4.20 Equilibrium Distributions of Clusters $H^+(H_2O)_n$ Predicted by Experimental Data.[115]

the change in mobility at constant total pressure and gas temperature will be as shown in Table 4.13 below.

Table 4.13 Effect of Hydration on Mobility of SO_2, NO_2 and O_3 Molecules

Number of water molecules, n	K_n/K_o		
	SO_2	NO_2	O_3
1	0.392	0.330	0.356
2	0.383	0.317	0.343
3	0.375	0.310	0.332

If this model is representative, the effect of adding the first water molecule is drastic, reducing mobility to about one third its dehydrated value. Thereafter, the magnitude of effect is diminished, but still amounts to a few percent.

Assuming the use of a cylindrical geometry, as shown in the enlarged version of the drift tube analyzer sketched in Figure 4.19, with a thin central electrode of radius c at potential V_B with respect to ground, a coaxial gas inlet aperture of radius b and a coaxial outer electrode of radius a, at ground potential ("zero"), the radial electric field strength at a distance $c > r > a$ is given by

$$E_r = V_B \ln\left(\frac{a}{c}\right)/r . \tag{4.61}$$

The velocity in the radial direction will be

$$v_r = \frac{dr}{dt} = KE_r . \tag{4.62}$$

Substitution from (4.61), separation of variables and integration between appropriate limits gives

$$\int_{\gamma}^{a} r dr = \int_{0}^{\Delta t} KV_B \ln (a/c) dt \tag{4.63}$$

which can be solved to obtain an expression for K, i.e.,

$$K = (a^2 - \gamma^2)/2\Delta t\ V_B \ln(a/c). \qquad (4.64)$$

The lower limit of integration along radial displacement in (4.63), γ , represents the uncertainty in starting position of an injected ion. It will start somewhere between the surface of the center electrode, $r = c$, and the outside of the injection aperture, $r = b$.

For analysis it is desired that only those ions with mobility in a narrow range ΔK about a central value $\overline{K}$ reach the collector electrode which is located a distance L longitudinally down the drift tube from the injection plane. The electrode width is 2w, centered on L. If the average longitudinal velocity component is u, the appropriate time factor, Δt, in equation (4.64) is given by L/u. Therefore

$$K = u(a^2 - \gamma^2)/2\ L\ V_B \ln(a/c). \qquad (4.65)$$

Because of the variations of the parameters in equation (4.65) there will be uncertainties in the precise value of K. This uncertainty, δK, is related to the magnitude of parameter variations by

$$\frac{\delta K}{K} = \frac{\delta u}{u} - \left(\frac{2c^2}{a^2 - c^2}\right)\frac{\delta\gamma}{\gamma} - \frac{\delta L}{L}. \qquad (4.66)$$

The velocity uncertainty can occur due to variations in flow rate. The second factor reflects the uncertainty in starting position, as mentioned before. The third factor indicates the finite width of the collector electrode.

A one percent variation in flow rate will cause a corresponding one percent uncertainity in mobility measurement. For the following assumed dimensions:

$c = 1 \times 10^{-3}$m $\quad a = 2 \times 10^{-2}$m $\quad w = 1 \times 10^{-3}$m

$b = 3 \times 10^{-3}$m $\quad L = 1.0$ m

the uncertainty due to a spread in starting positions will be 2% and the range of mobilities collected by the finite width electrode will be one percent.

The amount of current produced at a given pollutant concentration will depend upon the ionization efficiency of the pollutant. It appears that negative ions for mobility analysis would be feasible for NO_2, SO_2 and O_3. The electron affinity of NO_2 is very large, 4 electron-volts per molecule, and that of ozone is also large, about 2 electron-volts per molecule. While quantitative data are not available for SO_2, it is known that it does participate in charge transfer from other negative ions.

A simple model for the charge transfer process from reactant ions at density $N_R(cm^{-3})$ to "target" species (such as NO_2, SO_2 and O_3) at an initial density N_{AD} (cm^{-3}), which has been developed elsewhere,[116] shows that the number of ions formed per second is given by

$$n_I = (A\ V_I\ K_R\ \tau_R) N_R N_{AD} \tag{4.67}$$

where A is the cross-sectional area of the ion-molecule reaction region, V_I is the ion drift velocity, K_R the ion-molecule reaction rate, and τ_R the drift time in the reaction region. The pollutant concentration can be written in terms of pphm by volume at 300°K as

$$N_{AD} = 2.43 \times 10^{11} x \text{ molecules/cm}^3 . \tag{4.68}$$

Assuming only one electronic charge per molecule, and 100% current collection efficiency, the current developed per pphm of pollutant will be

$$I/x = 3.9 \times 10^{-8}\ (A\ V_I\ K_R\ \tau_R)\ N_R . \tag{4.69}$$

values of the parameters can be estimated by assuming that the ionization region is a tube of 6 mm ID and 2 cm length through which the sample air stream flows at 100 cm^3/min. It will be further assumed that the longitudinal drift field which selects the polarity of the ions to be analyzed is small, on the order of 10 V/cm. The value of K_R will be taken as the Langevin limit of $10^{-9} cm^3/sec$. The value of reactant ion density can be estimated from the value of current available from electron capture detector sources, about 10^{-8} amps, as around $10^9 cm^3$. Using these parameter values in equation (4.69) gives a value for I/x as about 20 nA per pphm. Since the saturated current value for the ion source was assumed to be 10 nA, it is apparent that saturation effects would start to limit current at well below 1 pphm.

It is this extreme sensitivity that makes the method subject to so many interferences. Any species present in the air sample which tends to form ions of the same polarity as the target species can interfere. If the interferent has a higher charge affinity than the target species, or is present in sufficient concentration, the ion current due to the target species can be severely depleted or suppressed altogether.

4.9.3 Projected Performance

While the method can be sensitive to very small concentrations of pollutant it is subject to many interferences and many errors unless a more sophisticated analysis scheme is used than has been outlined above.

4.9.4 Logistical Factors

The method requires active sampling at a rate which is easily accommodated by any of the pumps in Table 2.1. The electronic signal processing circuits and bias polarity sources are easily available from battery signals.

4.9.5 Dose Rate Information

A continuous electrical signal proportional to pollutant concentration in ambient air is available for periodic sampling, digitizing, and storage by techniques discussed in Section 5.0.

4.10 Piezoelectric Mass Monitor

The principle of the method is to coat a quartz crystal with a thin layer of selectively adsorbing material. The coated crystal is used in an electronic oscillator circuit as the frequency controlling element. The coated crystal is then exposed to a gas stream containing the component to be selectively adsorbed. An equilibrium point is reached after a sufficient time interval at which a certain amount of mass has been added to the crystal. This causes a reduction in resonant frequency. A calibration between component partial pressure and frequency change can be established to obtain a compact, relatively simple measuring device.

4.10.1 Prior Use

For many years the change in frequency of a quartz crystal due to mass loading has been used as a method for monitoring the deposition of thin films. King[117] proposed that this principle be used as a selective detector by using a selective sorbent to coat the crystal electrodes. For quartz crystals King gave the relation for change in frequency, ΔF, with mass, ΔW, as

$$\Delta F = 2.3 \times 10^6 F^2 \frac{\Delta W}{A} \tag{4.70}$$

where F is the original resonant frequency of the crystal (in MHz) and A the area of the coated electrode. At a typical resonant frequency of 9 MHz a frequency change of about 500 Hz per microgram was reported.

The King sorption detection has been reported as used in many different applications. Pertinent to the present application--to measure NO_2, SO_2 and ozone--Frechette and his coworkers[118] have examined various coatings to determine their applicability in the selective sorption of SO_2. They concluded that SDM polymer (a 1:1 copolymer of styrene--dimentylaminopropyl maleimide) was the best candidate for a selective sorbent and proceeded to evaluate the performance of a mass monitor using SDM.[118] They reported that both water vapor and NO_2 could interfere. In addition it was found that the frequency change, ΔF, per microgram of SO_2 decreased with increasing sample size and that the response thus increased with increasing sample size.

The longer time response with larger sample size is also not surprising since it is likely that appreciable diffusion of the gas into the sorbent must occur to allow transfer of more gas across the gas-sorbent boundary layer.

The non-linear behavior of frequency change with increasing mass is not surprising considering equation (4.70). It can be shown[119] that the integral form of this equation is

$$\Delta F = \frac{(\Delta W)\, B}{1 + (\Delta W) B / F_o} \tag{4.71}$$

where B is the mass sensitivity at frequency F_o. If the mass loading of the sorbent plus the adsorbed gas causes a frequency change that approaches

2% of the base frequency, a more detailed look at the relationship between the deposited mass and resonance characteristics of the crystal-deposit system indicates that a period measurement is more appropriate than a frequency measurement, and that it is possible that the acoustic properties of the deposit might have to be taken into account[120] when the mass loading is very large.

4.10.2 Model

Consideration of the use of piezoelectric mass monitors as portable continuous detectors is attractive because they can be made very compactly, use relatively simple circuitry, are relatively inexpensive and comparatively rugged. Prior to consideration of the method for continuous monitoring, however, the limitations of the device must be thoroughly understood. We now address these under two categories--the acoustic system (crystal, coating gas) and the adsorbent system (coating, reactant gas).

Acoustic System

The quartz crystal orientation most frequently used in the AT cut. Its orientation relative to the major crystal axes[121] is shown in Figure 4.21. Nominally it is cut at about 35°10' in order to get a relatively low shift of resonant frequency due to ambient temperature changes. The effect of orientation on this temperature-frequency relation can be appreciated by considering the curves[122] in Figures 4.22-4.25. At 27°V an AT cut of 35°10' gives a relatively small $\Delta f/\Delta T$, roughly 25 Hz for a ± 10° change for a crystal resonating at 9 MHz at 27°C. The sign of the frequency deviation will depend upon the exact orientation of the crystal cut. For example, the data of Figure 4.22 shows that a deviation of just 5 minutes of arc from the 35°10' figure can either rapidly increase the $\Delta f/\Delta T$ (increasing angle). Figure 4.23 shows a family of such curves. Ideally there is one curve, corresponding to one precise orientation, that will give zero temperature coefficient at a particular temperature. This relation is shown in Figure 4.24. A detailed portion of this curve for ΔT cuts is shown in Figure 4.25. These data indicate the desirability of knowing the exact orientation of the crystal to be used in order to select the operating temperature that gives negligible temperature effect on frequency for small deviations.

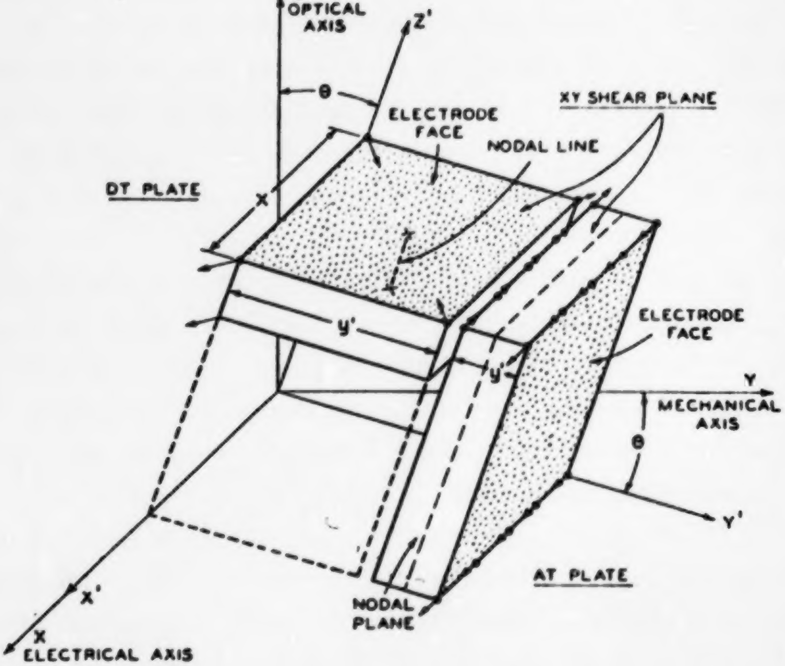
Z
OPTICAL AXIS
Z'
θ
ELECTRODE FACE
XY SHEAR PLANE
NODAL LINE
DT PLATE
x'
y'
ELECTRODE FACE
y'
Y
MECHANICAL AXIS
θ
Y'
AT PLATE
NODAL PLANE
X'
X
ELECTRICAL AXIS

Figure 4.21 Orientation of AT and DT Cuts with Respect to Major Axes of Quartz.[121]

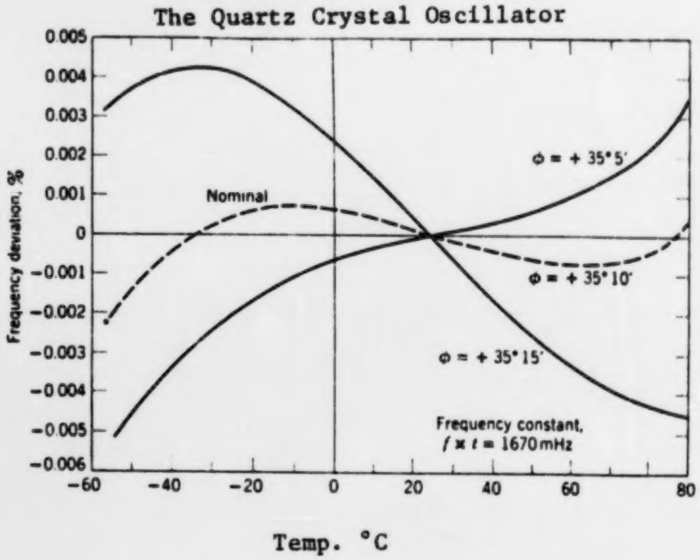

Figure 4.22 Effect of Minor Orientation Changes on Temperature Effects in AT Cut Quartz.[122]

THE QUARTZ CRYSTAL OSCILLATOR 147

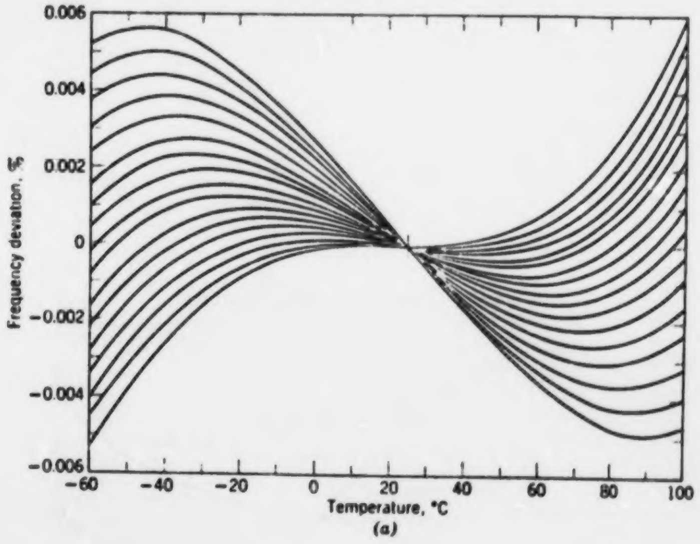

Figure 4.23 Family of Frequency vs. Temperature Curves for AT Cut Quartz.[122]

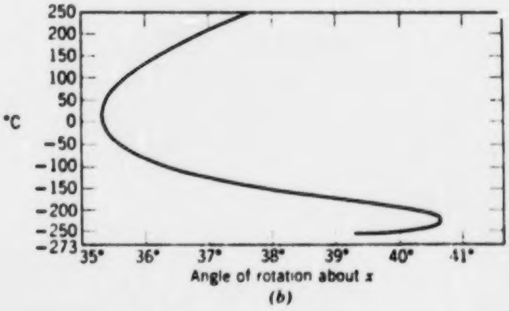

Figure 4.24 Zero Temperature Coefficient Operating Temperatures for AT Cut Quartz as a Function of Orientation.[122]

Another temperature related problem is the effect of a small transient temperature change on frequency.[123] A typical response is shown in Figure 4.26. This is thought to be due to the presence of a thermal gradient in the crystal. This type of spurious response could occur when the gas stream impinging on the crystal suddenly changed temperature, and could be avoided by controlling the inlet gas temperature.

The original theoretical justification for equation (4.70) was based on the assumption that the added mass was "equivalent" to the quartz of resonant crystal,[124] i.e., had the same acoustic properties. More often than not in applications of this measurement principle, it is not true. However, formula (4.70) is very closely followed when the amount of mass added is very small compared to the mass of the quartz crystal. A theoretical justification, based on a perturbation analysis due originally to Rayleigh, has been given by Stockbridge.[125] This analysis is based on mathematical arguments that do not rely on a physical model.

A treatment based on a one-dimensional model of acoustic waves propagating from the quartz crystal into a thin deposited layer of different acoustic properties has provided more physical insight[126] than the Stockbridge treatment. This model also leads to an equation similar to (4.70) for the case when the ratio of density-thickness products for the quartz and the deposited layer is very much smaller than unity. This treatment has been extended to the case of relatively thick layers, where it has been shown that when the mass loading shifts the frequency more than 2% the acoustic parameters of the deposit must be taken into account and, furthermore, the simple relation between frequency shift and deposited mass equation (4.70), no longer holds.[120]

Both of these two-layer models involving the acoustic properties of the quartz and the deposit assume that the material added to the quartz will support the shear wave generated by the AT cut quartz crystal. Furthermore, the material is assumed to be lossless. These assumptions are justified in the usual applications where such crystals are used to monitor the deposit of crystalline solids. In the applications initiated

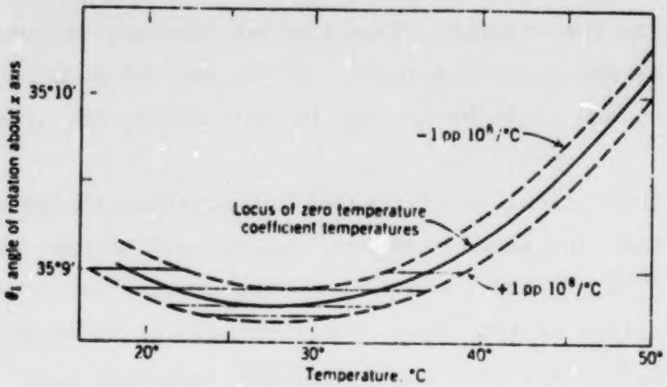

Figure 4.25 Detailed Portion of Figure 4.24 Near Room Temperature.[122]

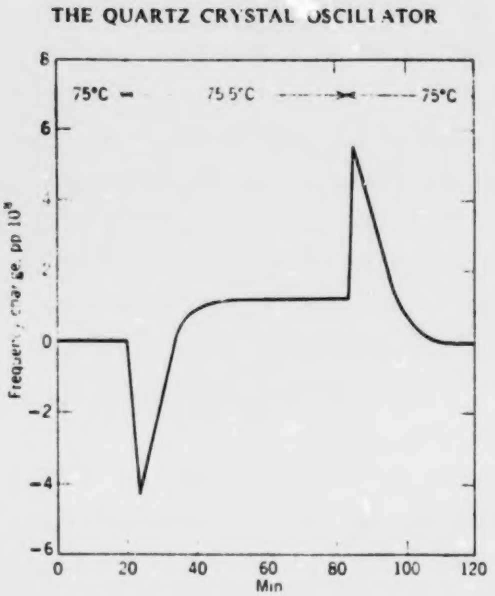

Figure 4.26 Typical Frequency Response to a Change in Ambient Temperature. Any Thermal Disturbance which Produces a Thermal Gradient in the Quartz will Produce a Similar Effect.[122]

by King,[117] however, where a "selective" sorbent layer is used to coat the crystal, these assumptions are not justified. Typically such a coating is an amorphous, visoelastic material. Although the problem of propagation of shear waves from a stiff medium, such a quartz, to a viscoelastic medium has been previously treated theoretically,[127] the problem of resonance of such an elastic/viscoelastic system apparently has not been modeled.

For ambient air monitoring, where the concentrations of pollutants to be "selectively" sorbed are generally a ppm or less, only a very thin coating of sorbent is required. Hence, the assumptions of Stockbridge's perturbational analysis are valid and the linear relationship of frequency change to added mass, given by equation (4.70), can be expected to hold.

Sorbent System

Providing the sorption is reversible, the thin coating of sorbent deposited on the surface of the crystal can be regarded as a permeable membrane characterized by a solubility parameter, S, and a diffusion coefficient, D. The equation for the mass of material absorbed from the gas phase into the membrane for a one dimensional system is,[128] assuming that Henry's law is obeyed, the pollutant gas is ideal, and the saturation concentration has not been attained,

$$\Delta m = MSA \left(\frac{Sp}{1 + Sp/C_s} \right) \left\{ 1 - \frac{8}{\pi^2} \sum_{n=0}^{n=\infty} \frac{1}{(2n+1)^2} \exp\left[\frac{-(2n+1)^2 \pi^2 Dt}{\delta^2} \right] \right\} \qquad (4.72)$$

where

M = molecular weight of absorbed gas pollutant

δ = thickness of sorbent

A = area of crystal covered by sorbent

p = partial pressure of gas pollutant in atmosphere

S = solubility constant

C_s = saturation concentration of gas in sorbent.

It should be noted that the diffusion coefficient of the gas in the sorbent, D, and also the solubility parameter, S, will be functions of temperature. As discussed above in connection with temperature effects on quartz crystal resonance, it is desirable to maintain the temperature of the quartz crystal constant. Therefore S and D will be regarded as constant. If the absorbed concentration is well below the saturation limit, or

$$C = Sp \ll C_s \qquad (4.73)$$

the amount of mass deposited will be, for all practical purposes, linearly related to the partial pressure in the gas phase. Also if the sorbent layer is sufficiently thin, the quantity

$$\tau_n \equiv \delta^2/(2n+1)^2\pi^2 D \qquad (4.74)$$

will be small, and the response of a step change in concentration, $\Delta C \ll C_s$, to a step change in gas partial pressure will give a change in mass which varies with time as

$$\Delta W = M\delta AS \ \ \Delta p \ [1 - \frac{8}{\pi^2} e^{-t/\tau_0}]. \qquad (4.75)$$

Therefore, for all practical purposes the time response is exponential with a time constant given by equation (4.74) with n set equal to zero.

This treatment has assumed that the absorbed species is relatively free to move within the sorbent. When the desorption step requires that an energy barrier (bond breakage) be overcome the effective diffusion constant, D, becomes much smaller than that operative for uptake of the gas, giving a much longer time constant for desorption than for adsorption.

It might also be expected that the heat of sorption of the gas in the sorbent would change with amount of gas adsorbed, similar to the behavior exhibited by water vapor in zeolites.[129] Thus, initially, small quantities of gas would be transported with a low diffusion coefficient. As the amount of gas in the sorbent layer increased, the effective diffusion coefficient would increase. The overall effect would be to alter the shape of the response from the exponential form of equation (4.75).

Using the model developed above, the response of a piezoelectric mass monitor can be estimated. Using typical dimensions for an AT cut quartz crystal resonating at 9 MHz, a diameter of 12 mm and a thickness of 0.15 mm, and the density of quartz crystal, 2.65 g/cm^3, the mass of the quartz crystal, Mg, would be about 45 milligrams. Triethanolamine (TEA) will be used as an example of sorbent because it has been used to collect both NO_2[130] and SO_2.[131] Assuming a layer of triethanolamine, density 1.124 g/cm^3 deposited on the crystal to a thickness of one thousandth of an inch, 25 micrometers, covering a circular region of diameter 0.6 cm, the added mass is 794 micrograms. This is slightly under 2% of the crystal mass so the frequency shift will be proportional to the added mass fraction, or about 640 KHz, according to equation (4.70).

In order to obtain a quantitative estimate, it will be assumed that the saturation concentration of TEA corresponds to one molecule of SO_2 (or NO_2) per molecule of TEA. On this basis a total mass of 340 μg of SO_2 and 245 μg of NO_2 could be ultimately absorbed. However, at the ambient air concentrations normally encountered, the amount absorbed will be well below this so the approximate formula, equation (4.75), can be used.

Two parameters of interest are the solubility parameter, S, and diffusion coefficient, D. These can be determined by experiment, using equation (4.74) with n=0, equations (4.75) and (4.70). Since the density of the sorbent, ρ_S, is known, the thickness-area product, δA, can be obtained from the measured frequency shift when the coating is applied to the electrode, ΔF_e, whose area A, can be measured directly. Thus

$$\Delta A = A(\Delta F_e)/2.3 \times 10^6 F^2 \rho_s \ . \qquad (4.76)$$

By introducing a step change in partial pressure, Δp, of the pollutant, e.g., SO_2, and determining the time constant of the corresponding response curve, τ_0, the diffusion coefficient can be determined from

$$D = \delta^2/\pi^2\tau_0 \qquad (4.77)$$

where the value of δ is obtained from equation (4.76), above.

The solubility, S, is determined from the steady state solution of equation (4.75) with ΔW determined from the measured frequency, ΔF_C, resulting from a step change of pollutant gas partial pressure.

An estimate of the response expected from a TEA coated sensor for measuring SO_2 can be obtained by estimating values for S and D. For non-reactive gases in liquids, diffusion coefficients are on the order of $10^{-5}cm^2/sec.$[132] In the case of water diffusing interstitially in zeolites, the diffusion coefficient is on the order of $10^{-7}cm^2/sec$ unless the structure is totally dehydrated, in which case the diffusion coefficient can be two orders of magnitude lower.[129] Assuming that for the SO_2/TEA combination $D = 10^{-7}cm^2/sec$ and that the TEA coating is 25×10^{-4} cm thick, the time constant will be, from equation (4.74)

$$\tau_0 \simeq (25 \times 10^{-4})^2/\pi^2 \times 10^{-7} = 6.33 \text{ seconds}.$$

From the study by Frechette, et al,[117] if it is assumed that TEA will have similar adsorptive behavior for SO_2 as tripropylamine, the frequency change expected for TEA would be about 9 Hz per ppm.

From a resolution of 1 ppb in the measurement, the circuit for measuring frequency change would have to be capable of measuring a shift of about 10^{-2} Hz. At the 5 ppb level, this would correspond to a period difference of about 4 sec. A maximum counting period of 30 sec, corresponding to about 4 ppb, would set the response time. The circuit design for this would be a straightforward application of current digital techniques.

Although TEA reversibly adsorbs SO_2, development would be required to find a coating that would reversibly adsorb NO_2. Use of selective filters would prevent interferences. There is no direct way that O_3 could be measured with such a system.

As discussed above, precise temperature control of the crystals and conditioning of the incoming gas is required to prevent frequency shifts.

4.10.3 Projected Performance

Assuming precise temperature control of the crystals and incoming sample air stream, the piezoelectric mass monitor should be capable of a dynamic range of 5 ppb to 1 ppm with a resolution of 1 ppb. A response time of about 30 seconds would be required if the measuring and reference frequency crystals are exact frequency duplicates.

4.10.4 Logistical Factors

Active sampling would be required. Flow rates would be moderate, well within the capabilities of the portable pumps listed in Table 2.1. Although the response is not dependent upon flow rate from the point of view of pollutant sorption, it can be indirectly (and drastically) affected by any temperature shifts caused by flow changes. For this reason flow control should be employed. A significant amount of power would be required to maintain a constant temperature, typically 50° to 60°C, for the crystals.

4.10.5 Dose Rate Information

A digital signal, proportional to pollutant partial pressure, would be available every 30 seconds for storage by techniques discussed in Section 5.0.

SECTION 5

5.0 DATA ACQUISITION

The function of a data acquisition system is to measure one or more parameters and record the result for future observation or processing. The data acquisition system for the personal dosimeter must accomplish this function under several constraints, specifically low power consumption, low mass and small size. The unit must consume minimal power to save as much power from the source as possible for use with the sensor instrumentation. Likewise, mass and weight should be kept to a minimum since the state-of-the-art allows a much greater degree of miniaturization in data acquisition system design than in continuous ambient air monitors.

5.1 General

Types of data acquisition systems adaptable to the personal dosimeter range from simple systems to versatile, complex systems. At the simplest end of the scale are data recording mechanisms which are an inherent part of the sensor. In this case, the sensors permanently record their measurements in the form of a stable chemical change. Both those instruments which integrate data over long periods of time, such as film badges, and those which sample continuously, such as tape samplers, fall in this category. These systems are characterized by specialized data recovery systems which are dedicated to the recovery of the information stored by the chemical process, such as photographic processing equipment and absorbance spectrometers. This type of data acquisition system lacks the capability of measuring parameters other than the ones for which it is specifically designed. This has two implications: (1) the system cannot easily be changed to record different parameters by simply changing sensors, and (2) the system cannot record parameters from a number of different sensors but is limited to measuring only one parameter.

A second type of data acquisition system adaptable to small, portable systems is the electrochemical type. Systems in this category most frequently consist of strip chart recorders. While these systems definitely serve a need because of their immediate visual readout of recorded data, the difficulty in taking a quantity of data off the charts for computer processing makes their exclusive use in environmental systems inconvenient. However, in systems where weight, size, and power permit, these recorders are useful for two purposes: (1) as a display which shows past data as well as present, and (2) as a back-up unit for recording data when the primary system becomes temporarily inoperative.

The third type of data acquisition system is the electronic systems which record signals in analog manner, typically on magnetic tape. These systems, in order to function, must run continuously, which results in two consequences: (1) if the duration of the data acquisition period is long, large data storage capacity must be provided resulting in a bulky package, and (2) due to continuous operation, power must be drawn continuously resulting in higher current drain than other type systems. These reasons make the use of this type of recorder inconvenient for personal dosimeter application where it is not essential to monitor the data continuously.

A fourth type of data acquisition system is the analog/digital system. This system is the type most frequently found where data is to be processed by computer at the time of acquisition or later. This system is characterized by electronic circuitry capable of signal conditioning, multichannel scanning, analog-to-digital conversion and digital storage. This system has the advantage of fast, quiet operation, powerful signal processing capability, high resolution and accuracy (if desired) and output in a form compatible with computerized bulk data handling systems. Also the systems can be miniaturized and designed for low power consumption by switching off those portions of the system when they are not actually needed for operation.

Of the four types of data acquisition systems mentioned here, the latter, the analog/digital system, is the one most suited to a minaturized, easily portable system when used with sensors for continual monitoring. The first system classification, chemical systems, is also suited to small, portable systems where immediate access of data is not needed and chemical processing of the storage medium can be accomplished. These systems are discussed in Section 6. The digital system, however, is a complete self-standing system capable of use with any sensor or instrument which has an analog voltage output.

A general data acquisition system block diagram is shown in Figure 5.1. This diagram shows the different sections of a data acquisition system which utilizes the analog-to-digital conversion approach. Not all of the blocks shown will exist in every system, for in some applications not all of them are needed. Signals enter the system from sensors at the signal conditioner. The signal conditioner consists of a group of amplifiers, filters, or other signal processors which convert the input to a form more compatible with the analog-to-digital converter. Examples of types of circuits found are integrators, differentiators, resistance-to-voltage converters, amplifiers, low pass filters and non-linear networks to linearize responses of non-linear sensors. By preprocessing the data with a signal conditioner, quite frequently some stringent system requirements are lessened on other parts of the system. For example, noisy signals when sampled at fixed intervals can yield misleading averages unless the sample rate is twice the highest frequency component of the input signal. However, if an integration or a low pass filter is installed at the input, high frequency components are removed and the sample rate may be dropped to the desired observation rate (i.e., typically once every 5 minutes for environmental data).

After conditioning, the signals are passed to a scanner. This unit connects each of the active channels to the analog/digital converter for conversion. Its rates are controlled by the system control unit which insures that (1) the scanner leaves an input connected to the analog-to-digital converter (A/D) long enough for the A/D to stabilize and complete its conversion, and (2) the sequence of scanning all channels is initiated once at the beginning of each interval of preselected length. The scan interval is selected at the start of a period of data acquisition based on the characteristics of the data being monitored and usually is not changed until the type of test is changed. The number of channels for which a scanner may be designed is practically limitless. However, for this application, an 8- or 16-channel system will be adequate to handle all data inputs as well as some parameters significant to system performance

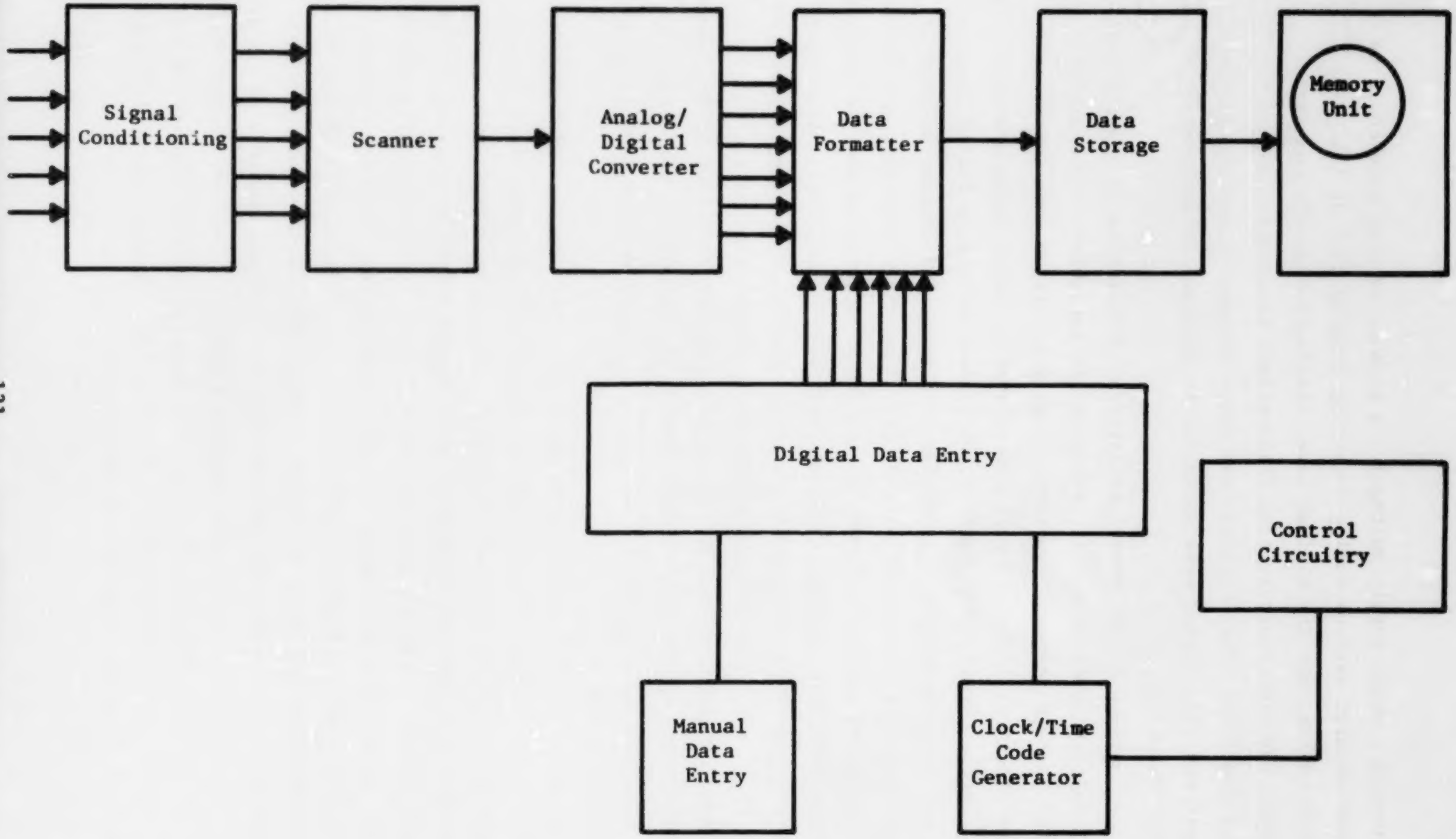
Signal Conditioning
Scanner
Analog/ Digital Converter
Data Formatter
Data Storage
Memory Unit
Digital Data Entry
Control Circuitry
Manual Data Entry
Clock/Time Code Generator

Figure 5.1. Generalized Data Acquisition System.

(for example, power supply voltage). A scanner of this size could be implemented with various analog switching devices such as relays or crossbar switch, but for minimal power dissipation on minimum size switches, the electronic-switch, field-effect transistors appear to be most feasible. They require less power because no mechanical coils are used and they occupy less space due to advances in integrated circuit technology.

The function of the analog-to-digital converter is to convert each analog voltage level to a digital representation which is compatible with the storage devices. Currently available devices are low power A/D converters utilizing Complementary Symmetry Metal Oxide Semiconductor (CMOS) logic. These units function on a power of only a few milliwatts while actually converting from analog to digital and consume microwatts while on standby. Eight-bit models offer resolution of 1 part in 256 which is adequate for state-of-the-art environmental monitoring and are available in single CMOS chip packages, making their use in this application very attractive. However, increased resolution may be obtained by utilization of 10- or 12-bit units, sacrificing only speed and some size.

Speed of these devices may be obtained at the sacrifice of low power consumption but scan rates of less than 10 per second are more than adequate for environmental monitoring and are considered very slow for digital acquisition systems.

The output of the analog-to-digital converter consists of 8 to 12 parallel bits of digital information. Before storage, some information must be added to this in order to produce a complete, usable unit of data. Information that must be associated with the data includes source of data (channel number), time of data, and events which occurred simultaneously with the data. For units where the amount of storage is not a premium, the channel numbers of each data point can be stored along with the data. For systems which use more expensive memory units (cost, power or size), some scheme may be worked out whereby the data for all channels is formatted sequentially in the order of the channel numbers. A unique, recognizable character group is inserted ahead of the group to mark the beginning of the data. The original channel of the data may then be determined by counting data points after the special character group.

A problem frequently encountered with data recovery from a data acquisition system is that of correlating the data with events which have an impact upon the data. Events in the case of personal dosimetry include location and activity of subject, time, range of instruments, among others. It is possible to correlate recorded data with events which occurred as the data was taken by at least two methods, each with its drawbacks. The first method entails the recording of pertinent events manually in a log either by the subject or an observer. Disadvantages in this procedure include the possibility of loss of important data either through loss of the physical data record or neglect of the person recording data to make the proper entries in the log. Another drawback of this procedure is the effect on the data brought upon by the time, effort, and concentration necessary for the subject (or an observer) to make notes and observations. The second method of correlation of the recorded data with pertinent events is the analysis of data to determine the point of occurrence of easily detectable events or changes of activity. This procedure is usually carried out in addition to log-keeping. An example would be the change in ambient temperature which occurs when the subject leaves a protected environment. The disadvantage here is that the variability of the events is so high that the data must be processed manually, significantly increasing the amount of human processing necessary before the data may be processed by computer.

A solution to this problem is the digital data entry system. This block on the functional diagram allows data already in digital form to be stored along with the digitized analog data. Data stored typically comes from an internal real time clock or binary coded decimal (BCD) digit switches. Prearranged codes allow the switches to be used to input data pertinent to the test in progress. This data then is located in chronological order along with the digitized data taken at the same time and contained on the same storage device. Both data can then be read directly into a computer and processed routinely without the input of excessive data from outside the storage device.

The data storage device is the unit which puts the data on the removable storage record. In the case of tape systems, it is the tape deck.

For solid state memories, it may include hardware which accepts a memory board and stores the data at appropriate addresses on that board. The data storage device is the device which determines the characteristics of the data acquisition system as a whole. For dosimeter applications which are to take data for periods of from 8 to 24 hours, magnetic tape memories and solid state memories appear to be the most feasible. This application requires 8 to 24 hours of data to be taken over one interval continuously. At sample rates of once per minute, at least some magnetic tape systems have a surplus of data storage capacity allowing storage of items of lesser importance (more digital inputs, analog signals indicative of other than primary importance). Solid state memory systems, however, are expanded in increments of 1024 or 4096 bits at a significant cost per bit ($0.25/bit for 4K MNOS). Consequently, for those memories it is more economically profitable to conserve memory space wherever possible.

Digital magnetic tape memories suitable for this application would have to be small and low power. This narrows down the selection of recorders to the cartridge and cassette data recorders available today. At least one manufacturer produces units which use the Phillips Cassette, a tape housed in a case approximately 6.4 x 10.1 x 1.4 cm (2 1/2 x 4 x 7/16 inches). The unit is an incremental unit which means that the tape is moved past the recording head a small amount during the recording of each bit and then stopped during periods of no data. Consequently, power is saved in two ways: (1) no temporary storage buffer is necessary to save up data so that it can be placed on tape at a fixed rate while the tape is moved at a constant speed and stopped between groups of data, and (2) incremental recording requires that power be drawn only while data is recorded and no power is consumed while in the standby mode.

The other option for data storage is solid state memory. There are three types of integrated circuitry memory devices, each with its own advantages for use in this application. Metal Oxide Semiconductor-Large Scale Integration (MOS-LSI) has the advantage of high density packaging so fewer circuits are needed. Complementary Symmetry Metal Oxide Semiconductors (CMOS) have lower power drain. However, power must be maintained on both these units or data will be lost unless a non-volatile memory such as the Metal Nitride Metal Oxide Semiconductor is used. Typical designs using these devices are described in Section 5.3.

As with the design of any system, there are a number of tradeoffs which may be made in obtaining a system which best satisfies the requirements dictated by the application. For personal dosimeters, requirements for small size and low power are more stringent than most other applications. However, if allowable package size does permit the use of a miniaturized tape recorder, one is assured that sufficient storage will be available for monitoring purposes for periods up to 5 days. However, with the tape system, if less storage is needed, no space can be saved by sacrificing half of the memory capacity. Solid state memories, however, can be designed into systems only in the quantity necessary to accomplish the task. This means the size of the system and power consumption may be varied depending on the amount of storage necessary. (An exception arises in that power consumption may not vary appreciably if (1) memory circuits do not draw substantial power relative to other circuitry or (2) they are non-volatile circuits such that power may be removed when data is not being stored. Therefore, additional circuits do not result in increased consumption.) Therefore, for given maximum size, power consumption, or cost, the maximum size memory system may be determined.

For a given fixed memory size, tradeoffs now exist for the parameters, number of channels scanned, resolution, and sample rate. Obviously, the amount of data recorded is directly proportional to the rate at which it is taken. Likewise, it is also directly proportional to the number of inputs which must be scanned each time. The desired resolution also has an effect on the storage because the greater the desired resolution, the more bits it takes to represent one reading.

Each of the above parameters may be determined from the application, and the size of the memory necessary can be computed. If a memory of sufficient size cannot be accommodated in the allowable weight and power budget, there are design alternatives which allow a reduction in storage necessary to record data pertaining to a given experiment.

First, as previously mentioned, either low pass filtering or integration can be used on the input to reduce the necessary sampling rate, thus saving memory. Another way of possibly conserving memory arises in the case where special processing is to be applied to the data. The processing may be done "on-site" by analog processing before the data is, frequently reducing the sample rate necessary for recording the data. Examples of this are where rates of change or repetition rates are desired, as found in heart rate or respiration rate. Here, rather than recording EKG at a fast enough rate to determine when each pulse occurs, analog processing can be used to determine the pulse rate and produce an analog voltage for digitization which is proportional to the pulse rate. Another approach which can be used where a count of events is desired is to simply bypass the analog-to-digital converter. In this case, the count is computed during each scan interval and placed in a register connected to the digital data entry point. This causes the data to be placed in memory along with the digitized data. The savings in memory space arises because the scan rate does not need to be made fast in order to allow special processing of the data to obtain a single value for a given parameter from a number of sample points. It is only necessary that the sample rate be fast enough to insure that the user can observe it as often as necessary.

Another option which may be exercised in cases where size or power requirements restrict the allowable size of memory is a histogram type memory. Instead of saving the measured parameter value for every point in time (one per minute for each input channel), the electronics package monitors the level of the input voltage. This unit is connected to a bank of counters, each counter representing a range of values within the expected readings. A periodic clock pulse is input to logic circuitry which determines which of the counters the pulse is used to increment. The end result at the end of the period of data acquisition is that each counter contains a number proportional to the amount of time the monitored value spent in the range of values corresponding to that counter. This information can then be plotted in the form of a histogram, yielding information concerning the average value and the variance of the data. However, information relating the data to time is lost. This is an example of one tradeoff which may be made at a sacrifice of one group of information. Substantial reduction in system cost, complexity, and power consumption may be made.

Unless data acquisition is to be an exercise in futility, some provision must be made for getting the data from the storage device to a place where it can be inspected or further processed. Typically, data is transferred into a computer where it is reformatted for inspection and placed on a computer compatible magnetic tape for further processing.

For magnetic tape systems, the problem of data recovery simply becomes removal of the tape cartridge, which is always a separate module. Therefore, the solid state memory must be self-standing once removed. This means that for volatile memories, some means of power supply (batteries) must be maintained in the memory modules. Certain memories require pulsing circuits to keep the memory refreshed as well. Non-volatile memories such as the MNOS memory do not require either power or refresh circuitry to keep data and may hold data for periods up to a year with no power applied.

The question of how much circuitry to include in the memory module other than memory itself is not one with an obvious answer. Some of the circuitry which is used to interface the memory board to the system has to be duplicated in the data recovery unit. This circuitry includes addressing circuitry, the aforementioned refreshing circuitry, and the memory control. Approaches used may vary from a self-contained complete data acquisition system to a system with only the memory circuits themselves in a module. The configuration used would depend pricipally on economic factors such as number of memory modules needed relative to number of data acquisition systems.

The following two sections illustrate example designs which could be implemented using magnetic tape systems (Section 5.2) or solid state memories (Section 5.3). The designs are intended to be typical for personal dosimeter application but would probably vary somewhat in specific details dependent upon application.

5.2 Magnetic Tape System

The configuration of a data acquisition system using magnetic tape would be exactly as that described in Figure 5.1 with the storage unit becoming a magnetic tape unit. No other modifications in the system would be necessary to accommodate the tape unit. The tape unit is a digital tape unit designed to interface to the digital output of the analog/digital converter through the data formatter.

Digital tape decks come in several forms ranging from the 7- or 9-track drives used in a large computer systems to new cassette drives small enough to be hand-held. Of the systems currently developed, only two general categories seem to be applicable to personal dosimetry. These two types are the cassette recorders and cartridge recorders. Cassette recorders use the Phillips Cassette which is a high quality version of the cassette used in many portable and home entertainment audio systems. Cassettes intended for digital use are manufactured to much tighter tolerance somewhat larger than cassettes and use wider magnetic tape (0.633 cm). At the present time there are a number of different cartridges available, because different manufacturers have introduced different systems of tape decks and cartridges within the past few years. One problem with adapting either of the two types of systems to personal dosimetry is size. While designers tried to keep the size of a tape cartridge to a minimum to facilitate handling, not much effort has been expended to reduce the size of the deck itself. However, there are some manufacturers who do produce relatively small, low power units, possibly suitable to this application.

Basically there are two different types of systems for transporting tape past the recording head, incremental and continuous. Incremental recorders move the tape in discrete steps placing one bit per track at a time on tape. Gaps are produced by advancing the tape a number of steps while not putting on any data. The continuous recorders put data on continuously while running. Consequently, considerations must be made in the supporting electronics package. Since the tape moves continuously while recording, room must be left between groups of data recorded at one time to allow for stopping and starting the tape. In order to make good utilization of available tape, these blocks of data should be long so that most of the tape is data separated by occasional gaps and not mostly gaps with short blocks of data. Since data will arrive at the tape unit at a non-constant rate, buffer storage must be provided to save data as it is input to the tape deck until enough is received to place on tape. The tape is then advanced and data is read from the buffer at a rate compatible with the tape unit. Gaps (inter-record gaps) are then left at the end of each block of data stored on tape to allow the recorder time to stop and start after data ended and before data is started.

Of the two types of recording systems, incremental seems the most desirable for several reasons. One, it does not require an external buffer for temporary storage of data before placing it on tape because it simply places it on tape as it receives it without waiting for a whole block of data to be received. Also, more efficient use of the tape can be gained because of better control of the tape by the capstan[*] which increments it past the head.

Magnetic tape systems have several advantages over other types of data acquisition systems. Some of these are listed as follows:

(1) Magnetic tapes have capability for storing a large quantity of data on one tape. A cassette in one typical system can hold 2.2×10^6 bits or 137,000 data points (16 bits each).

(2) Tapes provide a low-cost, high density permanent storage for data. With magnetic tape systems no additional translation step is necessary to get data to magnetic tape for archiving data in a computer compatible format.

Along with the advantages gained by a magnetic tape system come several disadvantages as well. Some of these are listed below:

(1) For systems where minimum data storage is needed, much storage space is wasted and the cost of the system per stored data point becomes high.

(2) It is difficult to miniaturize the system much after the electronic package is reduced due to the mechanical interface with the tape cartridge including motors, mounting plates, etc. This could become very significant when gas analyzer technology allows pocket size dosimeter.

Typical Design

A system suitable for monitoring the outputs of gas analyzer, physiological parameters, and ambient temperature/humidity is shown in

---

[*] Some continuous recorders do not use a capstan drive at all but regulate speed of tape by keeping hub speed constant. Bit density on tapes produced by this method may vary considerably as tape builds up on the hub pulling the tape past the recording head.

Figure 5.2. This system was designed to measure and store the following parameters:

- Integrated and peak value for ozone (2 channels)
- Integrated and peak value for NO (2 channels)
- Integrated and peak value for NO_2 (2 channels)
- Temperature
- Dew Point
- Heart Rate
- Respiration Rate

The system is to be able to store this data for a minimum of 8 hours and preferably 24 hours. The unit is to be composed of readily available modules illustrating state-of-the-art in off-the-shelf manufactured equipment. To keep costs of the designed systems to a reasonable level, no special developmental items such as further miniaturization of tape decks were included. Also all components used are proven in everyday usage, and consequently, the system could be assembled with confidence that its performance would meet the predicted specifications.

The unit was designed around a commercially available data acquisition system. This unit, built by DATEL, contains circuitry necessary to interface with 16 analog channels, digitize the data, and place it on a cassette via its own internal incremental cassette tape deck; it requires external clock, control circuitry, manual data entry hardware, and signal processing in order to make it a complete system. This unit was selected because it appeared to be representative of a system fabricated from individual components and its performance specifications determined.

Specifications for the unit may be found in Table 5.1.

Several options are available to modify this system depending on the specific application. These options include:

Repackaging -- The data acquisition could be repackaged in separate modules or a single module of a different shape. However, a requirement does exist for the smallest dimension to be at least 7.5 cm to accommodate the tape unit.

Expansion of input capability -- Due to the more than adequate size of the memory capacity, the input capability may be increased to 16 channels with no additional hardware. Expansion beyond that does involve more extensive control circuitry modifications and additional multiplexors external to the DATEL unit.

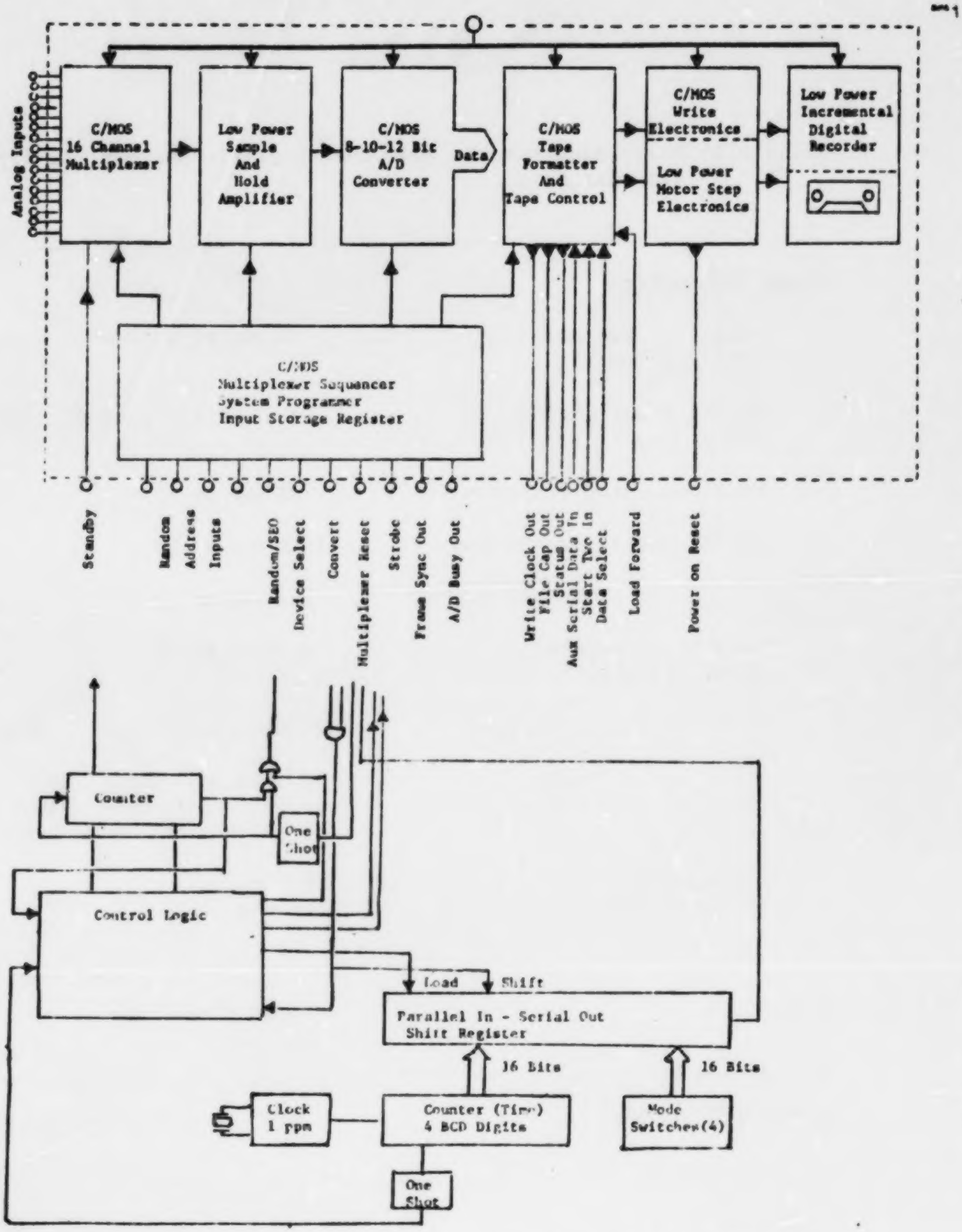
Analog Inputs
C/MOS 16 Channel Multiplexer
Low Power Sample And Hold Amplifier
C/MOS 8-10-12 Bit A/D Converter
Data
C/MOS Tape Formatter And Tape Control
C/MOS Write Electronics
Low Power Motor Step Electronics
Low Power Incremental Digital Recorder
C/MOS Multiplexer Sequencer System Programmer Input Storage Register
Standby
Random
Address
Inputs
Random/SEO
Device Select
Convert
Multiplexer Reset
Strobe
Frame Sync Out
A/D Busy Out
Write Clock Out
File Gap Out
Status Out
Aux Serial Data In
Start Two In
Data Select
Load Forward
Power on Reset
Counter
One Shot
Control Logic
Load
Shift
Parallel In - Serial Out Shift Register
16 Bits
16 Bits
Clock 1 ppm
Counter (Time) 4 BCD Digits
Mode Switches(4)
One Shot

Parts Count Estimate - 14 Flat Packs

Figure 5.2. Incremental Digital Tape Recorder Data Collection System.

Table 5.1 Power Requirements and Other Logistic Factors for Tape Recorder Unit

POWER CONSUMPTION		
Telemetry Reception (FM^2 Receivers)	14 ma at + 12 v	
Signal Conditioning (6 op-amps)	0.3 ma at + 12 v	0.3 ma at -12 v
Data Recording record mode 2 sec/min	80 ma at 12 v	
(DATEL Unit) standby mode	0.01 ma at 12 v	
average current	2.6 ma at 12 v	
Control Circuitry (CMOS Circuitry)	0.6 ma at 12 v	
Total Current, average	17.5 ma at + 12 v	0.3 ma at -12 v
peak	97.5 ma at + 12 v	0.3 ma at -12 v
SIZE	10.16 cm x 10.16 cm x 30.48 cm	
Includes DATEL unit, 2 control circuitry cords, 2 signal processing cards and 2 FM receivers		
WEIGHT	Less than 3 lbs	
TEMPERATURE RANGE	-10° to 60°C (limited by tape unit)	

Sample rate -- Also because of the abundance of memory space in the cassette, the rate at which the data is sampled may be increased without exceeding the memory capacity in an eight-hour day. Power consumption will be increased somewhat but will still be low enough to allow battery operation as planned.

Signal processing -- Options vary widely for signal processing. Simplest on the scale of complexity is point sampling in time. Options exercised in this design include integration over the sampling interval and peak detection during the interval.

5.3 Solid State Memory System

Solid state memories are the newest type of memory to be incorporated into system design. Their use is expanding into new areas such as computer memories where large quantities of memory storage are needed. They have also made possible production of memory systems which are smaller, faster, cheaper, and lower power then conventional memory systems. The major advantages of solid state memories are low power, fast read and write speed, and accessibility. The major disadvantages are that they are not well suited for mass storage of data and most types need power applied continuously to retain data.

There are several different types of solid state memories, each with its own advantages. This section will explore two different types of these memories, the most common type called MOS-LSI, and a newer, non-volatile type called MNOS. A data acquisition unit using these two memory types is described below. The unit is made up of two basic parts, the data control section and the memory section. The memory section is different for each type of solid state memory device, but the data control section would be the same for both solid state memories and the magnetic tape system. The next subsection describes the data control section and this is followed by descriptions of the two memory systems.

The function of the data control section is to take the data from the sensors and make it compatible with the memory for storage. A typical block design is shown in Figure 5.3. The basic parts include a multiplexor to successively select which data channel to be processed, an analog-to-digital converter (A/D) to transform the signal to a binary form, and a

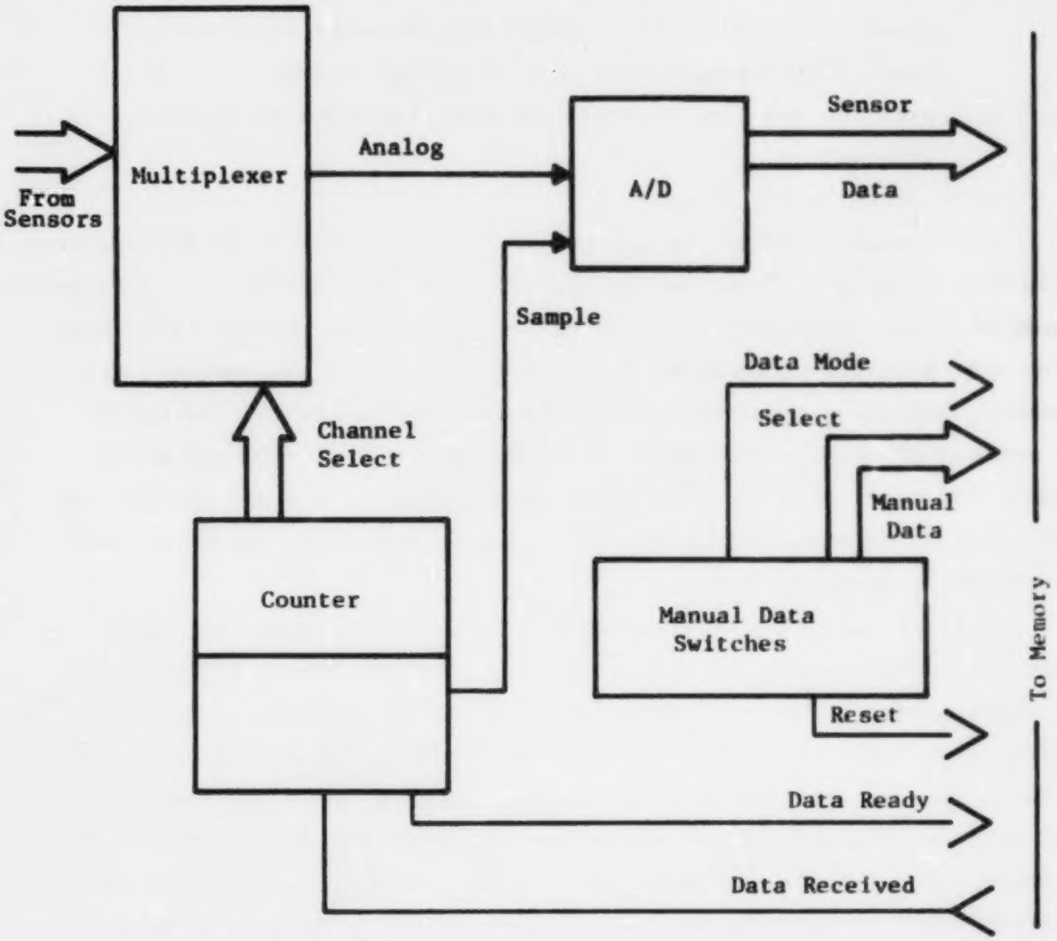
From Sensors
Multiplexer
Analog
A/D
Sensor Data
Sample
Channel Select
Counter
Data Mode
Select
Manual Data
Manual Data Switches
Reset
Data Ready
Data Received
To Memory

Figure 5.3. Data Selection Control.

counter/timer section to keep track of when to take new data. Also included would be a row of switches to be used to enter coded manual data. This section is basically the same as that described under magnetic tape systems.

5.3.1 MOS-LSI Memory Systems

The first type of memory system is built around the Metal Oxide Semiconductor-Large Scale Integration (MOS-LSI) circuits. This name, MOS-LSI, comes from the process used in their manufacture. The transistors are formed by depositing a layer of metal over an insulating layer of oxide on the silicon base. The individual transistors are so small that the manufacturers can integrate over 25,000 of them on the same piece of silicon. They then interconnect the transistors to achieve highly complex functions such as memories and registers. This is how the term "large scale integration (LSI)" developed.

The basic method of storing data in these devices uses the fact that once a memory transistor is forced into one of its two stable states, it stays in that state for a short period of time. To avoid loss of this information after this brief time, it is necessary to rewrite the data over itself. This process is known as refreshing and must be done continually to keep the data. In presently available units, refreshing must be done 500 times a second. However, a read or write cycle takes less than one microsecond, so there is still plenty of time between refresh cycles to record data.

This refreshing process makes it imperative to have a clock to keep track of when it is necessary to rewrite the data. Since it is impractical to write new data while refreshing, the control system must have logic circuitry to decide when to write and when to refresh. It is also necessary to have two counters to use as address registers. One of them is used to store the location of the next vacant data block in the memory, and the other counter retains the location of the next part of memory to refresh. Since it is convenient to be able to write manually into the memory to log events, this manual data as well as the necessary logic to control it should be included in the system. Perhaps the most complex part of the memory system is the timing. This circuitry must properly sequence the necessary pulses of the correct duration.

Presently it is possible to get MOS-LSI which have 4096 storage locations in a half-inch by one-inch package. This large memory size and small physical size make them perfect for portable applications. The proposed data system has a digital output that is 8 binary digits (bits) wide. That is to say that one sensor reading is represented as 8 bits in the memory. A memory system would consist of 8 of these memory packages side by side to accept all the data bits simultaneously. With an 8-package memory array (the smallest practical size), it would be possible to record 4096 sensor readings or about 400 readings for each of the ten sensors. At one reading per minute, this size memory array would hold 6.7 hours of data. Since this is not enough storage space, it is necessary to use two memory packages for each of the 8 data bits. This 16-package memory array would last 13.4 hours at one reading per minute. If a reading were taken every five minutes, this array would hold 67 hours of data. If a different number of channels or data sampling rate is necessary, the size memory needed can be found by using the formula:

$$S = 8\,C\,R\,H$$

where S = size in memory (in bits)
C = number of channels
R = number of readings per hour
H = number of hours data is to be taken.

To find the number of packages needed for an arbitrary size memory, it is necessary to divide the memory size by 4096 and round up to the nearest multiple of 8.

Figure 5.4 shows a typical block design using the MOS-LSI memories. The size of the memory (8K x 8) was chosen to be a reasonable size for this application. The following data is based on this size system. Since this memory needs a refresh cycle to maintain data, a small battery must be placed on the circuit board. Average power drain for this typical memory array is about 250 mw and the necessary control logic would consume

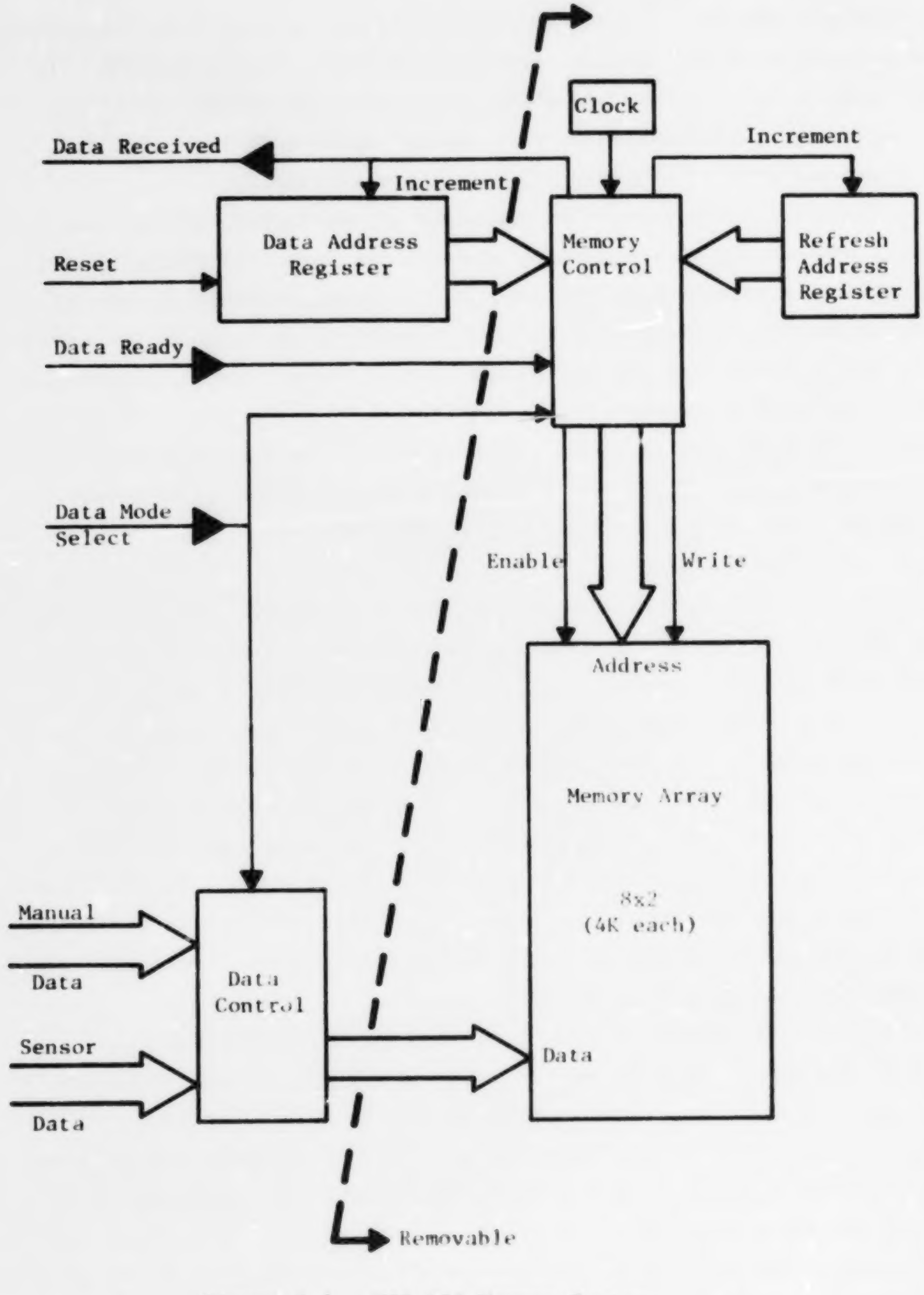
Clock
Data Received
Increment
Increment
Data Address Register
Memory Control
Refresh Address Register
Reset
Data Ready
Data Mode Select
Enable
Write
Address
Memory Array
8x2
(4K each)
Manual Data
Sensor Data
Data Control
Data
Removable

Figure 5.4. MOS LSI Memory System.

about 50 mw. The data selection control would require 20 mw, bringing the total to 320 mw. If a different size memory is selected, the power and cost would be the same for the data selection control section. In the memory array the cost and power is proportional to the number of packages, and in the memory control section about half the power and cost is fixed and half is proportional to the memory size.

The part of the circuit on the right of the dashed line in Figure 5.4 is the minimum logic necessary to maintain the data. If this circuitry and a battery were combined on one circuit board, it could be removed, another put in its place, and the system would be operational once more. The circuit board with the data could then be plugged into a readout device and the data would then be transferred to a computer. It would probably be easier to include everything except the data selection control on this removable circuit board. This additional logic would simplify the readout device and its interface considerably.

5.3.2 MNOS Memory System

The name Metal Nitride Oxide Semiconductor (MNOS) comes from the fabrication process of the devices. They are made by placing a metal layer over a layer of silicon nitride over a very thin layer of oxide which is placed on top of the silicon base. Binary data is stored by trapping charge in the oxide insulating layer. The charge changes the threshold of the transistor thus permitting non-destructive readout. The trapped charge remains in place even with no power applied, making it possible to keep the data with zero power dissipation. This ability to maintain information through power interruption gives them their other name of non-volatile memories. The transistors can be electrically reset so that they can be used repeatedly.

The control needed for this type of memory is less complicated than that of the MOS devices because it needs no refresh cycles. Like the MOS type memory, it needs a data control section to select the data from the manual switches or the data from the sensors. The control section also needs timing logic to pulse the memory array with the proper duration signals in the correct order to write into the memory. The memory control section must also confirm to the data section that the data has been stored in memory. In addition, it must increment the address counter used to store the next vacant memory location.

Presently non-volatile memories are available in a case size of 0.8 x 0.3 inches which contain 1024 memory locations. This is about half the density of the MOS memories. Although less dense, these memories make up for some of the additional circuit board space by requiring less control circuitry and do not require a battery on board. These non-volatile memories are perfect for small, ultra-low power memories. To store the same amount of data as in the MOS example mentioned earlier, an array of these packages 8 x 8 inches could be necessary. To determine the memory size for an arbitrary number of channels or length of time, use the same memory size formula as before. However, it is necessary to divide this total memory size by 1024 and round up to the nearest multiple of 8 to determine the number of packages necessary.

Figure 5.5 shows a typical block design using the non-volatile memories. The 64K memory size was chosen to make it comparable to the MOS design. Average power drain for the memory array is 3 mw and power drain for the memory control would be 10 mw. The cost per bit is relatively high now because the devices are new to the market, but the cost is expected to drop as volume increases. The data selection control section would be identical to the MOS type memory with power consumption at 20 mw, bringing the total power drain to 33 mw. If the cost or power consumption of a different size memory is needed, the control sections would remain essentially unchanged, but the cost and power of the memory array would be proportional to the number of packages.

If a removable circuit board is desired for this memory type, the minimum circuitry would be the memory array itself. To make it easier for readout, it would be better to include all of the memory section except the data control on this board. It would not be necessary to put a battery on this board and the life of the data would not be limited by the power of the battery as is the case with the MOS memory.

5.3.3 Summary

The major advantage of solid state memories is low power and small physical size in small and medium size memory applications. The best parts of the MOS memory are its small cost and small size. The disadvantages include large power consumption and complexity. The advantage of using the MNOS memory is ultra-low power consumption, but this is offset at present by higher cost.

Table 5.2 lists the major parameters of the solid state memory systems.

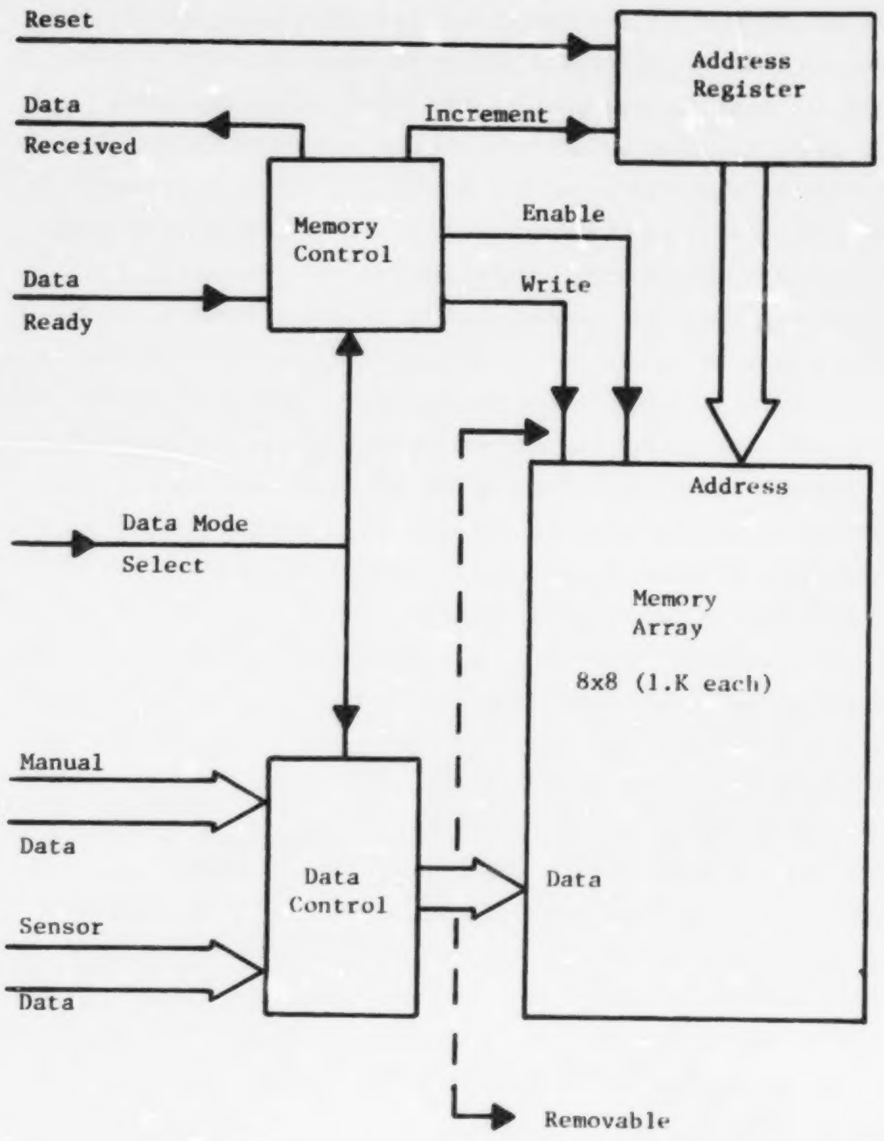
Reset
Address Register
Data Received
Increment
Memory Control
Enable
Data Ready
Write
Address
Data Mode Select
Memory Array
8x8 (1.K each)
Manual Data
Sensor Data
Data Control
Data
Removable

Figure 5.5. MNOS Memory System.

Table 5.2 Comparison of Memory Systems of 64K Bits

Section	Average Power mw	Equivalent Circuit Board Area sq. in.	Hardware Costs $
Data Control	20	18	280
MOS Memory	250	14	430
MOS Memory Control	50	9	70
KNOS Memory	3	32	1600
MNOS Memory Control	10	7	50
TOTAL MOS	320	41	780
TOTAL MNOS	33	57	1930

SECTION 6

6.0 INTEGRATED DOSE METHODS

These methods rely upon the collection of the pollutant gas and retention until analysis can be performed. The gas can be adsorbed onto a (presumably) specific adsorbent coated on a suitable solid substrate to give a high surface/volume ratio. Alternatively the air sample may be contacted with an absorbing liquid, selected for its collection efficiency and for its compatibility with subsequent analytical procedures used for readout of the dosage information.

With both types of collection media there are two forms of sample acquisition that can be used, either the passive diffusion methods or the active pumping methods discussed in Section 2.0.

These combinations of media/sampling will be briefly discussed to develop their main features relative to dosimeter development strategy. More detailed information is contained in the references cited.

Finally in this section the novel techniques of "packaged vacuum" sampling is briefly discussed.

6.1 Solid Adsorbents/Passive Sampling

As discussed in Section 2.0, the diffusion tube sampler collects a quantity of material that is directly proportional to the concentration-exposure time product for the pollutant provided the pollutant concentration is kept at zero by total adsorption at the collecting surface. The collecting material can be coated onto a metal screen disc[3] or a silica gel disc kept in position at the end of the diffusion tube. The mechanical design of the tube should allow rapid, easy removal of an exposed disc for subsequent analysis and replacement by a fresh disc.

The minimum detectable quantity of collected pollutant depends upon the analytical method used for readout. Using equation (2.2) from Section 2.1.2 and assuming a minimum detectable quantity of 1 μg, a diffusion coefficient of 0.2 cm^2/sec, and a diffusion tube 1 cm wide and 8 cm long, collection over a period of 10 hours would enable the detection of an average concentration of 1400 μg/m^3 or about 0.55 ppm of SO_2 or 0.75 ppm of NO_2. In order to detect a level of 5 to 10 ppb the analytical method would have to be able to detect 10 nanograms of pollutant.

An alternative method of achieving diffusive flow is to use a porous disc containing a large number, N, of small diameter tubes oriented parallel to each other, i.e., a honeycomb construction. The formula for diffusive flow through N parallel channels of length ℓ and cross-sectional area a is

$$Q = ND(\frac{a}{\ell})C_0t \ . \qquad (6.1)$$

By keeping a/ℓ the same as A/L in equation (2.2) and making N as large as practicable, a large enhancement of diffusive flow can be obtained. As indicated in Figure 3.2, molecular diffusion--such as experienced in bulk air--can occur in pores as small as 1 μm in diameter at normal temperature and pressure. Therefore, the use of thin porous discs as diffusion covers over a suitable absorber looks attractive. The practical limit to such a reduction is when condensible moisture in the sampled air can clog up the pores or appreciably reduce their diameter.

Colorimetric changes appear to be more sensitive. A paper impregnated with pH-sensitive dye has been reported to give a color change detectable by eye to concentrations of SO_2 of the order or 10 ppb 10 ppb following an hour's exposure.[133] However, the dye requires a humectant to provide water for the acid reaction which develops the color. The degree of development is dependent upon temperature, humidity and--in the simple flat plate geometry used--at low wind speeds, depends upon windspeed. This problem with "flat plate" absorbers has already been pointed out in Section 2.1. It is also probable that the developed color change is not stable, but fades with time.

A colorimetric indicator for nitrogen oxides using dephenyl benzidene decasulfonic acid (or an alkalai metal salt of this) on an inert solid support has been reported.[134] Another method for NO_2 is to deposit diphenylamineoxalic acid from alcoholic solution onto silica gel.[135]

6.2 Solid Adsorbents/Active Sampling

This approach uses a known, constant pumping rate to draw air sample through a tube containing a packed granular adsorbing bed. The adsorbed pollutant can be measured either through retention for subsequent chemical analysis or be development of a color, with the length of the colored zone being related to the concentration of pollutant.

Because of normal variation in packing density, the packed bed cannot be relied upon as the controlling restriction setting flow rate.[136] Such control is usually obtained by using a small diameter limiting orifice[137] on the vacuum pump side of the tube. In order to prevent plugging of this orifice, a fine pored filter should be used. The design of the flow system should insure that the pressure drop across the packed sampling tube and filter are kept as low as possible. Figure 6.1 shows schematically the components of pressure drop in the system.

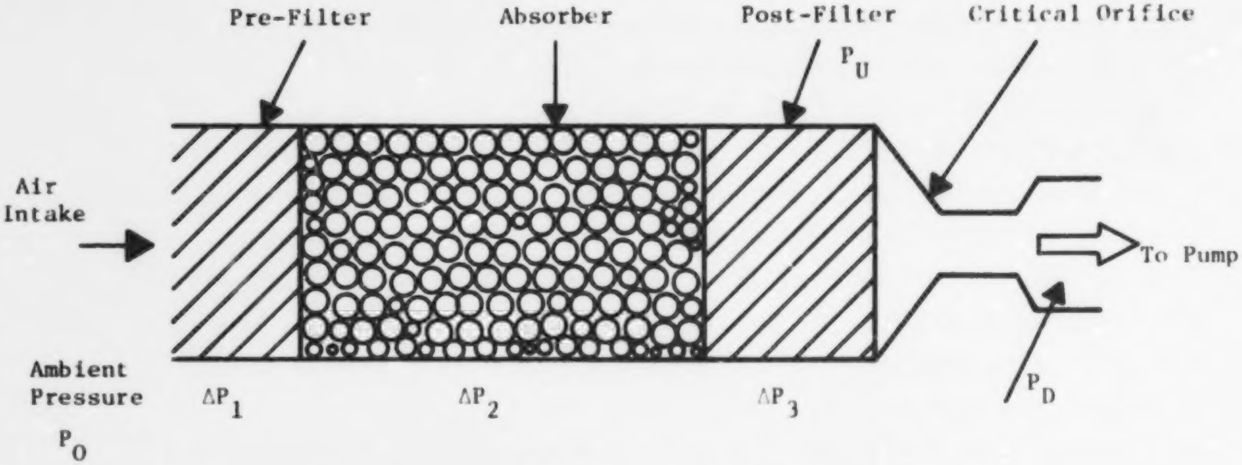
Pre-Filter
Absorber
Post-Filter
Critical Orifice
P_U
Air Intake
To Pump
Ambient Pressure
P_0
ΔP_1
ΔP_2
ΔP_3
P_D

Figure 6.1. Pressure Components in Packed Tube Samplers.

In order for the critical orifice to function properly, controlling the flow at the maximum, Q_{max}, the downstream pressure, P_D, must be less than 53% of the upstream pressure, P_U. The type of pump used will determine the suction pressure, P_D, at flow rate Q_{max}. In order to maintain the required pressure drop across the critical orifice, the sum of the pressure drops must satisfy the relation

$$\Delta P_1 + \Delta P_2 + \Delta P_3 < P_0 - 1.887 P_D . \qquad (6.2)$$

Even if this relation is maintained, there are still many sources of error.

The equation for the flow rate of air at critical flow is[135]

$$Q_{max} = 6.8 \times 10^4 \, CAP_U \sqrt{T} \text{ m}\ell\text{/min} \qquad (6.3)$$

where C = discharge coefficient, usually of unity order, (dimensionless)
A = critical orifice cross section area, cm^2
P_U = upstream pressure, atmospheres,
T = air temperature, °K.

With a 0.1 mm diameter orifice, at a pressure of 1 atmosphere and air temperature of 300°K, and assuming unity as the discharge coefficient value, the flow rate will be about 100 mℓ/min. As can be seen from equation (6.3) a 10°K change in temperature will give about 1.7% change in flow rates. This assumes that C is independent of temperature, which is dubious. In addition, P_U will vary as the ambient pressure varies, and will depend upon the pressure drops, ΔP_K, which will vary from tube to tube. All of these factors contribute to the uncertainty as to the volume of air which has been pulled through the packed absorber.

When the concentration of pollutant to be adsorbed is small, the length of packing, L, which has been coated with pollutant will be given by[138]

$$L = KC^{(1-n)}V \qquad (6.4)$$

where K = a proportionality constant

C = the volumetric concentration in air

V = the volume of air sampled.

The exponential term n is the same as that for the Freundlich isotherm equation for equilibrium absorption[139] of SO_2 on the adsorber.

The collected material may be analyzed by chemical methods, or, if a dye chemical is used, by photometric analysis of the length of stain. Linch has reviewed the latter practice in detail.[140]

Practical factors affecting the use of non-selective adsorbents such as silica gel and activated charcoal have been discussed by Linch.[141] Water vapor is usually a problem with such adsorbents. It can also be a problem on relatively selective adsorbents, although for a different reason. With the non-selective adsorbents, water vapor tends to preferentially cover the adsorbent surface and perhaps clog up the micropores of these materials. This "crowds out" the other molecular species, and can be construed as a physical process of interferance. If SO_2 and NO_2 react with adsorbed water to form acids, and these acids are in turn capable of chemical reaction with some coating material, the resulting chemical change of the surface might alter the uptake of pollutant. Such behavior has been noted for SO_2 in the presence of water vapor on SDM co-polymer.

6.3 Liquid Adsorbents/Passive Sampling

The method here is essentially the same as that described above in Section 6.1 except the collector is a liquid rather than a solid coated on a support of large surface area. This technique has been used by Palmes and Gunnison[142] to monitor SO_2 with TCM solution as the collecting fluid. The method is subject to the same drawback as the solid absorber--lack of sensitivity. In addition, the cell must remain vertically oriented in order to avoid spilling the collecting solution.

6.4 Liquid Adsorbents/Active Sampling

Bubblers, with an air sample drawn through an adsorbing solution, have been used for many years in air pollution monitoring. Spill-proof microimpingers have been reported[143] and are available commercially,[144] matched to suitable miniature sampling pumps to obtain integrating dosimeters.

6.5 Packaged Vacuum

A novel approach to sampling for air pollutant dosimetry has been taken by NRL scientists.[145] This consists of a small cylinder evacuated to high vacuum. In operation as a sampler, the cylinder is opened to the atmosphere through a precision orifice. As long as the pressure in the cylinder remains below 53% of an atmosphere, air flow through the orifice is essentially constant at critical flow--which was discussed above in Section 6.2.

The quantities of pollutants collected in the cylinder will be proportional to the time averaged values obtained during the measurement period. If conditions for critical flow are maintained, the amount of each pollutant will be given by

$$m = QM\bar{C}t \tag{6.5}$$

where m = weight of material collected, grams
Q = flow rate through critical orifice, cm^3/min
M = pollutant molecular weight, grams
$\bar{C}$ = mean pollutant concentration in air, $moles/cm^3$
t = duration of sampling.

Using a sampling time of 8 hours, with a flow rate of 0.1 cm^3/min, and assuming an analytical method capable of detecting 0.25 μg of SO_2, the minimum detectable average concentration is about 2 ppm.

This can be improved by increasing the amount of material collected, i.e., by increasing the flow rate. The limit on this is imposed by the size of collection container. Since the pressure in the container at the end of sampling must be about 0.5 atmosphere, or less, the total volume sample will be about half of the container volume. Another method of decreasing the minimum detectable quantity is to increase the sensitivity of the analytical method. Usually, however, this increases the cost of analysis.

In addition to these drawbacks, the critical orifice may present a problem due to the very small size that must be used to restrict the flow to a manageable value. Partial or total plugging can drastically change the flow rate. This could be checked by measuring the final pressure prior to "readout". Again, this is an additional processing step which can significantly increase the cost of using this method.

SECTION 7

7.0 DOSIMETRY SYSTEMS

Whether gathered in the form of an integrated sample or as a recorded signal proportional to a time varying concentration, in order to be of use as an exposure record correlated to activity of the human subject, a "readout" must be obtained. This section reviews the operational sequences that might be used in the deployment of dosimeters and discusses some of the methods that might be used for readout.

7.1 Integrated Dose Methods

At this point it is important to review the operation of the dosimeter system to put into perspective the factors which influence deployment and data quality. Figure 7.1 schematically presents the operational sequence in the deployment of dosimeters for integrated dose measurements. The dosimeter is considered to have 3 components: a "holder" that mechanically protects the collector and enables the device to be conveniently placed on the subject (weaver); a vessel which will contain the absorbing reagent; and a standard quantity of absorbing reagent. The dosimeter design could enable the holder to stay with a subject in the field, or could require that the holder/vessel/reagent be assembled in the laboratory each time prior to delivery to subjects in the field, with the holder and vessel recycled each time the dosimeter package is returned to the laboratory for read out.

Presumably in a health effects study the subjects would maintain an activity log which would be periodically submitted for comparison and correlation with exposure history. This would probably be supplemented by periodic health examinations.

There are many places where errors can be introduced into the measurement. These are indicated by numerals in parentheses in Figure 7.1. They include: (1) contaminated reagents at assembly; (2) spurious exposure of the blank, or partially or totally exposed measuring reagent due to improper mounting of the dosimeter in the field; (3) contamination during the decant/demount operation; (4) improper clean-up of vessels and/or holders; (5) contamination or reagent problems during sample processing; and (6) improper instrument calibration and operation during analysis.

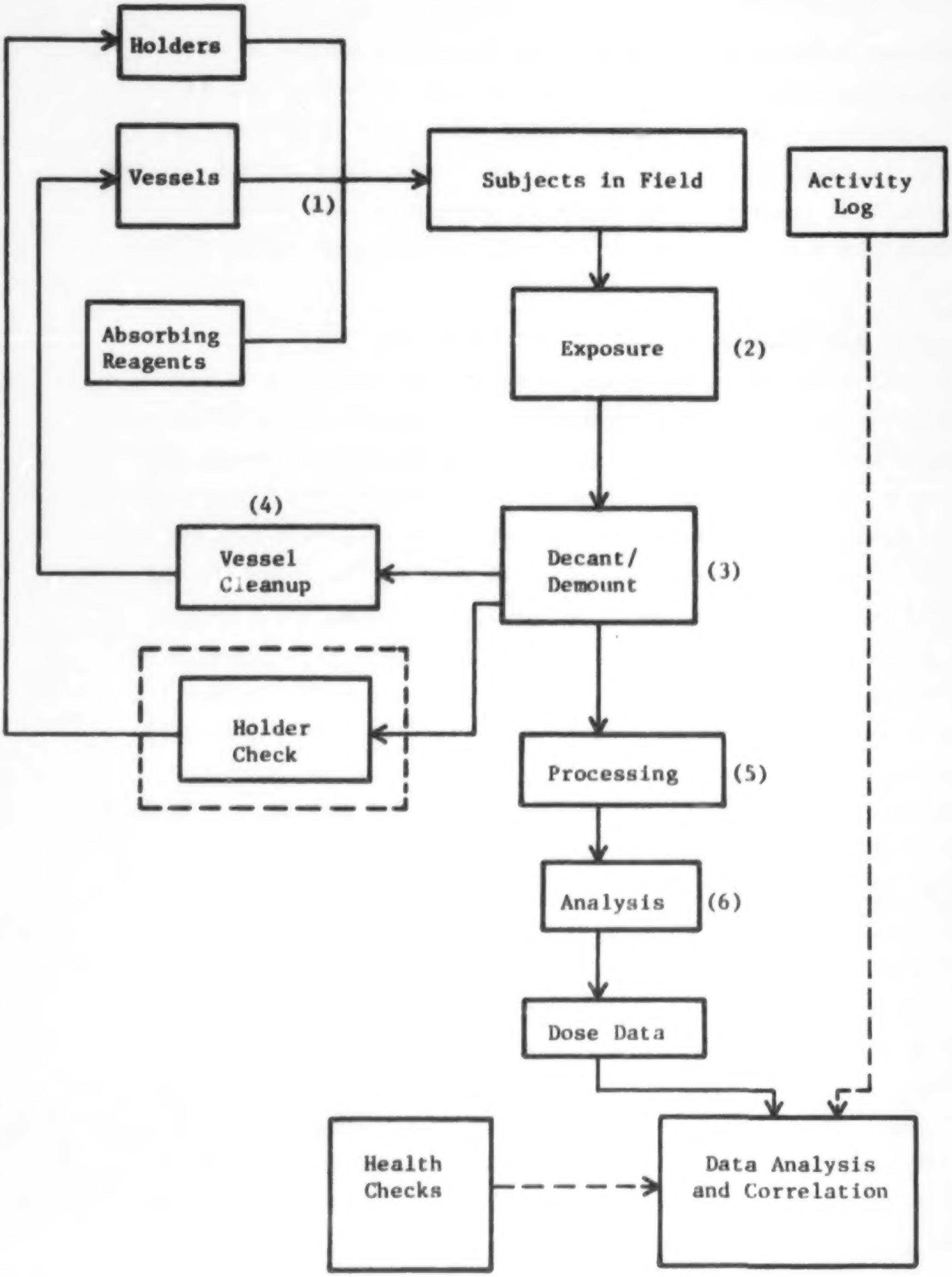
Holders
Vessels
(1)
Subjects in Field
Activity Log
Absorbing Reagents
Exposure
(2)
(4)
Vessel Cleanup
Decant/ Demount
(3)
Holder Check
Processing
(5)
Analysis
(6)
Dose Data
Health Checks
Data Analysis and Correlation

Figure 7.1. Integrated Dosimeter Operation Scheme.

Operating procedures should take these potential error sources into account and methods should be developed to minimize the possibilities of introducing spurious exposure data.

Figure 7.2 shows schematically the processing flow for obtaining dose measurements from the integral dose sampling methods of Section 6.0. Only collections via solid and liquid media are considered. The dashed line in the figure represents a blank sample which has gone through the same distribution, wear and collection process as the measurement sample, but has not been exposed (for a significant length of time) to air with the pollutant to be measured.

Material from solid adsorbers may be thermally desorbed to allow analysis or it may be removed by "wet processing". As an example of the former, assume that a brominated, amine modified silica gel cartridge (see Section 3.2) is heated to about 95°C for desorption and then carrier gas is used to conduct the desorbed SO_2 to a flame photometric detector. The analog signal from the detector could be used as a barographic record on a strip chart, or converted to digital form for printout on a paper tape or put on a magnetic tape in digital form. As an example of wet processing, assume that PbO, on a suitable substrate, is converted to the sulfate form by exposure to SO_2.[146] This is then converted to a barium sulfate colloidal suspension, the concentration of which is measured by nephelometer.[147,148] This signal can be used for barographic chart recording or digitized and further processed as discussed above.

As an example of processing of material collected in a liquid absorber, assume that a diffusion tube sampler, or alternatively an impactor sampler with a pump, has been used to collect SO_2 in TCM absorber solution. This solution would be decanted and analyzed by the standard West-Gaeke colorimetric method[149] in parallel with the blank solution. The signal from the colorimeter could be processed in the barographic or digital modes mentioned above to obtain a record.

This type of system would be labor intensive, particularly in the preparation and analysis stages. There would also be a lot of labor involved in the coding of dose data, activity data and health status data for subsequent analysis.

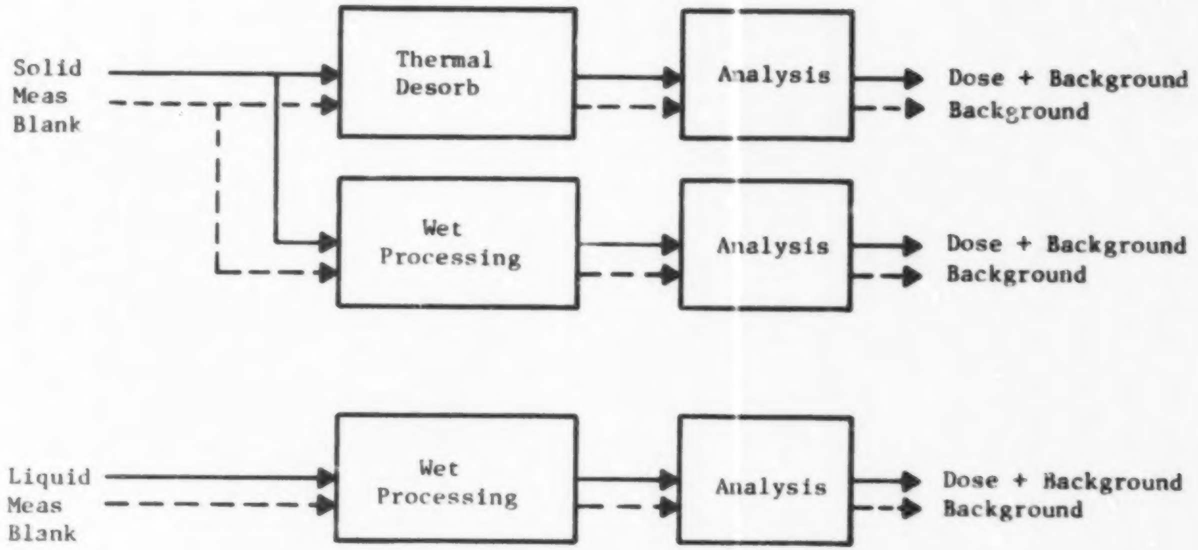
Solid
Meas
Blank
Thermal Desorb
Wet Processing
Analysis
Analysis
Dose + Background
Background
Dose + Background
Background
Liquid
Meas
Blank
Wet Processing
Analysis
Dose + Background
Background

Figure 7.2. Dose Measurements from Integral Methods.

7.2 Continual Dose Methods

Figure 7.3 schematically presents an operational sequence in the deployment of dosimeters for continual measurements. The components of the measurement package are: the instrument package containing all of the "hardware" for O_3, NO_2 and SO_2 measurement; transducers for activity monitoring and the data collection system; the calibration reagents; and the measurement reagents. The instrument package with reagents is delivered to the subjects in the field. Periodically, as required, calibration and measurement reagents are replenished, either individually, or possibly with the whole instrument package recycled (dashed line).

Although the instrument pakcage could--and probably would--have transducers to monitor subject activity (i.e., through heart rate or breathing rate measurements), it is likely that the subject would also be asked to keep an activity log which would be periodically submitted for comparison and correlation with exposure history, supplemented by periodic health examinations.

There are many places where error could be introduced into the measurements. These are indicated by numerals in parentheses in Figure 7.3. They include: (1) contaminated calibration or measurement reagents; (2) malfunction of instrument components in the field; (3) spurious errors in the data collection system; and (4) improper clean-up and check-out of the instrument package and reagent containers during recycle.

Operating procedures should take these potential error sources into account and methods should be developed to minimize the possibilities of introducing spurious exposure data.

The calibration reagents might be employed automatically in the operating system to obtain span and zero checks several times during a day, or they might be applied manually at less frequent invervals--say once a day. The frequency of such checks will involve a trade-off between system complexity and instrument cost on one hand and data reliability on the other.

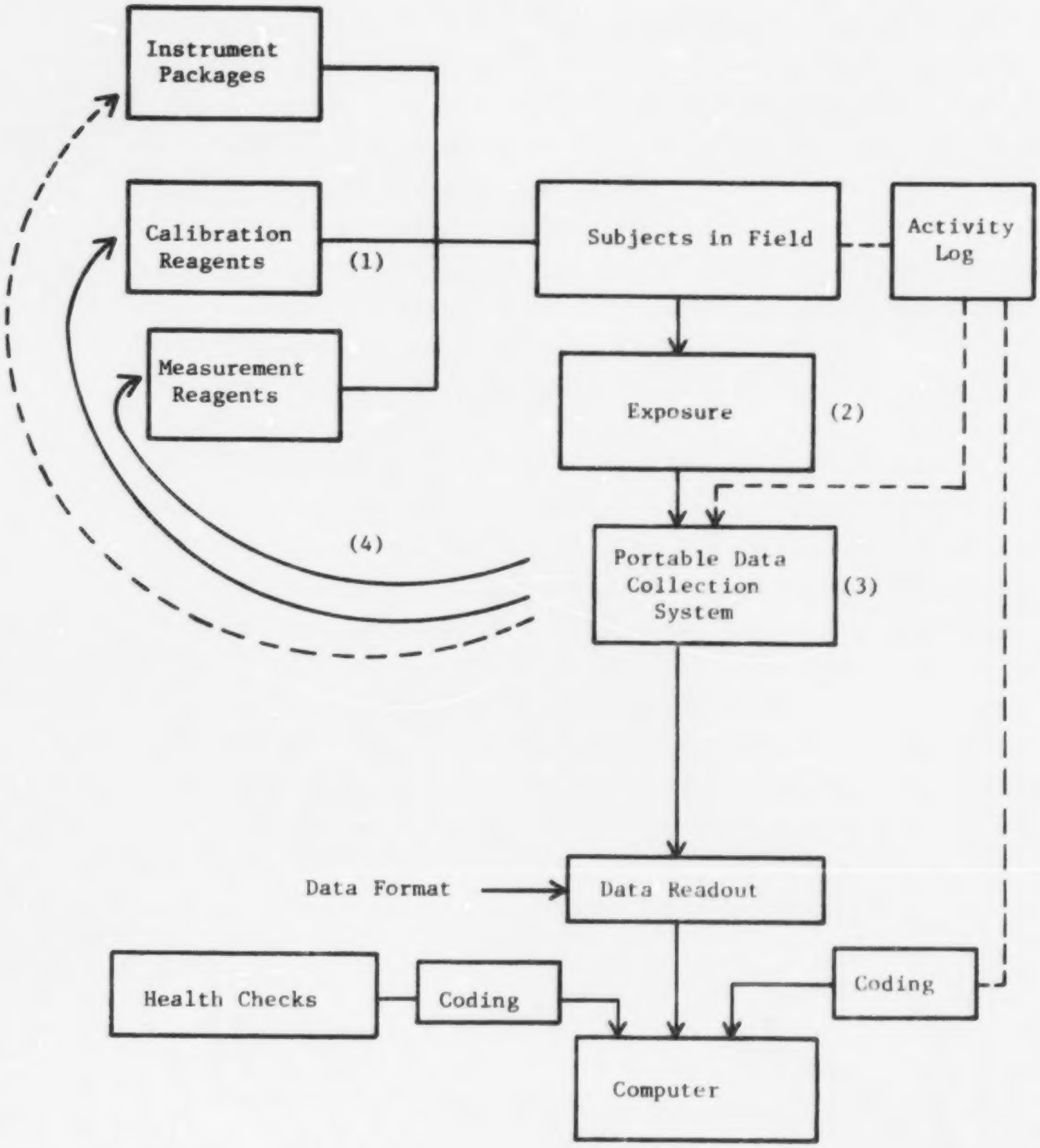
Instrument Packages
Calibration Reagents
Measurement Reagents
(1)
Subjects in Field
Activity Log
Exposure
(2)
Portable Data Collection System
(3)
(4)
Data Format
Data Readout
Health Checks
Coding
Coding
Computer

Figure 7.3. Continual Dose Rate Measurement Operational Scheme.

Figure 7.4 shows schematically the processing flow for data obtained in portable collection systems. If "volatile" MOS memories are used, a "keep alive" power system will be required to maintain the data intact in memory during transport from the field to the central data collection system. If MNOS or magnetic tape data storage is used, such an auxiliary power supply will not be necessary. Each of the three different storage media will require a unique interface design that will allow insertion of the memory module and cycling to dump the data into a buffer memory associated with a central processor (computer). This cycling will insert the data in a pre-determined format.

As indicated in Figure 7.3 it is probable that a supplementary activity log and health data will also be used. Data from both of these sources will have to be coded for entry into the data processing system.

For this dosimeter system the bulk of the labor required should be in the preparation, delivery and maintenance of the instrument packages and the required reagents. Because of the complexity of the devices, skilled instrument technicians or specialists will be required to maintain the instrument used in the deployment network. This will be true even when prototype instrument packages have been through a thorough development and "shakedown" test phase.

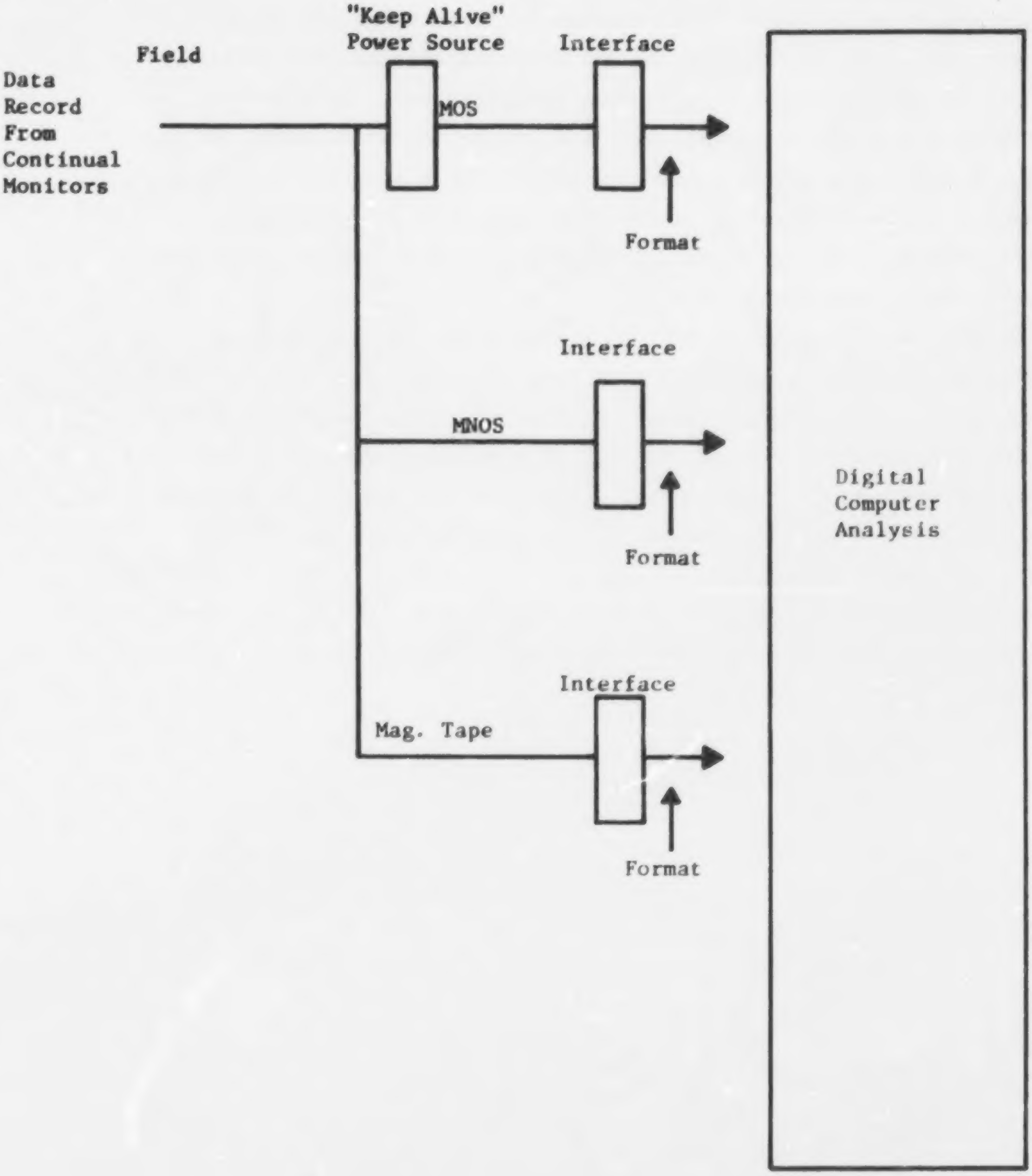
"Keep Alive"
Power Source
Field
Interface
Data
Record
From
Continual
Monitors
MOS
Format
Interface
MNOS
Format
Digital
Computer
Analysis
Interface
Mag. Tape
Format

Figure 7.4. Data Processing for Dose Rate Records from Continual Monitors.

SECTION 8

8.0 CONCLUSIONS AND RECOMMENDATIONS

A practical pollutant dosimeter system must be designed to be as simple and reliable as possible commensurate with the amount and quality of the data obtained. For reasons of economics and deployment logistics (which could also be translated back to economic terms) the system should use as many common components as possible. This minimizes initial costs through reduced design time and longer repetitive production runs. It reduces spare parts inventory requirements. It reduces the maintenance and trouble-shooting complexity.

If possible, the sensing principle(s) used should require little or no reagent supply. This minimizes the logistic burden of continual resupply, which is costly not only in terms of raw material costs but also in terms of the quality control measures required to assure that each batch of reagent is within specifications.

Finally, the sensing principle(s) should require a minimum amount of electrical power to be supplied during operation. This reduces initial costs by reducing battery size or by trading off increased battery size with longer operating time without recharge. Further, the weight of the instrument package can be reduced (making subject cooperation easier) if a smaller battery size is used.

With these considerations in mind, a comparison of the sensing principles analyzed in Section 4.0 indicates that only one method offers the possible combination of the characteristics cited above and at the same time appears to come close to the accuracy and precision desired (CHAMP Specifications, Section 1.1). This is the dual-cathode amperometric system modeled in Section 4.2.2. By using suitable adsorbing filters to select only one pollutant to be introduced to the cell for measurement, the same basic cell design can be used for ozone, nitrogen dioxide and sulfur dioxide. Such filters exist and have been described by Lindqvist[44] and Anderson, et al.[97] The system does use a liquid electrolyte and would, therefore, be orientation limited, but only occasional make-up water would have to be added to replace evaporative loss.

In order to improve the response to NO_2, if deemed necessary, research could be performed to determine additives for the electrolyte which could improve NO_2 absorption efficiency while not interfering with the electrode reactions.

The next choice from the list of continual sensors would be a tape transport colorimetric scheme, such as that outlined on pp. 89-93 in Section 4.5.2. A developmental model for NO_2 monitoring has been demonstrated by Lyshkow.[149] Further research and development work would have to be done to improve the mechanical tape transport design and to determine suitable colorimetric reagents for ozone and SO_2. As with the amperometric system cited above, selective filters could (and would probably have to) be used to eliminate interferences.

The third choice would be the luminol/H_2O_2 chemiluminescence system of Anderson, et al.[97] Although it uses a single detector, this method has the drawbacks of requiring liquid reagent re-supply, a mechanical device for alternately viewing each micro-reactor cell and a high voltage power supply for the photomultiplier tube.

All three of these methods require active sampling, but suitable portable pumps are already commercially available.

Of the data storage methods discussed in Section 5.0, the digital casette system appears to be the most desirable from the points of view of storage capacity, non-volatility and ease of entry into a computer system for subsequent verification and analysis.

Continual monitoring of ozone, nitrogen dioxide and sulfur dioxide at ambient levels by human subjects carrying a briefcase-sized instrument package entails the operation of a system of which the instrument packages are but a part. As discussed in Section 7.2, many operations are required to deploy instruments in the field and to process the data obtained in order to get meaningful information about the relation between pollutant exposure and general health status. Periodic calibration is a necessity. Periodic routine maintenance must also be performed to keep instrument performance within specifications. These operations require skilled instrument personnel in addition to the skilled personnel expected to be employed in the health checks and data interpretation. Adequate staffing must be considered in addition to hardware costs when cost estimates for system operation are made.

8.1 Recommendations

Current budgeting might not allow a large scale program to develop and deploy continual monitoring devices, and might not for some time. However, research and development of sensors and other components for these devices should be encouraged. This encouragement can come in several forms. EPA in concert with other interested governmental agencies can sponsor forums to discuss the problems associated with miniature sensor development, inviting industry and university participation. Hopefully this would stimulate the speculative development of prototypes in these sectors which could be improved for use either through strictly proprietary in-house development or through partial government funding. The trend of miniaturization and enhanced portability which began with the development of transistors twenty-five years ago, is inexorably and spontaneously leading to reduced instrument package size on the part of industry. The trend is most evident in what are regarded as strictly electronic instruments, i.e., voltage and current meters, signal generators and cathode ray oscilloscopes. In recent years, however, increasing numbers of portable gas sensing instruments for monitoring in the tens to hundreds of ppm ranges encountered in occupational environments have been developed and marketed. Knowledge of a potential market provides a powerful incentive for private development.

Another avenue is for EPA to conduct in-house research of one or more sensing principles and then underwrite the development by industry until viable types are available on the marked. Alternatively, EPA could contract out the research effort ab initio and then underwrite development or license for development and marketing.

Whichever strategy is used, it is recommended that at the initial stages of consideration of a particular sensing method, a modeling effort such as that carried out in Section 4.0 of this report be undertaken. The better (more complete) the model, the better will be the performance estimate. Such modeling techniques have been of great value in electronic systems design and in chemical systems design.[150] In addition, such modeling would serve to elucidate the design and operating parameters which influence the performance of the sensing method, calling to attention those parameters which must be controlled most closely in order to attain the desired sensitivity and stability of calibration. Such a technique has been used to advantage by McClenny *et al*[151] for a proposed NO_2 sensing method.

Further, it is recommended that consideration and analysis of sensing methods, at least mathematically and hopefully experimentally, be initiated as soon as possible in order to provide time for critical review and, hopefully, to stimulate alternate, competitive, approaches.

REFERENCES

1. Environmental Protection Agency, Russel E. Train, Administrator, Proposed Rule for Revision of "Significant Harm and Emergency Action Levels for Photochemical Oxidants" Federal Register 39:9672-9675, March 13, 1974.

2. Palmes, E.D. and A.F. Gunnison. Personal Monitoring Device for Gaseous Contaminants. Amer. Ind. Hyg. Ass. J. 34:78-81, February, 1973.

3. Gunnison, A.F., M.E. Gunnison and E.D. Palmes. Personal Samplers for CO, NO and NO_2 in Air - Annual Technical Progress. Report to U.S. Bureau of Mines on Grant No. GO 133066, June 1, 1973 to May 31, 1974. New York University Medical Center Institute for Environmental Medicine, June, 1974.

4. Gregg, S.J. and K.S. W. Sing. Adsorption, Surface Area and Porosity. New York, Academic Press, 1967. p. 9-19.

5. *ibid*. p. 36-49.

6. Rideal, E.K. Concepts in Catalysis. New York, Academic Press, 1968. p. 62.

7. Perry, R.H., C.H. Chilton and S.D. Kirkpatrick. Chemical Engineers' Handbook, Fourth Edition. New York, McGraw-Hill Book Co., 1963, p. 14-12-14-13.

8. Jost, W. Diffusion in Solids, Liquids, Gases, Third Printing with Addendum. New York, Academic Press, 1960. p. 420-423.

9. *ibid*. p. 14-14-14-15.

10. Adsorbents for Gas-Phase Odor Control or Liquid-Phase Heavy Metal Removal, Patent, *Japan Kokai*, 72 23,383.

11. Active Carbon for Adsorbing Sulfur Dioxide, *Japan Kokai*, 72 33,890.

12. Polystyrene or Nylon Foam Fibers Containing Activated Charcoal for Absorbing Toxic Materials from Air. *Japan Kokai*, 72 28,214.

13. Salek, J.M.. Adsorption of Gases on Gold Films. J. Phys. Chem. 77:1849-, 1973.

14. Hashida, I. *et al*, Kagaku Kaishi 1973:1195-, June 1973.

15. Bostrom, C. The Absorption of Sulfur Dioxide at Low Concentrations (pphm). Studied by an Isotopic Tracer Method. Int. J. Air. Wat. Poll. 9:333-341, 1965.

16. Frechette, M.W. *et al*. Evaluation of Substrates for Use on a Piezoelectric Detector of Sulfur Dioxide. Anal. Chem. 45:1765-1766, September, 1973.

17. Burwell, R.L. and O. Leal. Modified Silica Gels as Selective Adsorbents for Sulfur Dioxide. J.C.S. Chem. Comm. 1974:342-343.

18. Thomas, F.W. and D.M. Davidson. Monitoring Sulfur Dioxide with Lead Perioxide Cylinders. J. Air. Poll. Control Assoc. 11:24-27, 1961.

19. Huey, N.A. The Lead Dioxide Estimation of Sulfur Dioxide Pollution. J. Air Poll. Control Assoc. 18:610-611, 1968.

20. Boulerice, M. and W. Brabant. New PbO_2 Support for the Measurement of Sulfation. J. Air Poll. Control Assoc. 19:432-434, 1969.

21. See Ref. 15 above.

22. Bracewell, J.M. and A.E.M. Hodgson. The Hydrogen Perioxide Method for Sulfur Dioxide in the Atmosphere-Efficiency at Low Concentrations by a Radioactive Tracer Technique. Int. J. Air Wat. Poll. 9: 431-438, 1965.

23. Pellizzari, E.D. Electron Capture Detection in Gas Chromatography. J. Chromatography 98:323-361, 1974.

24. Weast, R.C. (ed.). Handbook of Chemistry and Physics, 46th Edition. Cleveland, Ohio, The Chemical Rubber Company, 1965. p. E-68.

25. Nash, T. Absorption of Nitrogen Dioxide by Aqueous Solutions. J. Chem. Soc. A 1970: 3023-3024, 1970.

26. Ma, Y. H. and C. Mancel. Diffusion Studies of CO_2, NO, NO_2 and SO_2 on Molecular Sieve Zeolites by Gas Chromatography. AICHE 18:1148-1153, 1972.

27. Altshuller, A.P. and A.T. Wartburg. The Interaction of Ozone with Plastic and Metallic Materials in Dynamic Flow System. Intern. J. Air Water Pollution. 4:70-78, 1961.

28. Haagen-Smit, A.J. and O.J. Brunelle. The Application of Phenolphthalein Reagent to Atmospheric Oxidant Analysis. Intern. J. Air Pollution 1:51, 1968.

29. Bovee, H.H and R.J. Robinson. Sodium Diphenylaminesulfonate as an Analytical Reagent for Ozone. Anal. Chem. 33:1115, 1961.

30. Egerow, M.S. Z. Lebensm. 56:355, 1928.

31. Bravo. H.A., and J.P. Lodge. Specific Spectrophotometric Determination of Ozone in the Atmosphere. Anal. Chemistry 36:671, 1964.

32. Hendricks, R.H. and L.B. Larsen. An Evaluation of Selected Methods of Collection and Analysis of Low Concentrations of Ozone. Am. Ind. Hyg. Assoc. J. 27: 81, 1966.

33. Bradley, E.C. and C.J. Haagen-Smit. The Application of Rubber in the Quantitative Determination of Ozone. Rubber Chem. Technol. 24:750, 1951.

34. Atyaksheva, L.T. *et al*. Physico-chemistry of Concentrated Ozone. Zh. Fiz. Khim., 46:2602, 1972.

35. Jonathan, N. Infrared Spectrosocpy Application to Chemical Kinetic Systems. NTIS *AD-683771*, 1968.

36. Atyaksheva, L.T. *et al*. Physico-chemistry of Concentrated Ozone. Zh. Fiz. Khim. 47:996, 1973.

37. Reimshuessle, H.K. and G.A. Mountford. J. Colloid Interface Sci. 25:558-63, 1967.

38. Hall, R.C. A Highly Sensitive and Selective Microelectrolytic Conductivity Detector for Gas Chromatography. J. Chromatog. Sci. 12:152-160, March, 1974.

39. Knipe, A.C. *et al*. A Fast Response Conductivity Ampiifier for Chemical Kinetics. J. Physics E:Scientific Instruments 7:586-590, January, 1974.

40. Tokiwa, Y. *et al*. Atmospheric Ozone Determination by Amperometry and Colorimetry. In:Determination of Air Quality, Proc. ACS Symposium, 1971, Mamantov, G. (ed.). New York, Plenum Press, 1972. p. 109-130.

41. Boyd, A.W. *et al*. New Determination of Stoichiometry of the Iodometric Method for Ozone Analysis at pH 7.0. Anal. Chem. 42:670-672, 1970.

42. Schechter, H. Spectrophotometric Method for Determination of Ozone in Aqueous Solutions. Water Research 7:729-739, 1973.

43. Kromhyr, W.D. Electrochemical Concentration Cells for Gas Analysis. Ann. Geophys. 25:203-210, 1969.

44. Lindqvist, F. A Differential Galvanic Atmospheric Ozone Monitor. Analyst 97:549-558 , 1972.

45. Skoog, D.A. and D.M. West. Fundamentals of Analytical Chemistry. New York, Holt, Rinehart and Winston, 1963. p. 378-380.

46. Philips Model PW9700.

47. Beckman Inst. Co. Model 906A.

48. Schulze, F. Versatile Combination Ozone and Sulfur Dioxide Analyzer. Anal Chem 38:748-752, 1966; Schulze, F. U.S. Patent No. 3,361,661, Jan. 2, 1968.

49. Byers, R.L. and J.W. Davis. Sulfur Dioxide Adsorption and Desorption on Various Filter Media. J. Air. Poll. Control Assoc. 20:236-238,1970.

50. Chand, R. and M. Shaw. Apparatus for Measuring Sulfur Dioxide Concentrations. U. S. Patent No. 3,622,488, November 23, 1971.

51. Chand, R. and M. Shaw. Apparatus for Measuring Nitrogen Oxide Concentrations. U. S. Patent No. 3,622,487, November 23, 1971.

52. Dynasciences Corp., Los Angeles, California.

53. Environmental Instrumentation Group, Lawrence Berkeley Laboratory. Instrumentation for Environmental Monitoring AIR, LBL-1, Volume 1. University of California, Berkeley, CA, May 1, 1972. p. 17-19.

54. Pasternak, R. A., M. V. Christensen and J. Heller. Diffusion and Permeation Oxygen, Nitrogen, Carbon Dioxide, Nitrogen Dioxide Through Polytetrafluoroethylene. Macromolecules 3:366-374, 1971.

55. Chand, R. and P. R. Cunningham. Characterization of Organic Solvents for Electrochemical Air Pollution Sensors. IEEE Trans. Geosci. Electronics GE-8:158-161, July 1970.

56. Ruch, W. E. Chemical Detection of Gaseous Pollutants. Ann Arbor, Michigan, Ann Arbor Science Publishers, 1966. p. 168-173.

57. Saltzman, B. E. Direct Reading Colorimetric Indicators. In: Handbook of Analytical Toxicology.

58. Linch, A. L. Evaluation of Ambient Air Quality by Personnel Monitoring. Cleveland, Ohio, CRC Press, Inc., 1974. p. 19-78.

59. Patterson, G. D., Jr. and M. G. Mellon. Colorimetric Determination of Sulfur Dioxide. U. S. Patent No. 2,785,959, March 12, 1957.

60. See Reference 22.

61. See Reference 15.

62. Lyshkow, N. A. System for Analysis of Gases in Trace Amounts. U. S. Patent No. 3,535,045, October 20, 1970.

63. Cummings, W. G. and M. W. Redfearn. Instruments for Measuring Small Quantities of Sulfur Dioxide in the Atmosphere. J. Inst. Fuel 30:628-635, 1957.

64. DHEW, Title 42, Chapter IV, Part 410, Appendix A. Reference Method for the Determination of Sulfur Dioxide in the Atmosphere (Pararosaniline Method). Federal Register 36:8187-8189, April 30, 1971.

65. See Reference 53. p. 5-13.

66. See Reference 56. p. 140-149.

67. See Reference 56. p. 151-156.

68. Boyd, A. W. *et al*. New Determination of Stoichiometry of the Iodometric Method for Ozone Analysis at pH 7.0. Anal. Chem. 42:670-672, May 1970.

69. See Reference 40.

70. Shechter, H. Spectrophotometric Method for Determination of Ozone in Aqueous Solutions. Water Research 7:729-739, 1973.

71. Kortüm, G. Reflectance Spectroscopy. New York, Springer-Verlag, 1969.

72. Lyshkow, N. A. Colorimeter and Elements Therefor. U. S. Patent No. 3,617,136, November 2, 1971.

73. Nederbragt, G. W. *et al*.

74. Warren, G. J. and G. Babcock. Portable Ethylene Chemiluminescence Ozone Monitor. Rev. Sci. Instr. 41:280-282, 1970.

75. DHEW, Title 42, Chapter IV, Part 410, Appendix D. Reference Method for the Measurement of Photochemical Oxidants Corrected for Interferences Due to Nitrogen Oxides and Sulfur Dioxide. Federal Register 36:8195-8197, April 30, 1971.

76. Hodgeson, J. A. *et al*. Comparison of Chemiluminescent Methods for Measurement of Atmospheric Ozone. in: Progress in Analytical Chemistry, Volume 5, (ed). New York, Plenum Press, p.

77. Clyne, M. A. A. *et al*. Kinetics of the Chemiluminescent Reaction between Nitric Oxide and Ozone. Trans. Fradaday Soc. 60:359-370, 1964.

78. Fontijn, A. Chemiluminescent Method of Detecting Ozone. U. S. Patent No. 3,528,779, September 15, 1970.

79. Fontijn, A. *et al*. Homogeneous Chemiluminescent Measurement of Nitric Oxide with Ozone. Anal. Chem. 42:575-579, May 1970.

80. Hodgeson, J. A., *et al*. Application of a Chemiluminescence Detector for the Measurement of Total Oxides of Nitrogen and Ammonia in the Atmosphere. Paper 71-067, Joint Conference on Sensing of Environmental Pollutants, Palo Alto, CA, Nov 8-10, 1971. Proceedings available from AIAA Library, 750 3rd Ave., New York, N. Y. 10017.

81. Winer, A. M. *et al*. Response of Commercial Chemiluminescent NO-NO_2 Analyzers to Other Nitrogen-Containing Compounds. Environ. Sci. Tech. 8:1118-1121, December 1974.

82. Wooten, G. W. et al. Chemiluminescent Method and Apparatus. U. S. Patent No. 3,749,929, July 31, 1973.

83. Benson, S. W. et al. Detection Device. U. S. Patent No. 3,647,387, March 7, 1972.

84. Halsted, C. J. and B. A. Thrush. Chemiluminescent Reactions of SO. Photochem. Photobiol. 4:1007-1013, 1965.

85. Clyne, M. A. A., et al. The Kinetics of Elementary Reactions Involving the Oxides of Sulphur. Part I, The Nature of the Sulphur Dioxide Afterglow. Proc. Roy Soc. (London) 295A: 355-362, December 1966.

86. Clyne, M.A.A. and B.A. Thrush, Mechanisms of Chemiluminescent Combination Reaction Involving Oxygen Atoms. Proc. Roy. Soc (London) 269A: 404-418, 1962.

87. Fontijn, A., et al., Absolute Quantum Yield Measurements of the NO-O Reaction and Its Use as a Standard for Chemiluminescent Reactions. J. Chem. Phys. 40:64-70, January, 1964.

88. Mettee, H. Foreign Gas Quenching of Sulfur Dioxide Vapor Emission. J. Phys. Chem. 73: 1071-1076, 1969.

89. Schwarz, F.P. and H. Okabe. Fluorescence Detection of Sulfur Dioxide in Air at the Parts per Billion Level. Anal. Chem. 46: 1024-1028, July, 1974.

90. Halsted, C.J. and B.A. Thrush. The Kinetics of Elementary Reactions Involving the Oxides of Sulphur. Part III, The Chemiluminescent Reaction between Sulfur Monoxide and Ozone. Proc. Roy. Soc. (London) 295A: 380-397, December , 1966.

91. See Reference 77.

92. Steffenson, D.M. and D.H. Stedman. Optimization of the Operating Parameters of Chemiluminescent Nitric Oxide Detectors. Anal. Chem. 46: 1704-1709, December, 1974.

93. Harrison, J.W. and G.E. Spangler. Evaluation of Chemiluminescent Detection Methods. In: Comparative Evaluation of Trace Gas Technology Volume II-Analysis and Evaluation of Instrumental Methods, Final Report on Contract DAAK02-73-C-0128, Harrison, J.W. (ed). Research Triangle Park, N.C., Research Triangle Institute, December 1972. AD777868. p. 495-518.

94. Bowman, R.L. and N. Alexander. Ozone Induced Chemiluminescence of Organic Compounds. Science 154: 1454-1456 , 1966.

95. E. H. White et al "Energy Transfer in Chemiluminescence" pp. 479-492 in E. C. Lim (ed.) International Conference on Molecular Luminescence, W. A. Benjamin, New York 1969, 910 pp.

96. Bersis, D. and E. Vassiliou. A Chemiluminescence Method for Determining Ozone. Analyst 91: 499-505, 1966.

97. Anderson, H.H. *et al*. System and Method of Air Pollution Monitoring Utilizing Chemiluminescence Reactions. U.S. Patent No. 3,659,100, April 25, 1972.

98. Stepanova, A.G. *et al*. Luminescent Method for Determining Ozone in Gas Mixtures. USSR Patent No. 329,451, February 9, 1972. Cited in Chem. Abstr. 77, 1972. Abstract No. 42859.

99. __________. Silicon Photodiode Application Notes, D3000 B-1. Salem, Mass, EG&G, Inc. Electro-Optic Div., March, 1973.

100. Regener, V.H. Measurement of Atmospheric Ozone with the Chemiluminescent Method. J. Geophys. Res. 69: 3795, 1964.

101. Tommerdahl, J.B. *et al*. Chemiluminescent Ozone Meter for Continuous Air Monitoring Project. Final Report, Contract No. CPA 70-27. Research Triangle Park, N.C., Research Triangle Institute, January, 1971.

102. Hodgeson, J.A. *et al*. Chemiluminescent Measurement of Atmospheric Ozone. Anal Chem 42: 1795-1802, 1970.

103. Guicherit, R. Ozone Analysis by Chemiluminescent Measurement. Z. Anal. Chem. 256: 177-182, 1971.

104. Lyshkow, N.A. Apparatus and Method for Analysis of Gas Streams. U.S. Patent No. 3,712,793, January 23, 1973.

105. Lukác, S. and J. Sevík. A Discussion of the Detection Mechanism and the Response Character of the Helium Detector. Chromatographia 5: 258-264, 1972.

106. Pellizzari, E.D. Electron Capture Detection in Gas Chromatography. J. Chromatography 98: 323-361, 1974.

107. Krejci, M. and M. Dressler. Selective Detectors in Gas Chromatography. Chromatographic Rev. 13: 1-59, 1970.

108. McDaniel, E.W. *et al*. Ion-Molecule Reactions. New York, Wiley-Interscience, 1970.

109. Loeb, L.B. Basic Processes of Gaseous Electronics. Berkeley, Calif., Univ. of Calif. Press, 1955. p. 8-39.

110. Registered Trademark of Franklin GNO Corp., W. Palm Beach, Fla.

111. McDaniel, E.W. and E.A. Mason. The Mobility and Diffusion of Ions in Gases. New York, Wiley-Interscience, 1973.

112. Vree, P.H. and A. Fontijn. Method of Determining Trace Amounts of Gases. U.S. Patent No. 3,540,8451, November 17, 1970.

113. Murrmann, R.P. et al. Vehicle Detection Classification Using Chemical Sensors. Sepcial Report 181, U.S. Army Cold Regions Research and Engineering Laboratory, Hanover, N.H. August, 1972. AD751740. 57p.

114. Lovelock, J.E. Improvements in or Relating to the Detector of Trace Gases. Brit. Patent. No. 1,266,869, March 15, 1972.

115. Kebark, P. Higher-Order Reactions - Ion Clusters and Ion Solvation. In: Ion-Molecule Reactions, Volume 1, Franklin, J.L. (ed). New York, Plenum Press, 1972. p. 346.

116. Harrison, J.W. Analysis of the Plasma Chromatograph. In: Comparative Evaluation of Trace Gas Technology, Volume II-Analysis and Evaluation of Instrumental Methods, Final Report on Contract DAAK02-73-C-0128, Harrison, J.W. (ed). Research Triangle Park, N.C., Research Triangle Institute, December, 1972. AD 777868. p. 41-101.

117. King, W.H., Jr. Piezoelectric Sorption Detector. Anal Chem. 36: 1735-1739.

118. Frechette, M.W. et al. Evaluation of Substrates for Use on a Piezoelectric Detector. Anal Chem. 45: 1765-1766, 1973; ____________. Simple Piezoelectric Probe for Detection and Measurement of SO_2. Environ. Sci. Tech. 7: 1135-1137, December, 1973.

119. King, D. and G.R. Hoffman. Observations on a Quartz Crystal Deposition Monitor. J. Phys. E., Sci. Instr. 4: 993-998, 1971.

120. Lu, Chih-Shun. Improving the Accuracy of Quartz Crystal Monitors. Research/Development: 45-50, March, 1974.

121. Mason, W.P. Uses of Piezoelectric Crystals and Mechnanical Resonators in Filters and Oscillators. In: Physical Acoustics Principles and Methods, Volume I, Part A, Mason, W.P. (ed). New York, Academic Press, 1964, p. 375.

122. Warner, A.W. MicroWeighing with the Quartz Crystal Oscillator-Theory and Design. In: Ultra Micro Weight Determination in Controlled Environments, Wolsky, S.P. and E.J. Zadnauk (eds). New York, Interscience, 1969. p. 137-161.

123. Warner, ibid., p. 141.

124. Saurbrey, G. Schwingquarze zur Wagung dunner Schichten, Z.Phys. 155: 206, 1959 (German)

125. Stockbridge, C.D. Resonance Frequency Versus Mass Added to Quartz Crystals. In: Vacuum Microbalance Techniques, Behrndt, K. (ed). New York, Plenum Press, 1966. p. 193-205.

126. Miller, J.G. and D.I. Boleff. Acoustic Wave Analysis of the Operation of Quartz Crystal Film Thickness Monitors. J. Appl. Phys. 39: 5815-5816, 1968.

127. Mason, W.P. Physical Acoustics and the Properties of Solids. Princeton D. Van Nostrand, 1958. p. 27-32.

128. Jost, W. Diffusion in Solids, Liquids, Gases, Third Printing with Addendum. New York, Academic Press, 1960. p. 303.

129. Jost, *ibid*. p. 300-304.

130. Bracker , J.H. Triethanolamine for Collecting Nitrogen Dioxide in the TLV Range. Am. Ind. Hygiene Assoc. J. 34: 390-395, September, 1973.

131. Homolya, J.B., Emission Measurements Research Branch, CPL/NERC, Research Triangle Park, N.C. Private communication.

132. Jost, *ibid*. p. 465.

133. Linch, A. L. *ibid*. p. 3.

134. Brauer, L. W., Indicator for Nitrogen Oxide. U. S. Patent 3,388,075, June 11, 1968.

135. Rakowski, R. F., Colorimetric Dosimeter for Nitrogen Dioxide. U. S. Patent 3,574,552, April 13, 1971.

136. Linch, A. L. *ibid*. p. 31

137. Nelson, G. O. Controlled Test Atmospheres. Ann Arbor, Mich., Ann Arbor Science Publishers, 1971. p. 45-49.

138. Linch, A. L. *ibid*. p. 36.

139. Szepesy, L. *op. cit.*, p. 42.

140. Linch, A. L. *ibid*. p. 19-73.

141. Linch, A. L. *ibid*. p. 91-105.

142. Palmes, E. D. and A. F. Gunnison, Personal Monitoring Device for Gaseous Contaminants. Am. Ind. Hygiene Ass. J. 34:78-81, 1973.

143. Linch A. L. *ibid*. p. 82.

144. Bendix Environmental Science Div., Baltimore.

145. Williams, F. W. and H. G. Eaton. A New Concept in Personal Samplers. Paper No. 88, presented at the 1975 Pittsburgh Conference, March 3-7, 1975, Cleveland, Ohio.

146. N. A. Huey. The Lead Oxide Estimation of Sulfur Dioxide Pollution. J.A.P.C.A. 18:610-611, September, 1968.

147. Boulerice, M. and W. Brabant. New PbO_2 Support for the Measurement of Sulfation. J.A.P.C.A. 19:432-434, 1969.

148. Keily, H. J. and L. B. Rogers. Nephelometric Determination of Sulfate Impurity in Certain Reagent Grade Salts. Anal. Chem. 27:759-764, 1955.

149. Lyshkow, N.A. private communication.

150. Himmelbau, D.M. and K.B. Bischoff. Process Analysis and Simulation. New York, John Wiley & Sons, 1968.

151. McClenny, W.A., J.A. Hodgeson and J.P. Bell. Photofragment Detection of Nitrogen Dioxide. Anal. Chem. 45: 1514-1518, July, 1973.